Lunar and Planetary Laboratory
Department of Planetary Sciences

Canyons of Mars and Earth

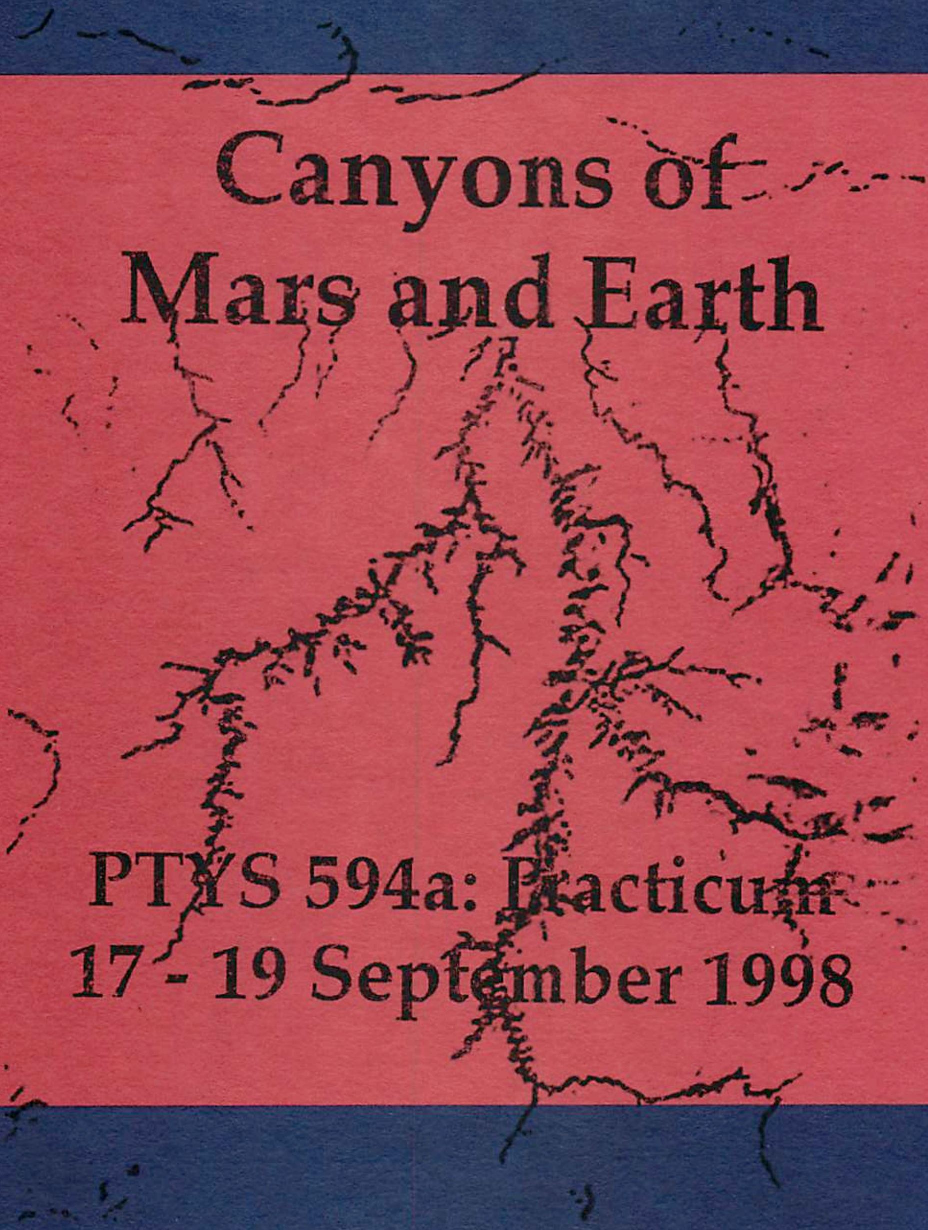

PTYS 594a: Practicum
17 - 19 September 1998

The University of Arizona
Tucson, Arizona

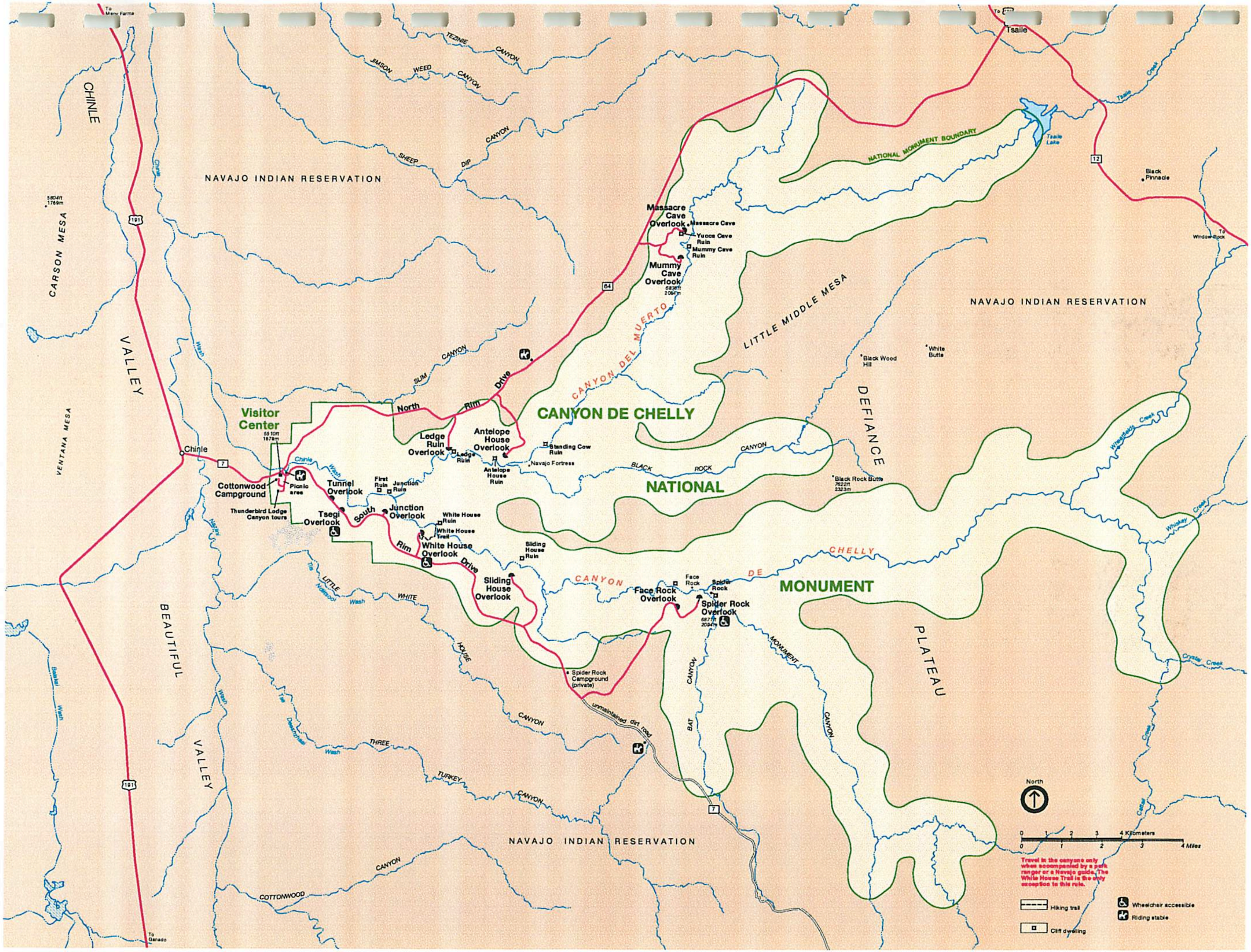
CANYON DE CHELLY
NATIONAL
MONUMENT
Visitor Center
5510ft 1679m
Cottonwood Campground
Thunderbird Lodge Canyon tours
Picnic area
Tunnel Overlook
Tsegi Overlook
First Ruin
Junction Ruin
Junction Overlook
White House Ruin
White House Trail
White House Overlook
Sliding House Ruin
Sliding House Overlook
Ledge Ruin Overlook
Ledge Ruin
Antelope House Overlook
Antelope House Ruin
Standing Cow Ruin
Navajo Fortress
Massacre Cave Overlook
Massacre Cave
Yucca Cave Ruin
Mummy Cave Ruin
Mummy Cave Overlook
Face Rock
Face Rock Overlook
Spider Rock
Spider Rock Overlook
Spider Rock Campground (private)
unmaintained dirt road
North Rim Drive
South Rim Drive
CANYON DEL MUERTO
BLACK ROCK CANYON
CANYON DE CHELLY
MONUMENT CANYON
BAT CANYON
NATIONAL MONUMENT BOUNDARY
LITTLE MIDDLE MESA
DEFIANCE PLATEAU
NAVAJO INDIAN RESERVATION
NAVAJO INDIAN RESERVATION
NAVAJO INDIAN RESERVATION
CHINLE VALLEY
BEAUTIFUL VALLEY
CARSON MESA
VENTANA MESA
Chinle
Tsaile
Tsaile Lake
Black Pinnacle
White Butte
Black Wood Hill
Black Rock Butte
To Window Rock
To Many Farms
To Ganado
TEZNIE CANYON
JIMSON WEED CANYON
SHEEP DIP CANYON
SUM CANYON
WHITE HOUSE CANYON
THREE TURKEY CANYON
COTTONWOOD CANYON
Whiskey Creek
Crystal Creek
North
Travel in the canyons only when accompanied by a park ranger or a Navajo guide. The White House Trail is the only exception to this rule.
Hiking trail
Cliff dwelling
Wheelchair accessible
Riding stable
4 Kilometers
4 Miles

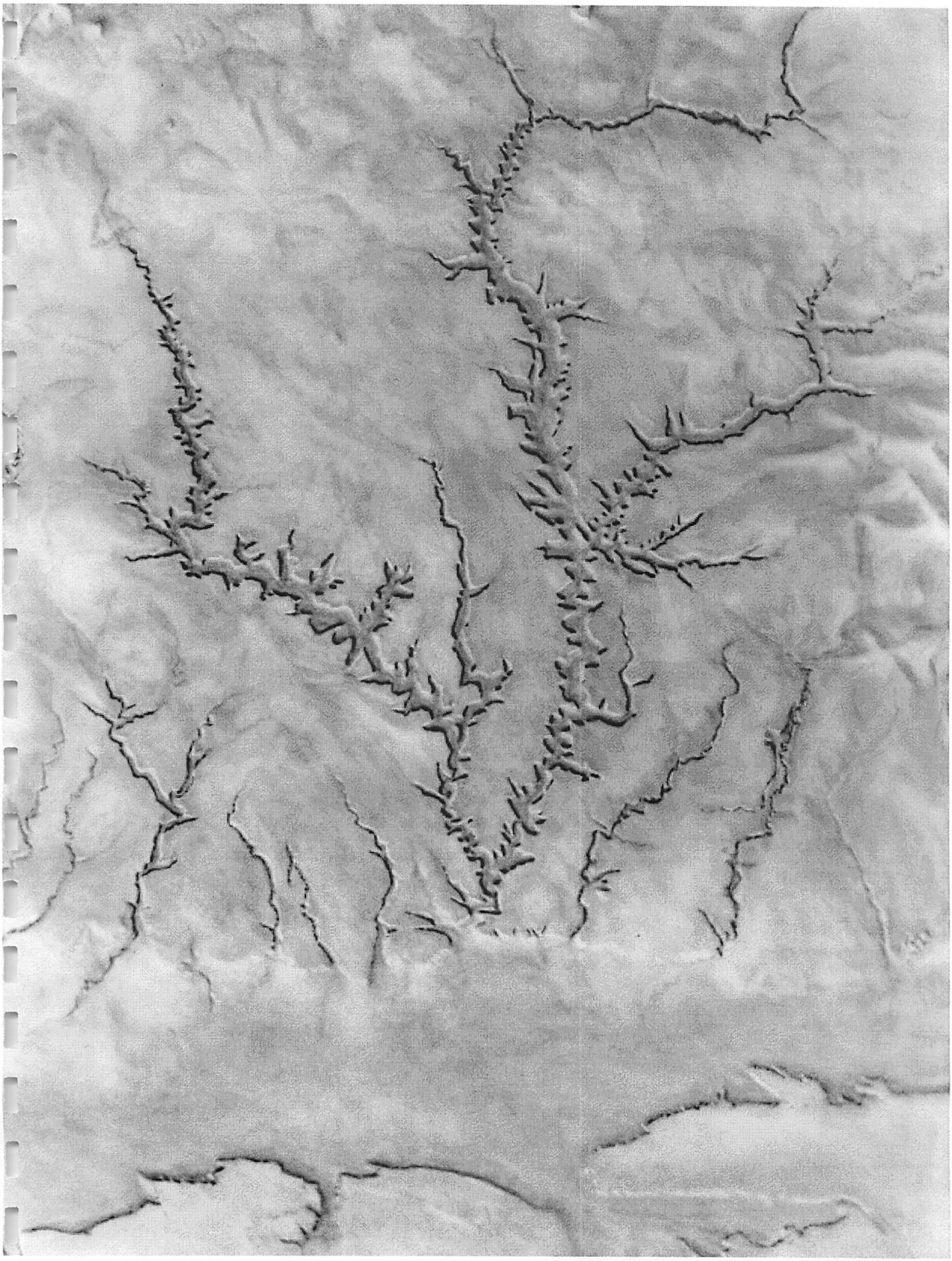

Dedication

"The whole world rides on the backs of graduate students."

Jay Melosh, 10 September 1998

Canyon de Chelly

Planetary Geology Field Practicum
PTYS 594a
17-19 September, 1998

PTYS 594a,

PLANETARY FIELD GEOLOGY PRACTICUM

Itinerary, Field Trip 17-19 September 1998

H. J. Melosh, 353 Space Sciences, 621-2806

We will depart at 8:30 am *sharp* on Thursday, 17 September from the LPL loading dock off Warren Street. We will have six U. of Arizona vans plus Lazlo Keszthelyi's truck. Try to be at LPL by 7:30 am to get the vans loaded, radios installed, etc. Please be sure that you have had breakfast beforehand, have ice for the coolers, etc. before we are scheduled to leave: breakfast and ice runs just before departure have caused long delays in the past!

Our approximate itinerary is:

Thursday, 17 September:

8:30 am Distribute handouts. Overview of Tucson area Tectonics from the roof of LPL, **D. Trilling**. Depart LPL, drive N on Oracle blvd.
9:00 am Stop to observe pediments and stream terraces of the Canyon del Oro drainage on W. side of the Catalina mountains –**W. Jaeger**
Drive rte. 77 toward San Manuel: Pirate fault to the East, Oracle granite underfoot.
10:30 am Stop to observe San Manuel mine/economic geology --**D. O'Brian** .
11:30 am Stop 10 mi S. of Mammoth at Camel Canyon fossil site –**T. Hurford**
Return to rte. 77, drive N toward Winkelman, Globe
12:00 noon Lunch Stop to observe/discuss giant landslides at milepost 153–**J. Head**
Caution: Exit here is steep and visibility poor. Drivers exit with care!
1:30 pm Continue N on rte 77 to Globe, turn onto rtes 60/77 to Salt River Canyon
2:30 pm Stop at Hieroglyphic point overlook of Salt River Canyon –**M. Milazzo.**
3:00 pm Stop in bottom of Salt River Canyon. Continue N on Rte. 60.
4:00 pm Stop to observe rim gravels and discuss uplift of the plateau –**J. Fields**
6:30 pm Camp in Sitgreaves National Forest near Show Low.

Friday, 18 September:

8:00 am Break Camp, continue N on rtes 61/180 to Petrified Forest. Discuss Springerville Volcanic field between Show Low and Concho – **P. Withers and L. Keszthelyi. F. Ciesla** will discuss the modern hydrology of the Little Colorado River.
9:30 am Arrive S. entrance Petrified Forest National Park.
9:45 am Stop to observe Chinle Formation, Fossils on short hike near Visitor's Center –**R. Mastrapa, B. Cohen**. Drive N through Park to intersection with I-40. Stop briefly at Painted Desert overlook.
11:00 am Continue west on I-40 toward Holbrook. Turn North on Rte. 77 at Sun Valley.
12:00 am Lunch Stop to discuss Hopi Buttes diatremes –**A. Eckholm**. Turn East on Route 15, drive to junction with Rte. 191, then North to Chinle.
2:30 pm arrive Chinle,

3:00 pm hike down to White House ruin –**B. Pierazzo and Z. Turtle** on Anasazi Archeology

5:00 pm return to vehicles, begin drive around S. rim – **A. Alpert and R. Beyer** on Sapping features, **J. Barnes and P. Lanagan** on general geology of canyon and vicinity

7:00 pm camp (Group Site 1) Fireside Chat by **A. Rivkin** on the Navajo Indian Nation.

Saturday, 19 September:

8:00 am Break Camp, drive N rim of canyon –**Alpert, Beyer, Barnes and Lanagan. Jim Rice** will describe/compare valley networks in the Artic.

10:00 am Depart Canyon deChelly, drive S. on 191 to Ganado, then proceed W. on 264 across Hopi mesas to Tuba City. **R. Lorenz** will probably find ample opportunity to discuss the physics of washboard roads on this segment. Stop to observe dinosaur footprints –**J. Spitale.**

1:30 pm depart Tuba City, continue W. on 160, then S on 89 to Flagstaff

2:30 pm depart Flagstaff for Tucson

7:00 pm (with luck) arrive Tucson, unpack vans, go home.

Additional Information:

Primary Drivers: J. Barnes, B. Cohen, J. Fields, J. Spitale, D. Trilling

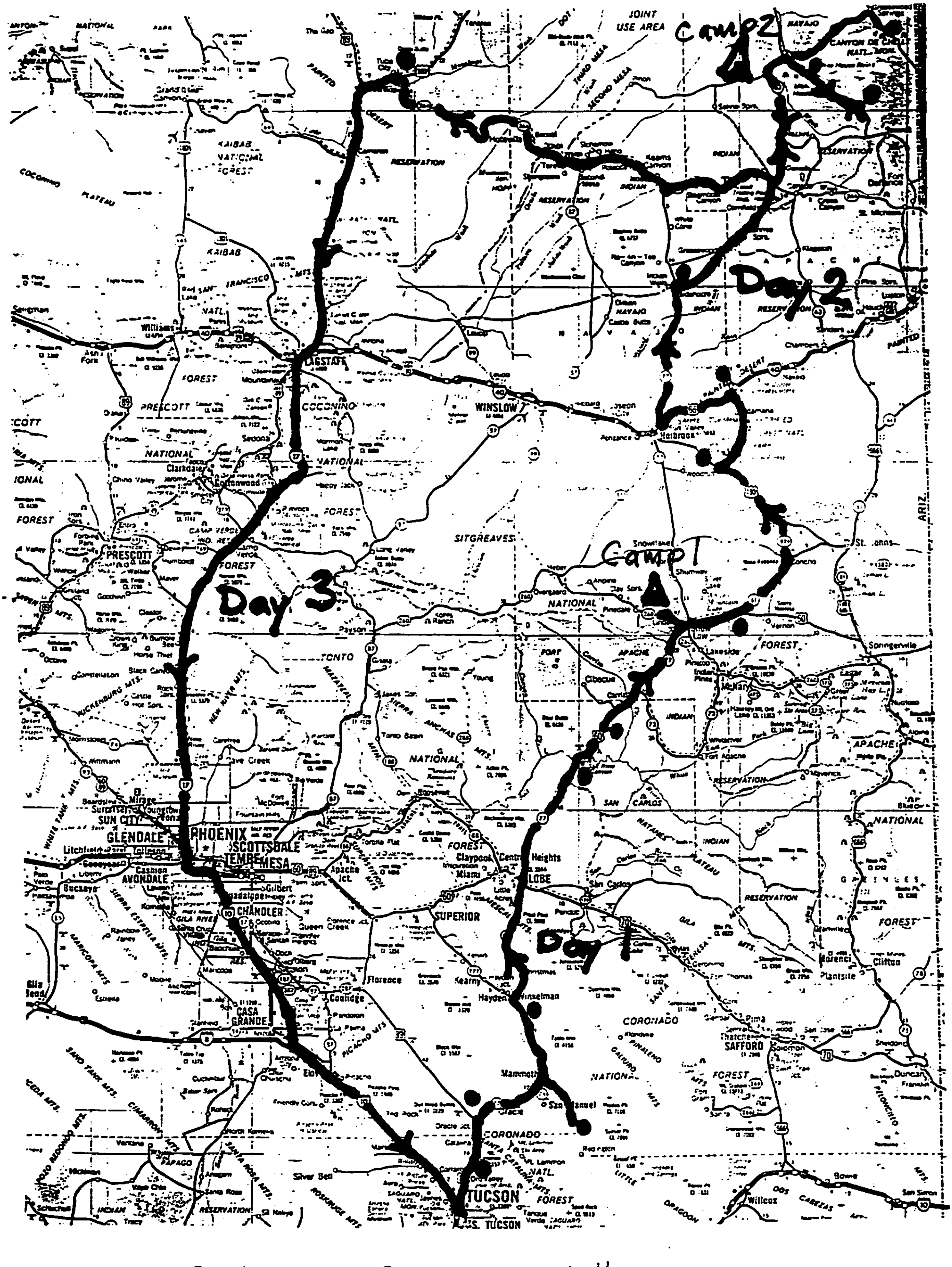

Route Map, Canyon de Chelly Trip

17 – 19 September 1998

ERA	PERIOD	EPOCH	AGE (mil yr)	DOMINANT LIFE FORMS	EVENTS IN ARIZONA
CENOZOIC Age of Mammals	Quaternary q	Holocene		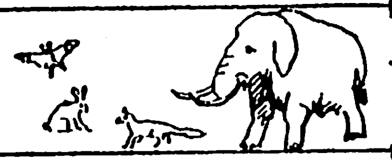	Present erosion cycle gouges Pleistocene and Tertiary deposits. Basalt volcanism continues near San Francisco Peaks and at a few other sites.
			.01		
		Pleistocene			Regional uplift accelerates erosion; cyclic erosion creates terraces. Basalt volcanism occurs in several areas; San Francisco Peaks grow, collapse, and are glaciated. Colorado River flows through to Gulf of California. Pluvial lakes occupy some valleys.
			2		
	Tertiary t	Pliocene		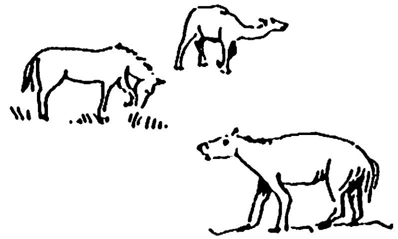	Colorado River turns west, initiates canyon cutting on Colorado Plateau. Little Colorado reverses as recurrent movements lift plateaus. In south, basins fill with stream and lake deposits.
			5		
		Miocene			Basin and Range Orogeny 15 to 8 million years ago creates fault-block ranges with NW-SE grain. Basalt volcanism widespread.
					Mid-Tertiary orogeny 30-20 million years ago pushes up mountains with NE-SW grain. Metamorphic core complexes form. Colorado Plateau rises; Colorado River flows south, east of Kaibab Arch. Downdropped Verde Valley intercepts northward drainage. Explosive volcanism common, with calderas in Chiricahua and Superstition Mountains.
			24		
		Oligocene			Tension faulting in south is accompanied by volcanism and intrusion of dikes, stocks, laccoliths. Intermountain valleys fill with debris from mountains. Verde Valley begins to form.
			38		
		Eocene			Laramide Orogeny ends 50 million years ago, leaving undrained intermountain valleys, some with lakes. No volcanism or intrusions mark "Eocene magma gap." Northbound streams deposit rim gravels.
			55		
		Paleocene			In south, Laramide Orogeny creates mountains with NE-SW trend; overthrusting may have occurred. Explosive volcanism occurs. Abundant small intrusions appear, some containing copper, silver, gold. In north, plateaus begin to form as large blocks are lifted or dropped.
			63		
MESOZOIC Age of Reptiles	Cretaceous K				Seas invade briefly from west and south; volcanism widespread. Laramide Orogeny begins 75 million years ago as west-drifting continent collides with outlying plates.
			138		
	Jurassic J				Deserts widespread; thick sand dune deposits in north. Explosive volcanism in south and west is followed by erosion.
			205		
	Triassic Ꞧ				Extensive coastal plain, delta, and dune deposits spread north from mountains in central and southern Arizona. Faulting, small intrusions, explosive volcanism occur in south.
			240		
PALEOZOIC Age of Fishes	Permian P			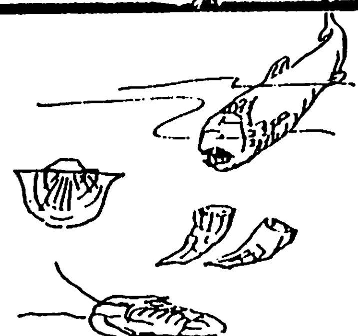	Dunes form across northern Arizona, then a western sea invades briefly. Alternating marine and non-marine deposition in south and west.
			290		
	Pennsylvanian ℙ				Marine limestones deposited in south and south-central Arizona; floodplain and desert prevail in north.
			330		
	Mississippian M				Widespread deposition of fossil-bearing marine limestone is followed by emergence and development of karst topography with sinks and caves.
			365		
	Devonian D				Marine deposits form, then are removed from many areas by erosion.
			410		
	Silurian S				No record.
			435		
	Ordovician O				Brief marine invasion, then no record.
			500		
	Cambrian ∈				A western sea advances across denuded continent, depositing conglomerate and sandstone, then shale and limestone.
			570		Great Unconformity — long erosion.
PRE-CAMBRIAN p∈	Younger				Several episodes of mountain-building and intrusions of sills and dikes are followed by marine and near-shore sedimentation, faulting, and uplift.
			1700		
	Older				Sedimentary and volcanic rocks accumulate, then are compressed and altered into NE-SW-trending ranges extending beyond Arizona. 1.7 billion years ago granite batholiths intrude these older metamorphic rocks.

Minerals

TABLE 1–3. Some Common Minerals and Their Physical Properties

Mineral	*Chemical Composition*	*Common Colors*	*Luster*	*Hardness*	*Cleavage*
Quartz	SiO_2	Clear colorless, milky white, pink, gray, etc.	Glassy	7	None, conchoidal fracture
Plagioclase	$NaAlSi_3O_8$ $CaAl_2Si_2O_8$	White, gray, colorless	Glassy to Pearly	6	Two directions, intersect at about 90°
Orthoclase (K-feldspar)	$KAlSi_3O_8$	Pink, white, gray, colorless	Glassy	6	Two directions, about 90°
Muscovite (white mica)	$KAl_2Si_3O_{10}(OH)_2$	Clear to silvery green, or yellow	Silky or Pearly	2–2.5	One direction, cleaves to thin sheets
Biotite (black mica)	$K(Mg,Fe)_3AlSi_3O_{10}(OH)_2$	Dark brown to black	Silky or Pearly	2.5–3	One direction, cleaves to thin sheets
Hornblende (Amphibole Group)	$Ca_2Na(Mg,Fe)_4(Al,Fe)(Al,Si)_8O_{22}(OH)_2$	Dark green to black	Glassy	5–6	Two directions, intersect at 56° and 124°
Augite (Pyroxene Group)	$Ca(Mg,Fe,Al)(Si,Al)_2O_6$	Dark green to black	Glassy	5–6	Two directions, intersect at 90°
Olivine	$(Mg,Fe)_2SiO_4$	Green to brown	Glassy	6.5–7	None, conchoidal fracture
Calcite	$CaCO_3$	Colorless to white	Glassy to Earthy	3	Three directions, intersecting at 75° and 105°
Pyrite	FeS_2	Pale brass-yellow	Metallic	6–6.5	none
Chalcopyrite	$CaFeS_2$	Brass yellow	Metallic	3.5–4	none

TABLE 1–4. Moh's Hardness Scale.

10	Diamond	↑
9	Corundum	
8	Topaz	
7	Quartz	
6	Orthoclase feldspar	increasing hardness
5	Apatite	
4	Fluorite	
3	Calcite	
2	Gypsum	
1	Talc	

Intrusive Rocks

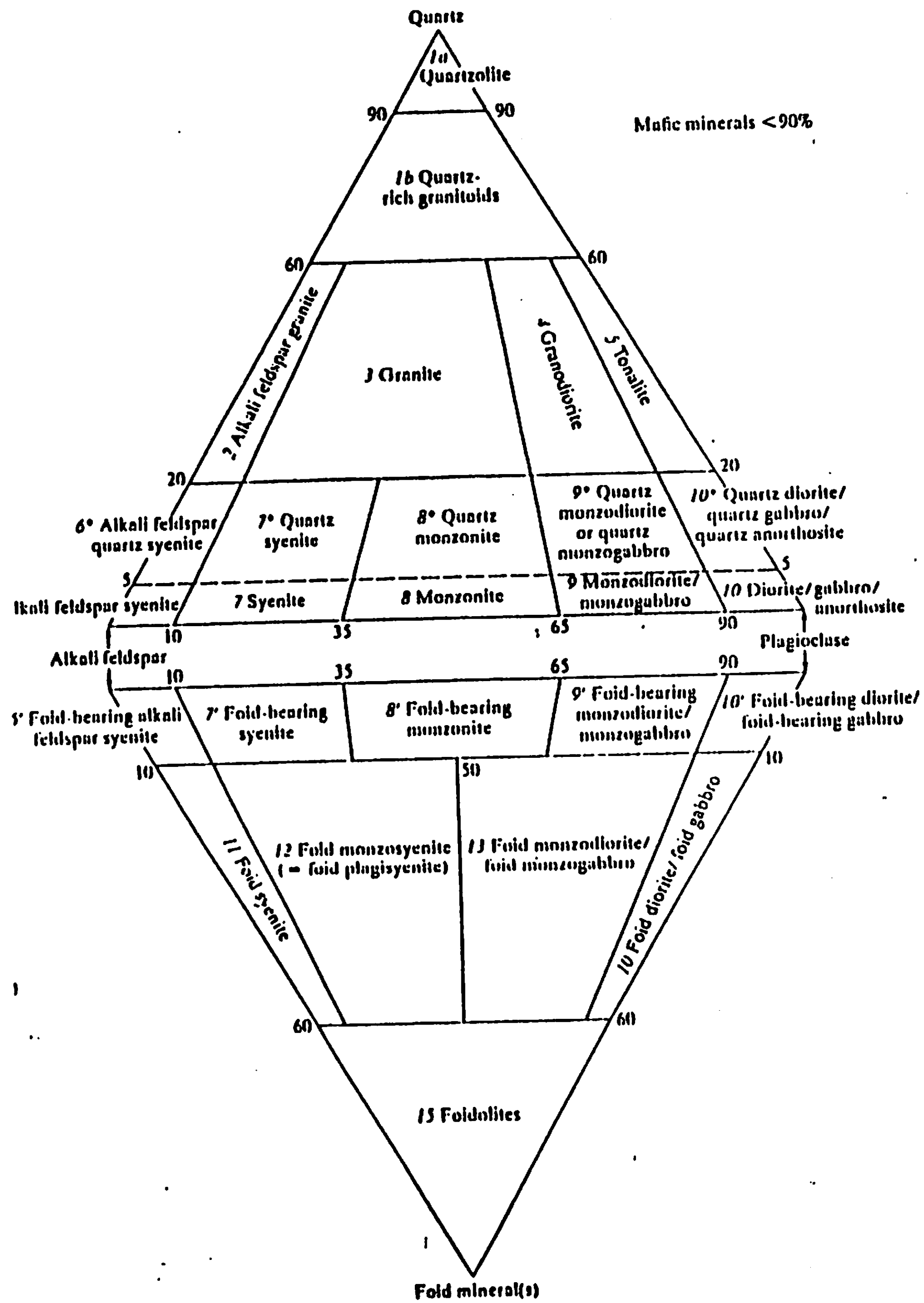

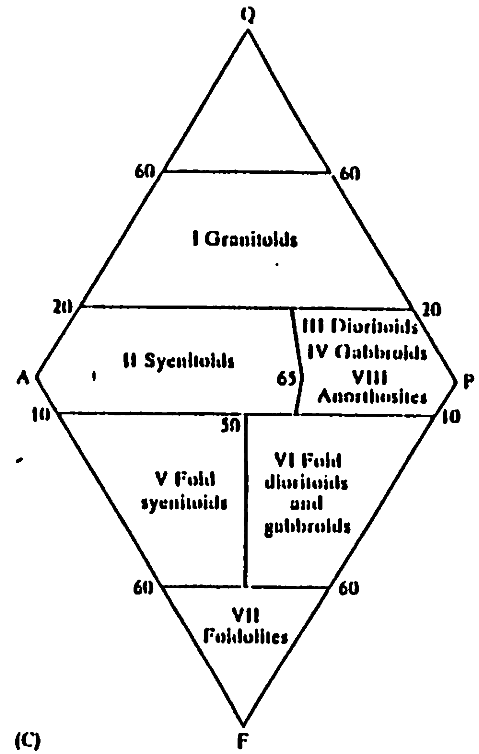

(C)

Figure 4–1
(A, B) The classification of plutonic rocks. In order to be included in these triangles, the igneous rock must be phaneritic. The rock must contain at least 10% plagioclase, alkali feldspar, and either quartz (triangle A) or feldspathoid (triangle B). The relative amounts of these minerals are recalculated to 100% and plotted within the appropriate triangle by the technique shown in Figure 4–2. Appropriate modifying terms are based upon mafic mineral composition or distinctive texture. (C) Generalized group names (for field use) when mineral percentages cannot be determined with precision. In fields II, III, and IV the qualifier "foid-bearing" should be used when feldspathoids are present. [From A. L. Streckeisen, 1976, *Earth Sci. Rev., 12*, Fig. 1a.]

(see Figure 4–1B). A rock cannot appear on both triangles, because quartz and feldspathoid are chemically incompatible; when mixed they will react to form a compound (feldspar) of intermediate silica content.

The volcanic igneous rocks are named on the basis of a similar triangular arrangement (see Figure 4–3). Distinction between basalt and andesite is made mainly on the basis of silica content (a rock with more than 52% SiO_2 is andesite, and a rock with less than 52% SiO_2 is basalt, as shown in part D), or less accurately on plagioclase composition (a rock with a plagioclase composition more sodic than An_{50} is andesite).

Extrusive Rocks

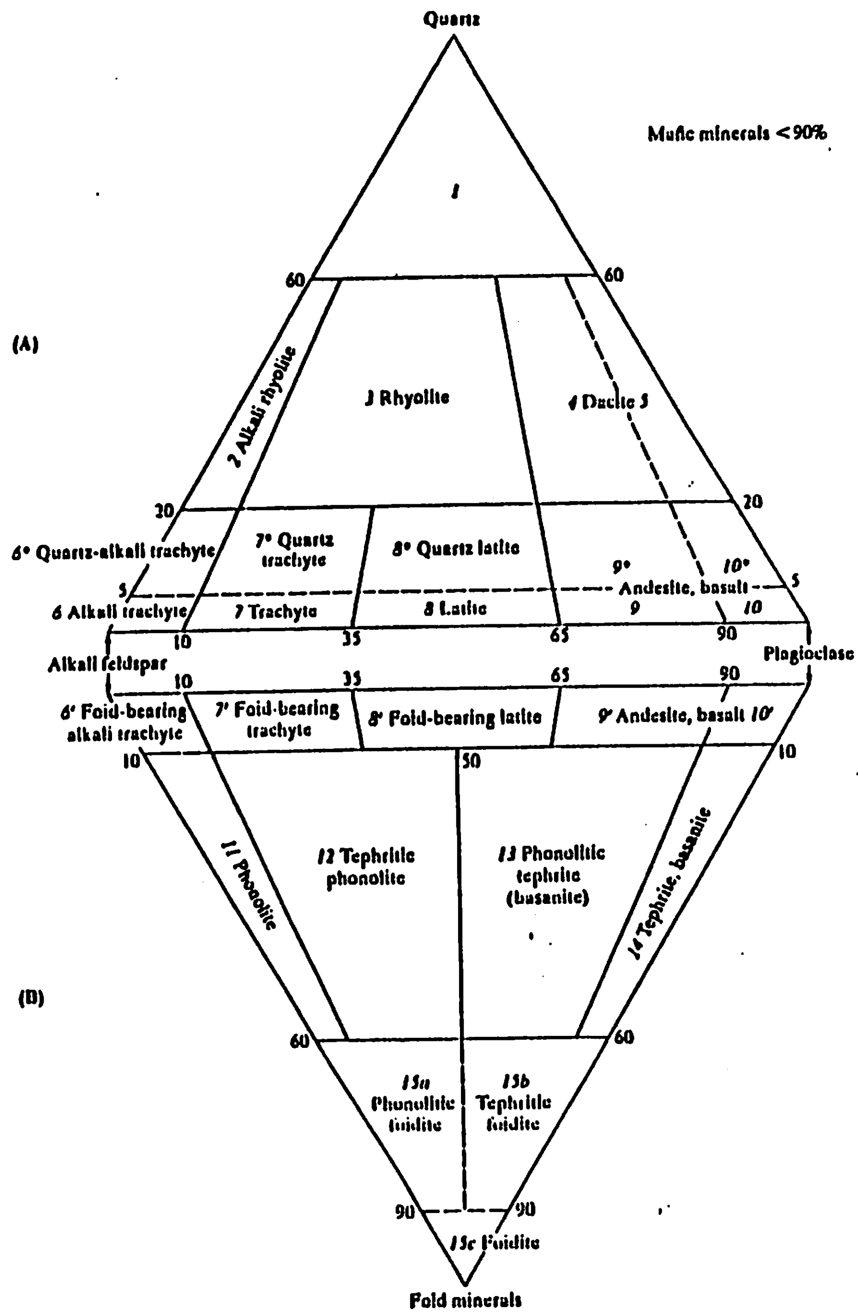

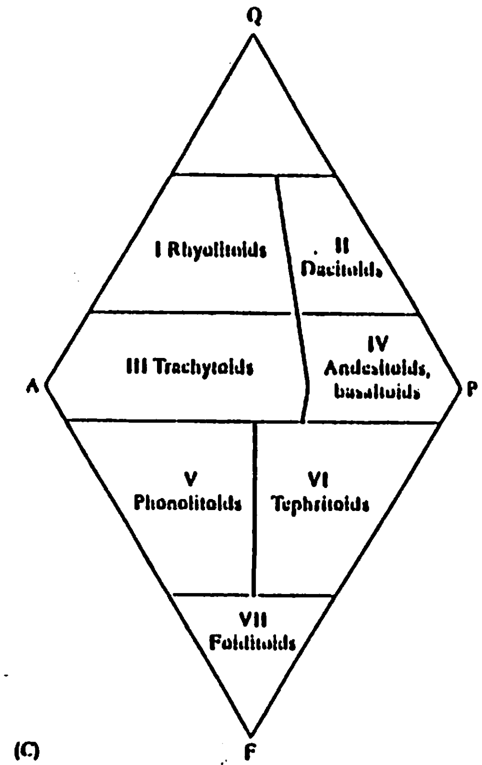

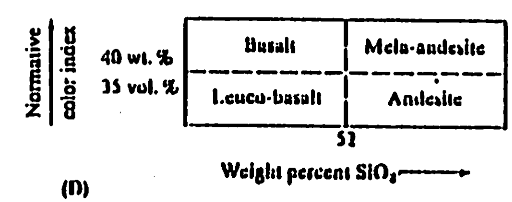

Figure 4–3
(A, B) The classification of volcanic igneous rocks. In order to be included within the triangles an igneous rock must be aphanitic. The rock must contain at least 10% plagioclase, alkali feldspar, and either quartz or feldspathoid (foid). The relative amounts of these three minerals are recalculated to 100% and plotted within the appropriate triangle, as shown in Figure 4–2. Appropriate modifying terms are used based upon mafic mineral composition or distinctive texture. In the case of those rocks whose matrix is too fine for determination, a tentative classification can be based upon minerals present in phenocrysts. (C) Generalized group names (for field use). (D) Distinction between basalt and andesite is based on color index (volume percentage of mafic minerals) and silica content. [From A. L. Streckeisen, 1979, *Geology*, 7, Figs. 1, 2; and A. Streckeisen, 1979, personal communication.]

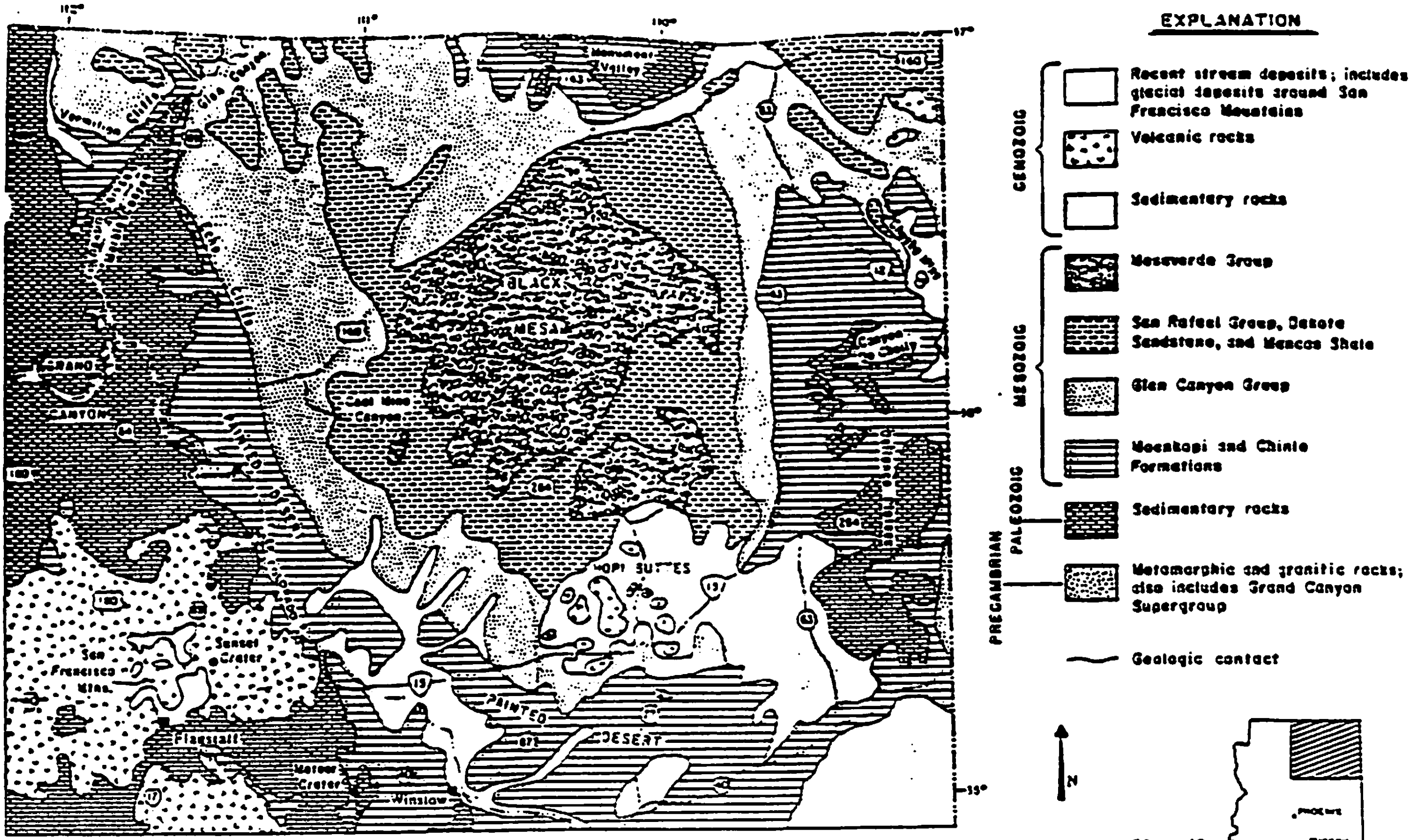

Generalized Geologic Map of Northeastern Arizona

Stratigraphic Position of Geologic Features

COMPOSITE STRATIGRAPHIC SECTION

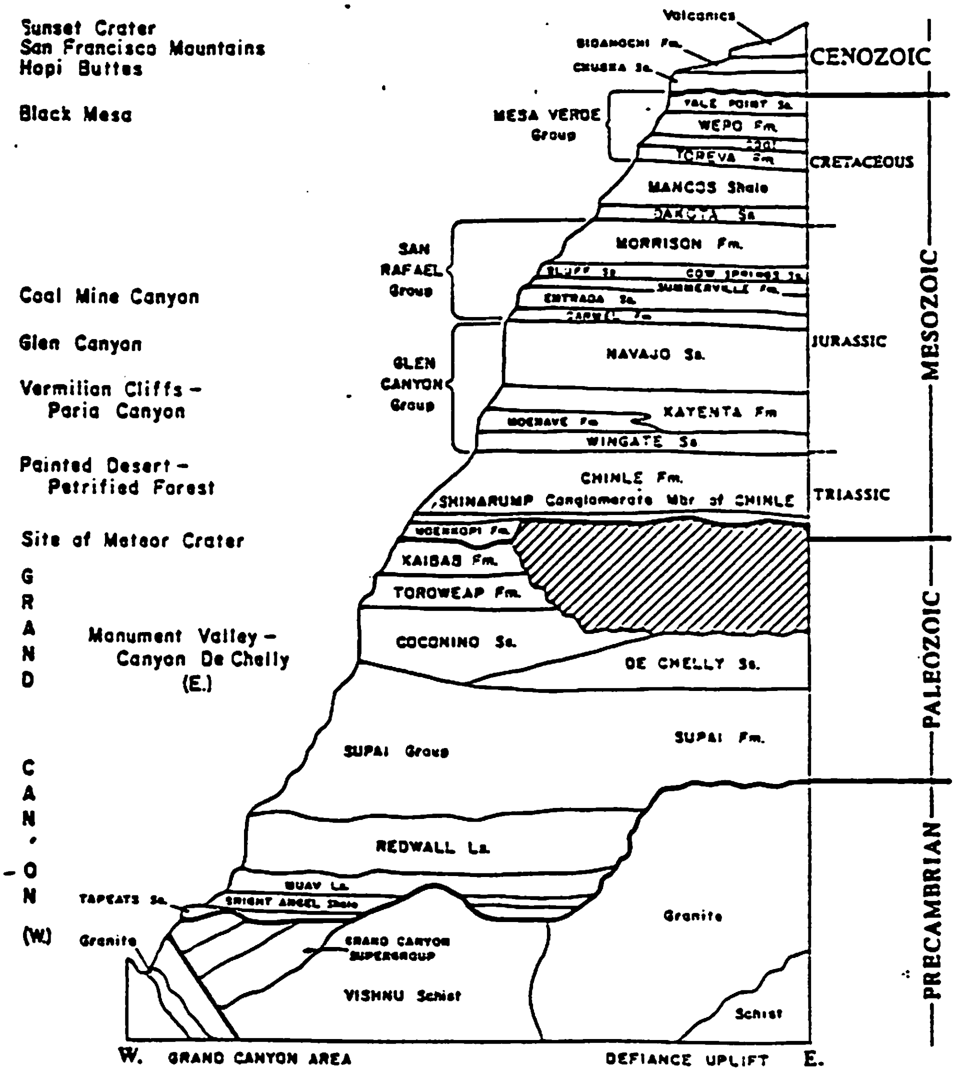

Geology of Northern Arizona

The G-rated Geology and Tectonics of the Tucson Basin Area

trilling!

I-10 TO PHX

SANTA CRUZ R. TO GILA, TO COLORADO

Tucson and surrounding area overview

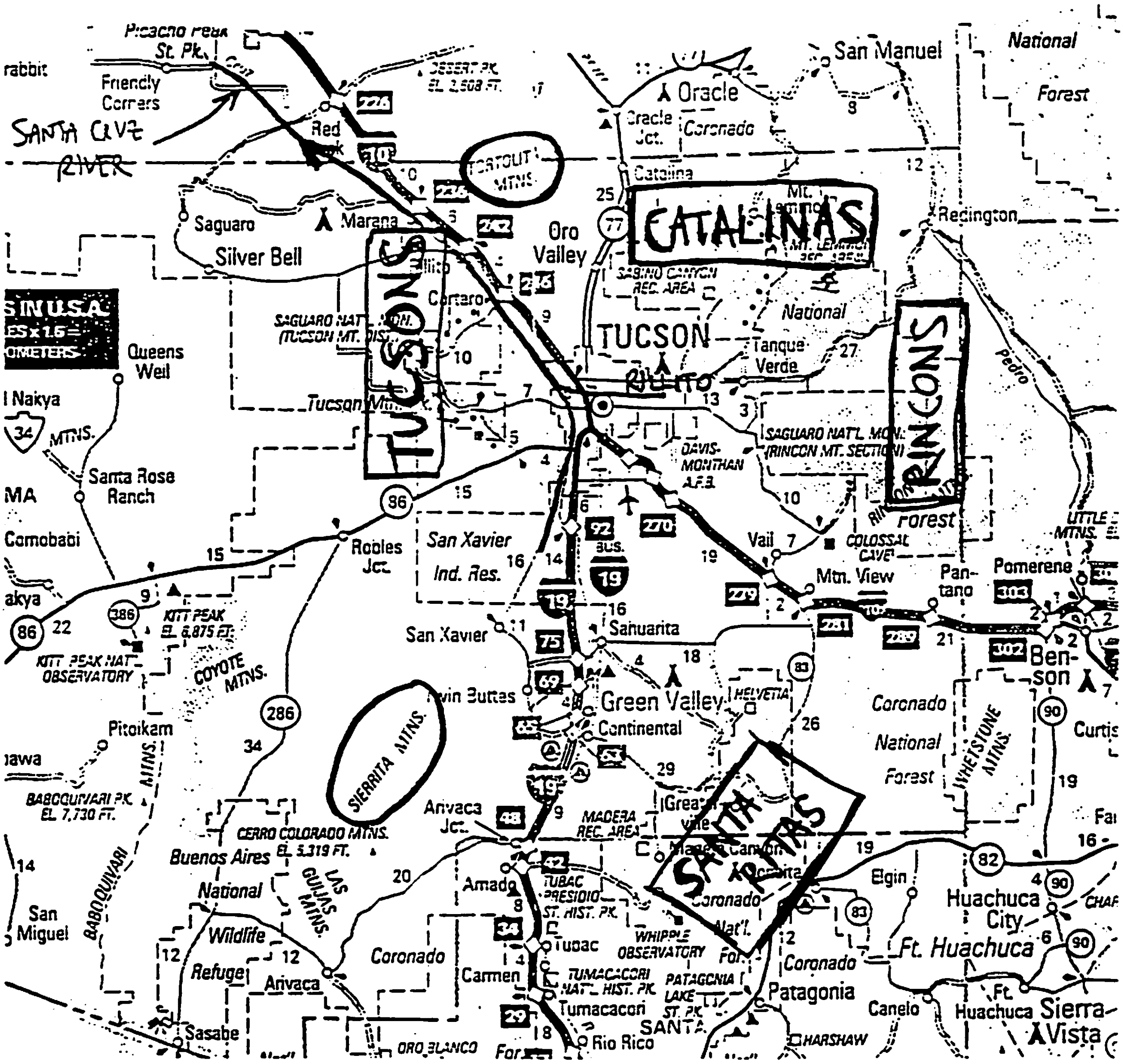

I-10 TO NM, T

I-19 TO NOGALES

Basin and Range overview (Dickinson 1991)

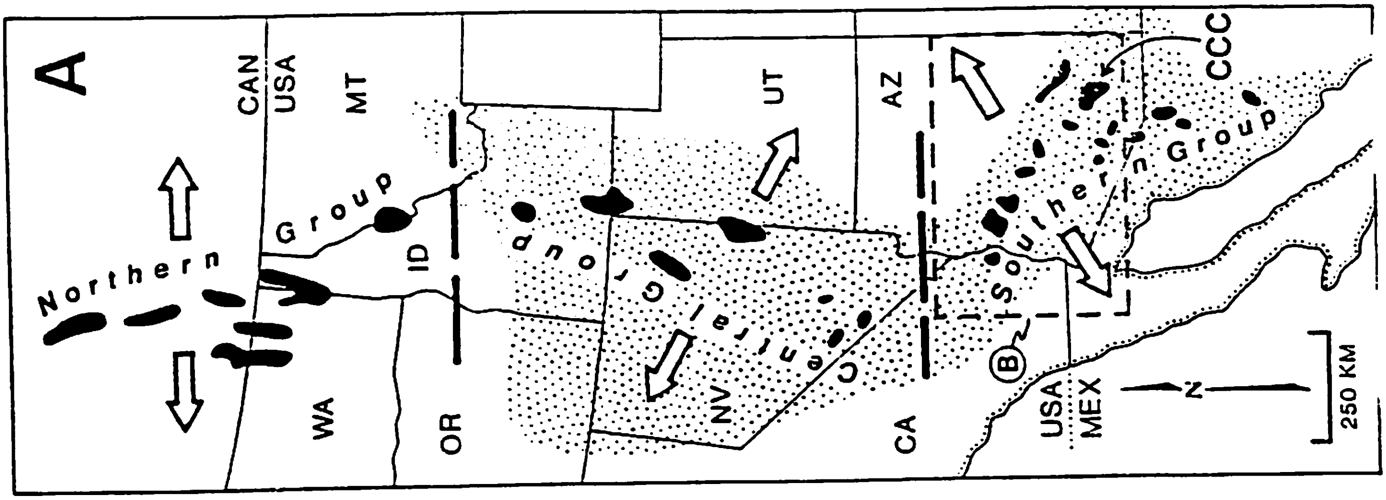

How a detachment fault works (Kring, unpublished)

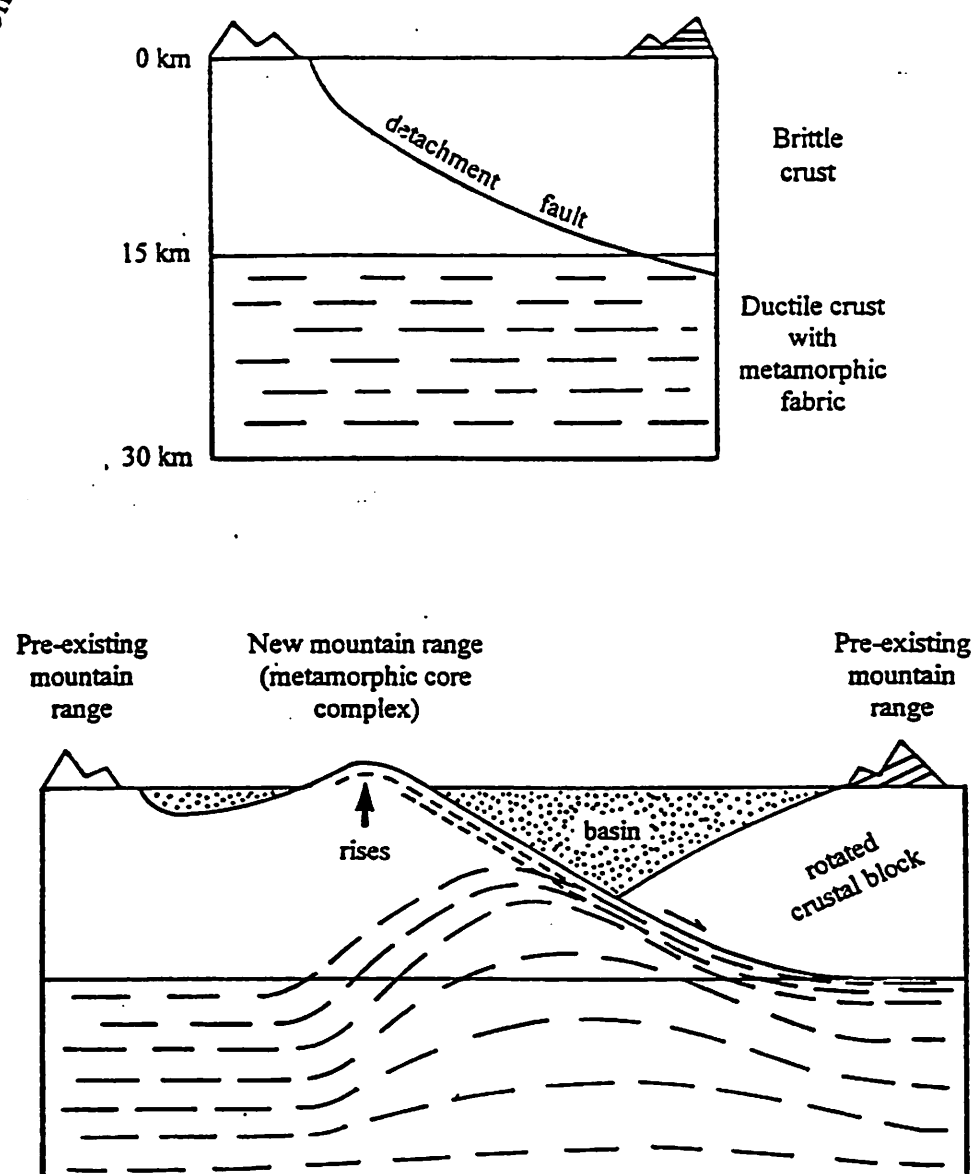

Tucson basin, unroofed metamorphic core complex, and the Tucson mountains (Dickinson 1991)

W. R. Dickinson

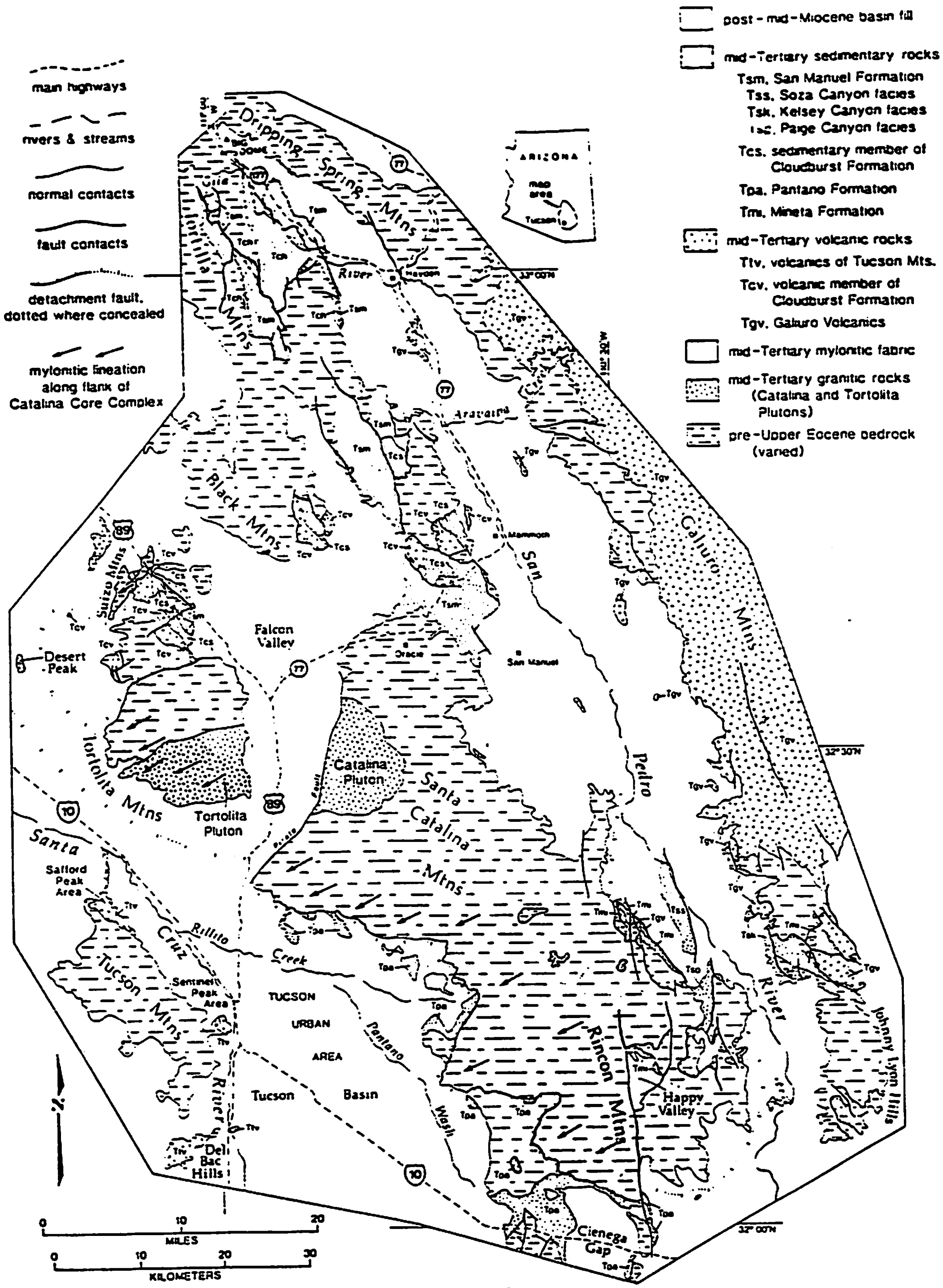

Figure 2. Geologic sketch map of Catalina core complex (mylonitic foliation and lineation along southwest flank) and San Pedro trough (traversed by San Pedro River and by Gila River below their confluence) showing areal distribution of tilted homoclines of mid-Tertiary volcanic and sedimentary successions in relation to exposures of older bedrock and younger basin fill; modified after Dickinson and Shafiqullah (1989).

Schematic result for the Tucson mountains (T[illegible]er)

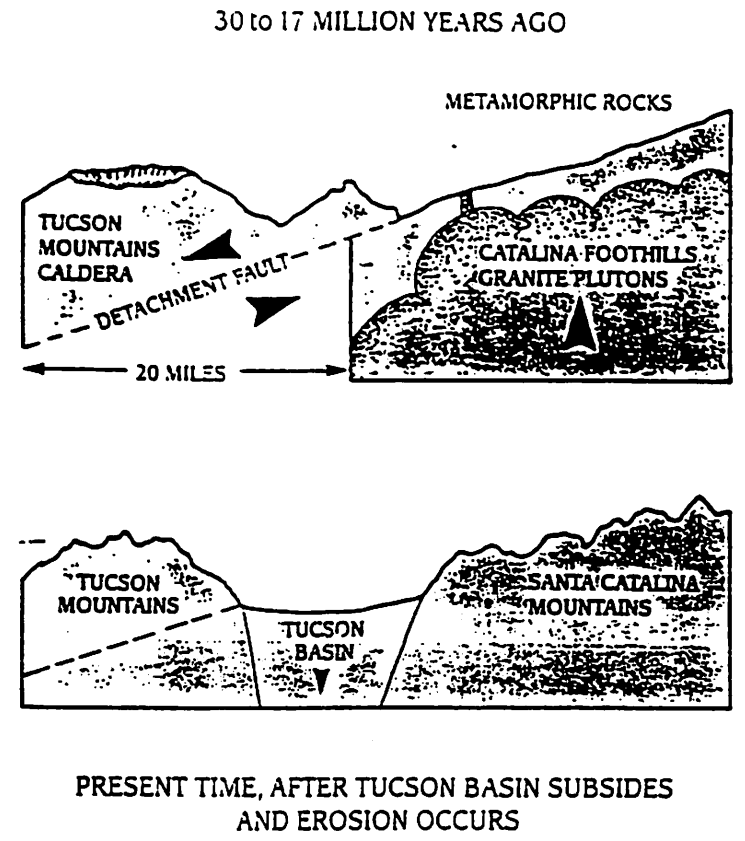

Santa Rita sequence:

Paleocene volcanics (Gringo Gulch Volcanics)
Cretaceous sandstones (Bisbee Group)
red beds
Triassic/Jurassic volcanics and sandstones
Paleozoic shallow marine sediments
pre-Cambrian schist and plutons

(after Drewes; Riggs and Haxel)

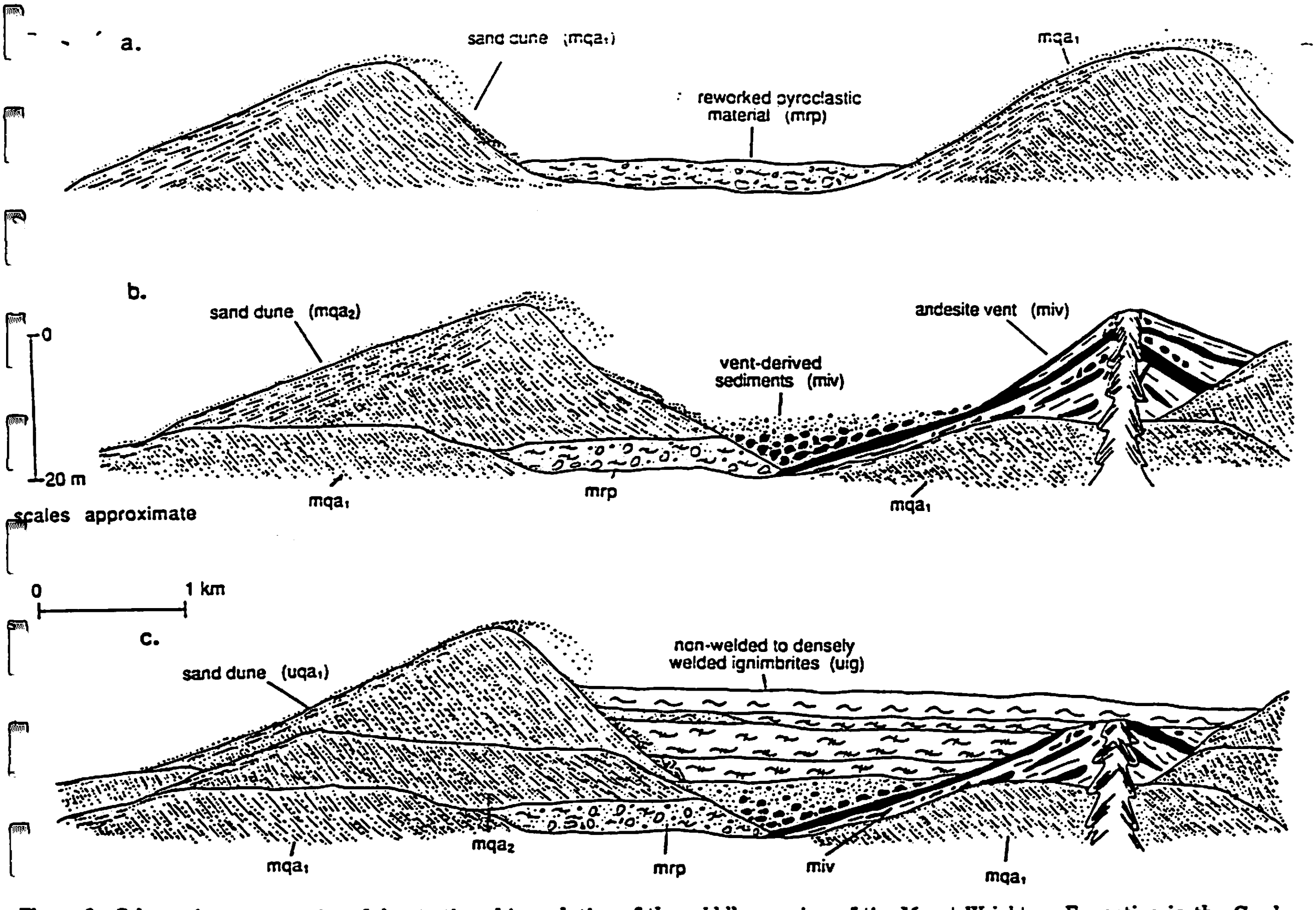

Figure 8. Schematic reconstruction of the stratigraphic evolution of the middle member of the Mount Wrightson Formation in the Gardner Canyon area, in cross-sectional view. Letter symbols refer to Figure 7 explanation, without 'J'. (a) Reworked pyroclastic debris is funnelled by ephemeral streams between sand dunes. (b) Following deposition of more eolian deposits, a valley is eroded into the eolian and reworked pyroclastic deposits; a small andesitic vent complex forms within the valley. (c) Ignimbrites fill the valley and partially cover the vent complex.

The mid-Jurassic Mount Wrightson Formation in the Santa Ritas (Riggs and Haxel 1990)

Stream Terraces of the Canada del Oro Valley and the Oracle Pediment

Windy Jaeger

Stream Terrace: *One of a series of level surfaces in a stream valley, flanking and more or less parallel to the stream channel. It is above the level of the stream, and represents the dissected remnants of an abandoned flood plain, stream bed, or valley floor produced during a former stage of erosion or deposition.*

How do stream terraces evolve?

1. The stream incises a path through a valley by the processes of downcutting and headward erosion.

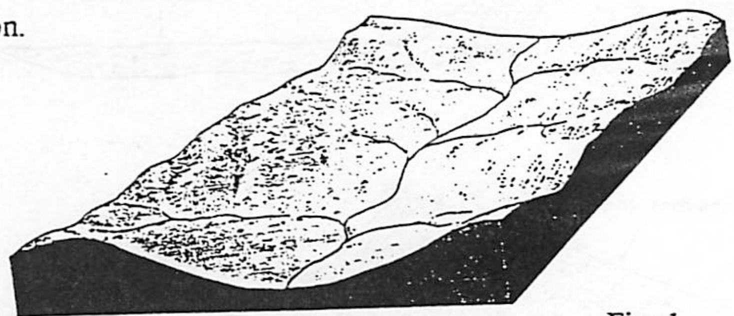

Fig. 1

2. Changes in climate, base level, or other factors that reduce flow energy cause the stream to partially fill its valley with a thick layer of sediment forming a broad, flat floor.

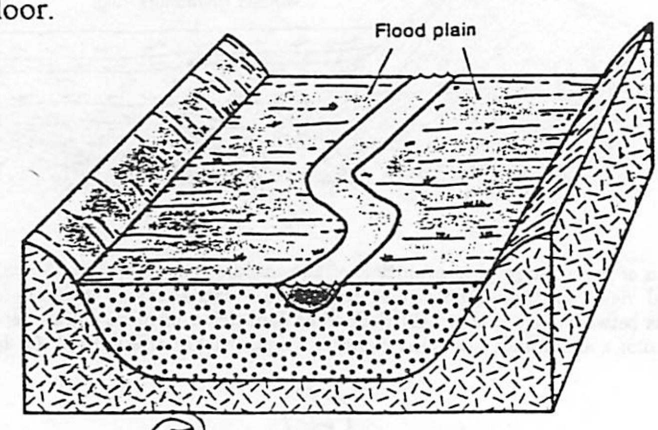

Fig. 2

3. An increase in flow energy causes the stream to erode through the previously deposited alluvium. A pair of terraces are left as remnants of the former floodplain.

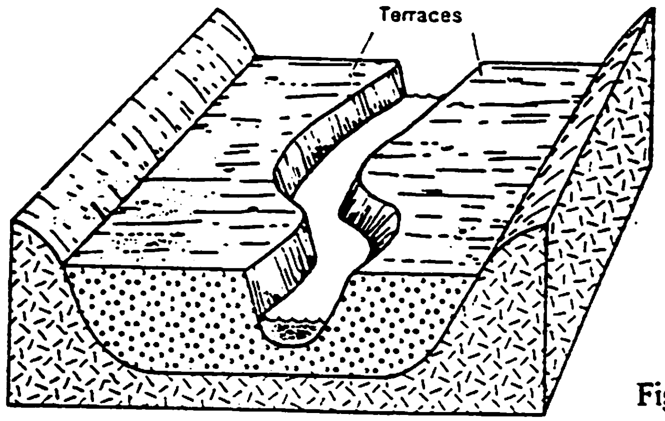

Fig. 3

4. The stream shifts laterally and forms lower terraces as subsequent changes cause it to erode through the older valley fill.

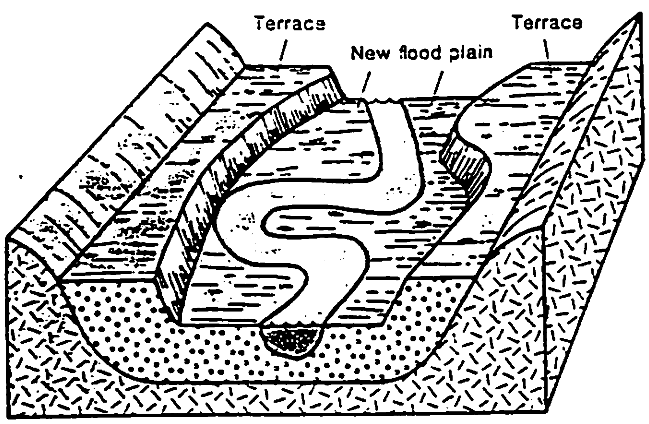

Fig. 4

Profile of Stream Terraces in the Rillito Wash

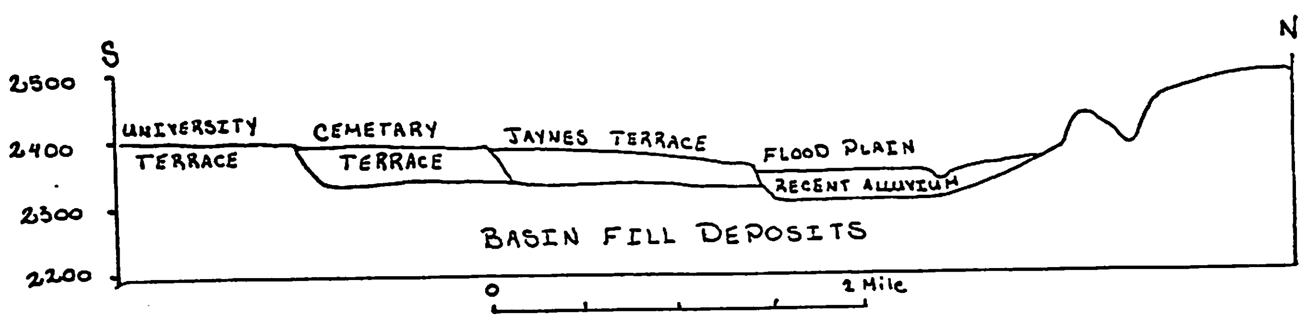

Fig. 5

Profile of Canada del Oro Stream Terraces

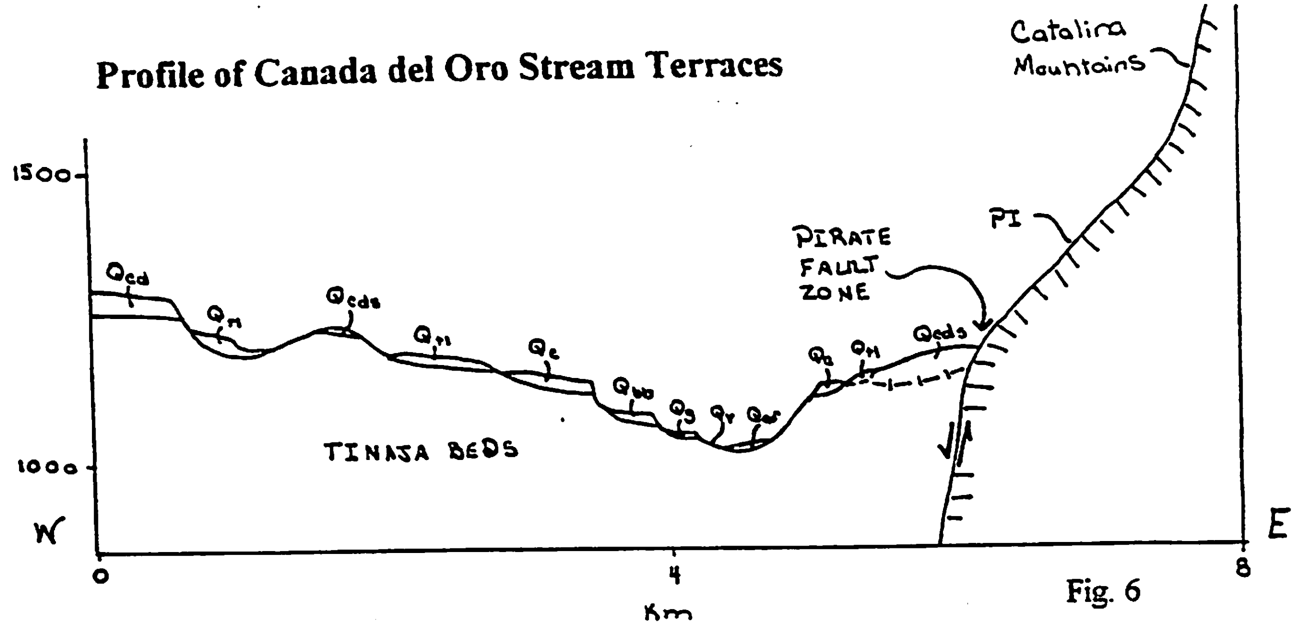

Fig. 6

Description of Canada del Oro Stratigraphy & Geomorphology

Symbol on X-sec.	Landform	Soil Color
PI	Pediment	Yellowish gray
Q_{cd} (Cordonnes Surface)	Alluvial fans	Reddish orange
Q_{cds}	Hillslopes of Q_{cd}	Gray-white
Q_{tl} (Twin Lakes Surface)	Terraces & associated alluvial fans	Reddish orange
Q_c (Catalina Terrace)	Terrace	Orange
Q_{bb} (Brave Bull Terrace)	Terrace	Reddish brown
Q_g (Golder Terrace)	Terrace	Brownish gray
Q_{af}	Active alluvial fans	Light brownish gray
Q_v	Active channels, floodplains	Ligh brownish gray

Pediment: *A broad, gently sloping erosional surface cut in bedrock at the base of an abrupt and receding mountain front. It is separated from the backing hillslope by a sharp change of gradient. The bedrock may be bare but is more often mantled with a thin, discontinuous veneer of alluvium derived from the upland masses and in transit across the surface. Pediments most commonly occur in semiarid or desert regions.*

Basic Model for Pediment Formation

1. Basin and Range style normal faulting produces maximum relief. (Playa lakes may develop in the central parts of the basins.)

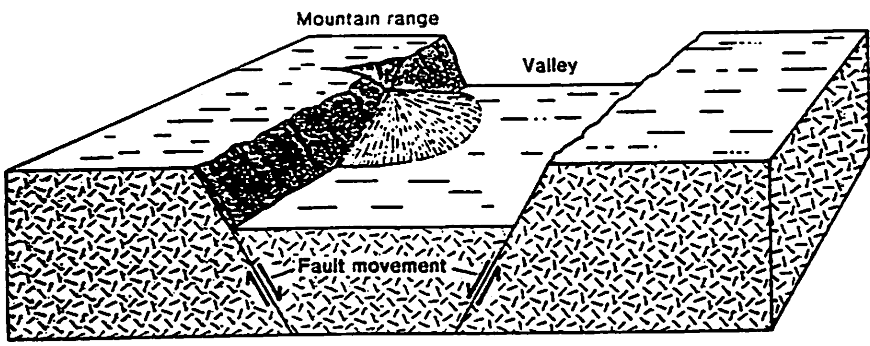

Fig. 7

2. As the mountain front retreats pediment develops and alluvial fans spread out into the valley.

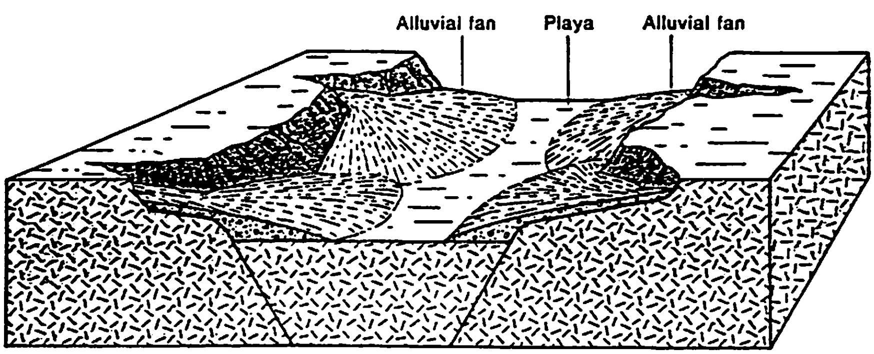

Fig. 8

3. The basins become filled with sediment. Erosion wears down the mountain ranges to small isolated remnants. The pediments expand and are buried by the alluvial fans. which merge to form bajadas.

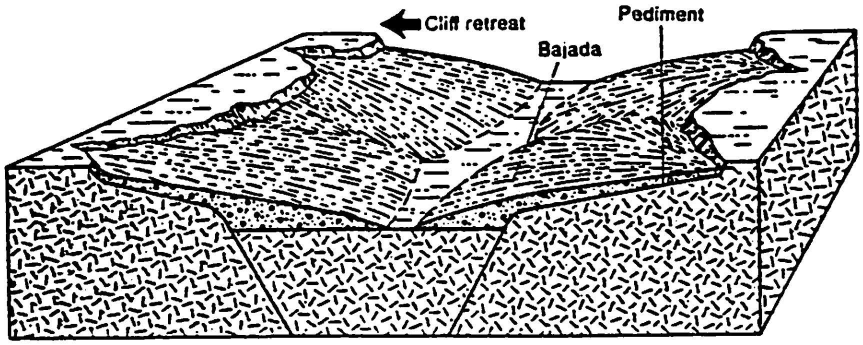

Fig. 9

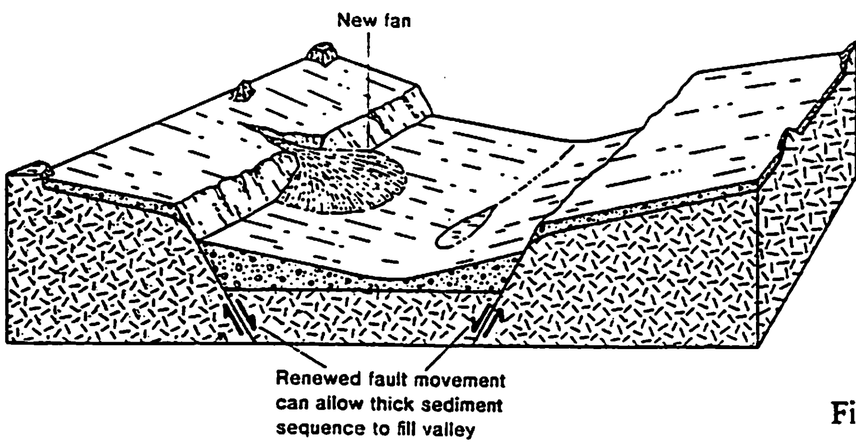

Fig. 10

Hypotheses of pediment formation and evolution

1a. Retreat of backing hillslope (see fig. 7-10)

1b. Retreat of backing hillslope combined with the erosional force of sheetfloods and rills

2. Lateral planation by shifting streams

3. Mantle-controlled planation (i.e. chemical weathering under the alluvium veneer)

References

Mabbutt, J. A., Desert Landforms, pp. 81-118, The MIT Press, Cambridge, Massachusetts, 1977.

McFadden, L.D. Soils of the Canada del Oro Valley, southern Arizona, The University of Arizona, M.S. Thesis, 1978.

McGeary, D. and Plummer, C. C. Physical Geology, Earth Revealed, pp. 375-377, 440-441, Wm. C. Brown Publishers, Dubuque, Iowa, 1994.

Geomorphic Surfaces in the Tucson Basin, Arizona, A Field Guidebook, compiled by L.L. Ely and V. R. Baker, The University of Arizona, 1985.

San Pedro River Valley:

Geology and Archeology of the Area

Terry Hurford

The San Pedro River Valley contains important clues to the lifeways of prehistoric man. This unique area provided the first links between man and now extinct animals in the southwest. Understanding the process of change in Southern Arizona sheds light on its history and geological background.

Present Climate:

Present climate of the San Pedro Valley is described as semi-arid and mesothermal. The area receives about 13 inches of rain a year, the majority of it falling during the rainy period between July and September. The yearly temperatures range between 44 ° F and 62° F. This still allows the San Pedro to be perennial, with minimal discharge in the dry season and many stretches of subsurface flow. There never exists a water surplus in the San Pedro during any season.

The San Pedro provides for three life zones; arid grasslands, encinal, and montane. The valley floor is characterized by the arid grassland. A plethora of grass species exist and are encroached upon by mesquite trees and other small shrubs. Relict islands of cottonwoods , willows and oak remain confined to the channel of the stream itself. The encinal zone on the hills along the valley are characterized by growth of oaks. Here too mesquites are quite common. Finally the montane area of pine and spruce rim the valley area.

Resent Climate:

Within the last century noticeable changes can be seen to have taken place in the San Pedro Valley. The current entrenchment of the stream began in 1883 and moved 125 miles in ten years. This entrenchment began at the mouth and moved headward as the arroyo eroded the river channel. The entrenchment excavated the stream. One example comes from Hereford, Az. where in 1910 a narrow channel of 3 feet in depth flowed. Prior to that in 1890 the stream was a series of grassy swells.

Before the 1800's accounts by Spanish explorers and Father Kino tell of a valley with a river running through it that could support native fish and beavers. These early Spanish settlers introduced cattle and horses to the valley, finding it a suitable place for grazing.

Prehistoric Climate:

At the end of the last ice age Southern Arizona had a much wetter, cooler climate. Since that time the area has been growing more arid. Now extinct animals like the Mammoth used to thrive in this area having migrated into the New World through a land bridge between Alaska and Asia. The water level used to be much higher too. Ancient prehistoric lakes and swamps have been identified in the San Pedro valley.

San Pedro Sediments and Artifacts:

The San Pedro is know for its rich archeological record. In 1952 at Naco and 1955 at Lehner ranch Mammoth remains were found with human spear points associated with them. These spear points showed that man was present and organized enough to hunt the large creatures around 10,000 yrs ago. The remains of the Mammoth were found after an arroyo had eroded into sediments that had been deposited since the kill. The kill itself was found in association with a prehistoric perennial stream. They were then covered by deposits of material identified as a swamp. This rich material was covered by gravels and river deposits. The lowering of the water table accelerated by livestock and human inhabitancy allowed the stream to erode quickly to the kill site.

The site itself is higher then other sediments from that time period 10,000 yrs. ago. Thermal upwelling in the San Pedro area has lifted the level of the site. This allowed the river to cut down to its level and recently expose the kill site.

CENOZOIC

STRATIGRAPHIC COLUMN
SAN PEDRO RIVER VALLEY
STUDY AREA

Formation Name	Yrs x 10^6	Description
Unnamed gravels	≤ 2	Pleistocene and Recent: river gravels and alluvial fan deposits (possibly the informal Tres Alamos Fm of Montgomery, 1963).
Quiburus Fm	4-7	Pliocene: fine-grained lacustrine deposits with some fluvial deposits in places overlain by unnamed Pleistocene gravels and alluvial fans. The main sedimentary unit exposed in the river valley in the area of study.
Galiuro volcanic	22-29	Oligocene and Miocene: rhyolite to andesite lava flows and ash flow tuffs.
"Teran" beds	≥ 27	Oligocene: fanglomerates, sandstone, shale and mudstone with a centrally situated andesite

Figure 3

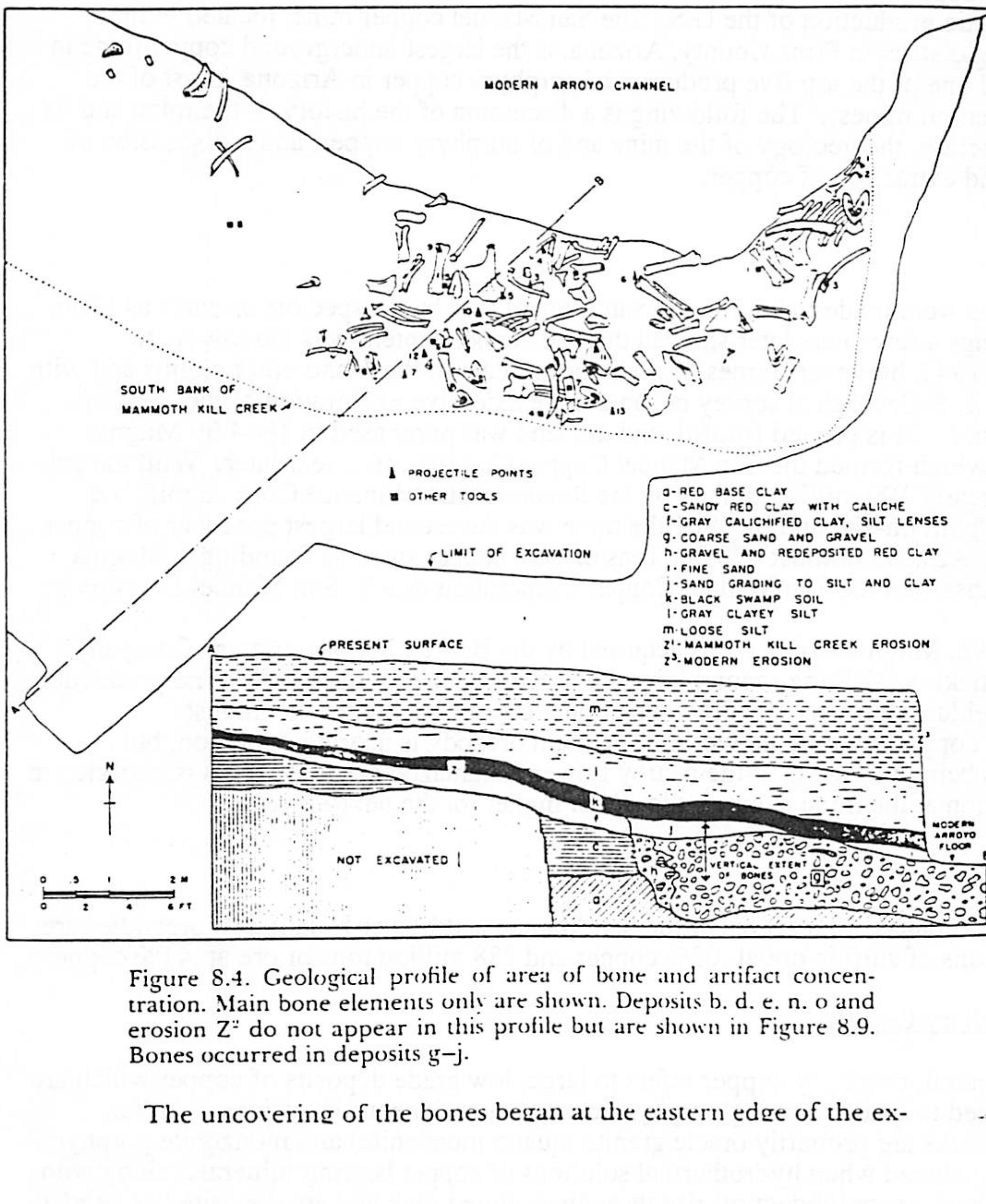

Figure 8.4. Geological profile of area of bone and artifact concentration. Main bone elements only are shown. Deposits b, d, e, n, o and erosion Z^2 do not appear in this profile but are shown in Figure 8.9. Bones occurred in deposits g–j.

The uncovering of the bones began at the eastern edge of the ex-

By the time th
ments of eight m
Bones of bison, r
three teeth and v
of the bone bed.
between two ribs
jectile points, eig
and eight miscella
sent refuse from
the projectile poi
of charcoal becam
upstream end or
for radiocarbon d
only after the sec
ruary, 1956.

The San Manuel Copper Mine and Porphyry Copper

by Dave O'Brien

Introduction

Porphyry copper is by far the most common type of copper deposit in Arizona, and production of copper from these deposits in Arizona accounts for well over half of the current domestic production of the U.S. The San Manuel copper mine, located in the Oracle mining district in Pima County, Arizona, is the largest underground copper mine in the world and one of the top five producers of porphyry copper in Arizona (most of the others are open pit mines). The following is a discussion of the history of the mine and its current production, the geology of the mine and of porphyry copper, and a discussion of the mining and extraction of copper.

History

Claims were made to land in the San Manuel area by prospectors as early as 1906, but test drillings a few years later showed that the copper content was too low to be feasible. By 1942, however, James M. Douglas purchased these and other claims and with the aid of the U.S Geological survey began a more extensive exploration of the area for copper deposits. This proved fruitful, and the land was purchased in 1944 by Magma Copper Co., which formed the San Manuel Copper Corporation a year later. With the aid of a loan of nearly 100 million dollars by the Reconstruction Finance Corp., a mill and smelter were built on-site and by 1961 the mine was the second largest producer of copper in the state of Arizona (almost 470,000 tons of pure copper since its founding). Magma Copper Co. absorbed the San Manuel Copper Corporation into its San Manuel Division in 1962.

In 1996, Magma Copper was acquired by the Broken Hill Proprietary Company Ltd.(BHP), making BHP the second largest copper producer in the world. The production at San Manuel last year was 107,000 tons of pure copper, making it the largest underground copper mine in the world. The main orebody is nearing depletion, but production is being phased in at the nearby Lower Kalamazoo orebody. This is expected to keep production at the mine at current levels or higher for the next 12 years.

Reserves

The estimated ore reserves of the San Manuel and Lower Kalamazoo orebodies are 222 million tons of sulfide ore at .63% copper and 288 million tons of ore at .41% copper.

What is Porphyry Copper

In general, porphyry copper refers to large, low grade deposits of copper which are spatially related to quartz-bearing porphyritic or granular igneous intrusions. At San Manuel, the rocks are primarily oracle granite (quartz monzonite) and monzonite porphyry. Copper is introduced when hydrothermal solutions of copper bearing minerals (along with other metals such as molybdenum) rise through shattered rock and are deposited as veinlets and disseminated grains in the rock. The primary copper ores present in the rock are chalcocite and chalcopyrite (sulfides) and cuprite (an oxide).

Geology of the Region

A map of the rock types in the area and their ages is attattached at the end--please refer to that (1). The oldest rock in the area is the quartz monzonite, which dates to pre-cambrian times. This rock is covered in some areas by alluvial slope deposits and conglomerate, and intruded in other areas by monzonite porphyry. Several faults pass through the area, as shown on the map. Many smaller faults have weakened and shattered the rock, making it easier for hydrothermal solutions to intrude and also making block caving the easiest method of ore removal (see below).

A multilayer map of the ore deposit is attatched at the end (2)

Due to the block caving method of mining the ore (explained below), the ground above the main caves has subsided to a fairly large degree--an effect easily visible from the surface. Please refer to the attatched set of handouts (3) describing the process of subsidence at the mine.

Mining and Extraction of Copper

Copper ore is mined by a process called block caving. Basically, this involves making a tunnel below part of the ore and drilling fingers up into it, allowing it to fall down and be removed. Due to the loose and fractured character of much of the ore, this is the quickest process for removal, removing a large amount of ore in a relatively small time. A side effect of this procedure is subsidence of the overlying ground, as mentioned above.

Once the ore is hauled out, it is taken to a plant where the copper is extracted and purified. Consult the attached handout (4) for a description of the refining process.

References

Schwartz, George M., Geology of the San Manuel Copper Deposit, Arizona, Geological Survey Professional Paper #256, United States Government Printing Office, Washington D.C., 1953

Arizona Bureau of Mines, Mineral and Water Resources of Arizona, Bulletin 180, 1969

Hatheway, Allen W., Engineering Geology of Subsidence at San Manuel Mine, Pima County, Arizona, 1966

AZ Dept. of Mineral Resources, History of Mining in Arizona, 1963

http://www.azma.com (Arizona Mining Association Homepage)

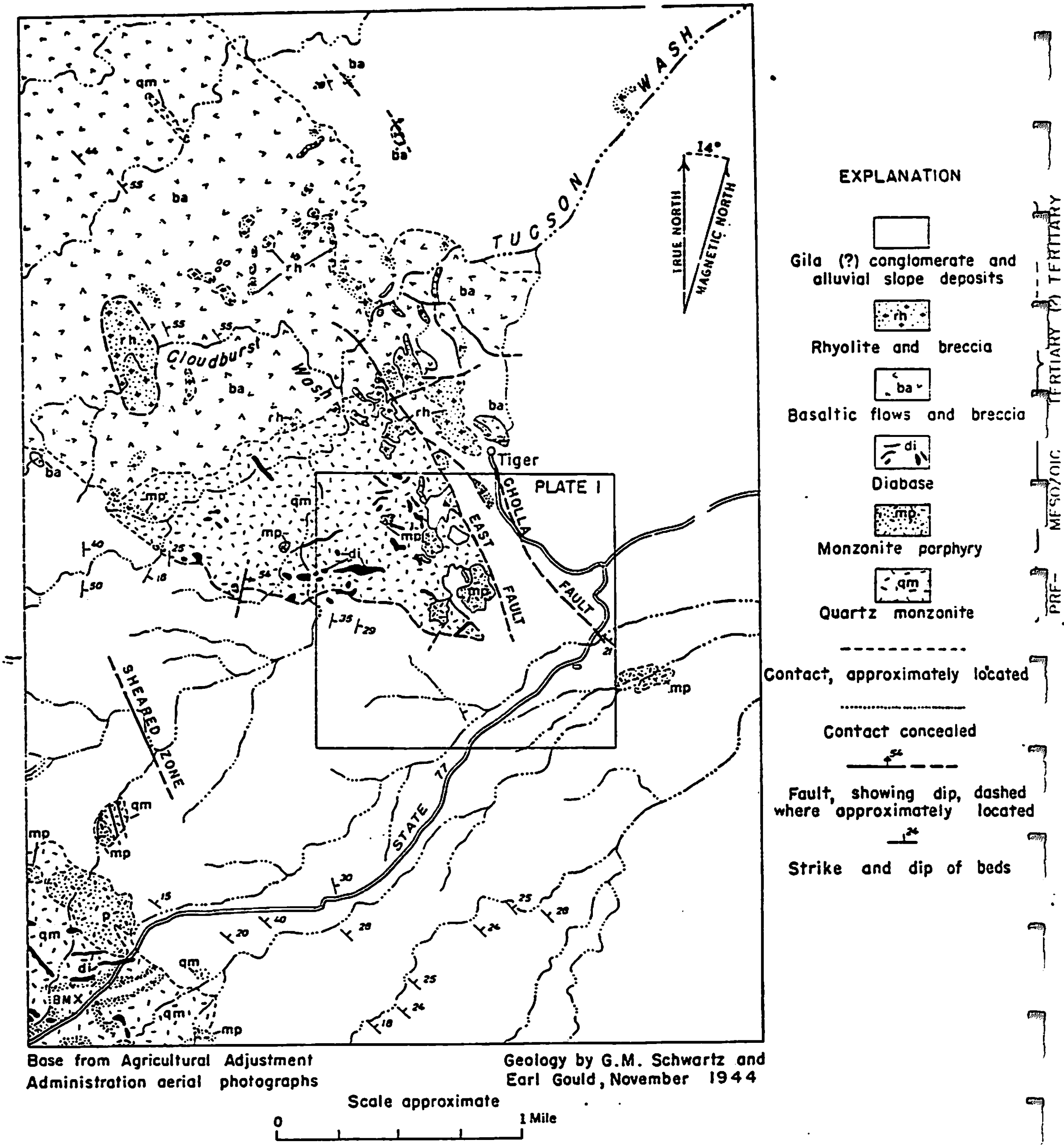

FIGURE 3.—Geologic map of area around San Manuel and Tiger, Ariz.

Handout 1

(17)

from Geology of The San Manuel Copper Deposit, Arizona

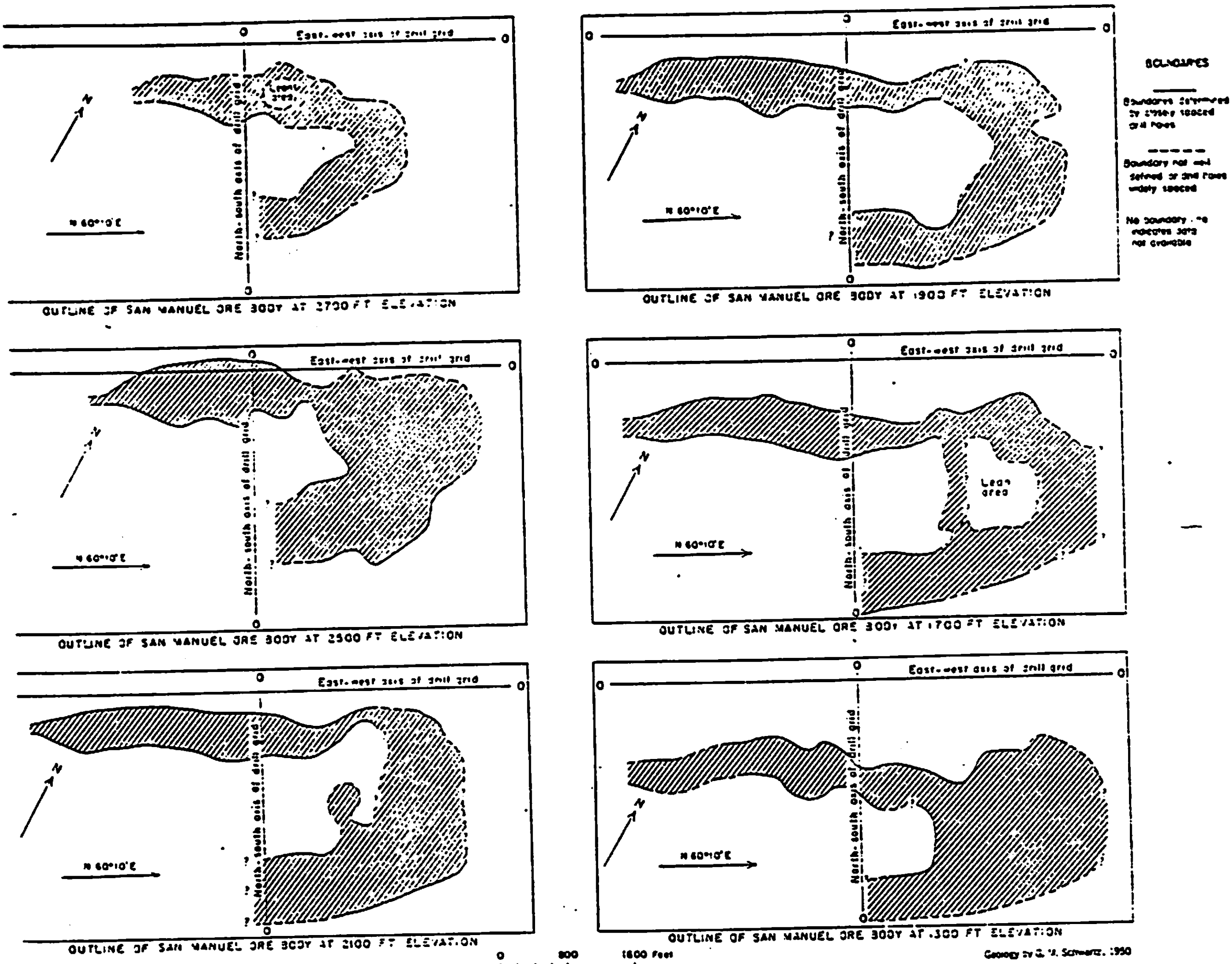

FIGURE 5.—Diagram showing outline of the San Manuel ore body at six altitudes.

Handout 2

from Geology of the San Manuel Copper Deposit, Arizona

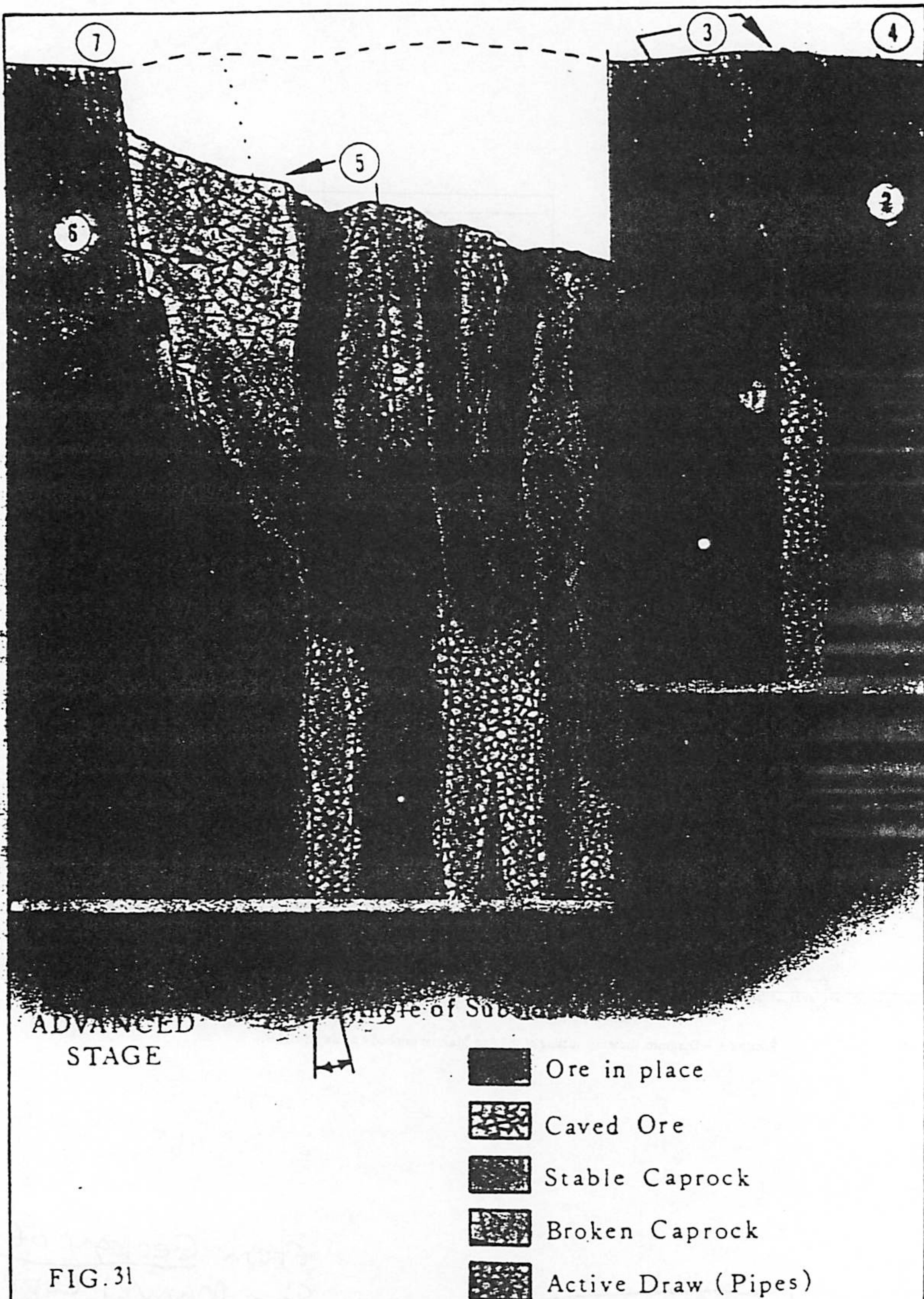

FIG. 31

Mechanics of Subsidence

(19) Handout 3

from Engineering Geology of Subsidence at San Manuel ...

Summary of the subsidence process

A chronological summary can be developed for the subsidence process at the San Manuel Mine. The steps are keyed to the two hypothetical cross sections found in figure 31:

1. Static loading begins with the removal of ore and disturbance of the material supporting the overlying caprock. Upward, near-vertical caving occurs mainly along stopes in the form of pipes.

   Voids formed by the pipes occur directly over the areas of draw with little or no lateral deviation at the surface. Pipes have always occured within the boundaries of the caved area. These features form in the granitic rocks largely by tension, induced by lithostatic pressure, and in the conglomerate by both tension and by parting and spalling along bedding planes.

   Spalling and uneven breakage of the granitic rocks occurs at the free faces bordering the pipes in response to relief of residual and active stresses in the immediate vicinity.

2. A pipe is shown extending to the interface between granitic rocks and the conglomerate at the plane of the San Manuel fault. A small amount of lateral breakage occurs, followed by readjustment and continued vertical expansion of the pipe into the conglomerate.

3. As a pipe reaches the surface, downward pressure begins as masses of conglomerate begin to weaken and break or separate along fractures and faults within the mass. Breakage is the result of tangential stresses surrounding the surface of the pipe. Because altered rocks are weakest under shear stress, the pipes are probably enlarged laterally by this type of failure.

4. Tension fractures open along planes of weakness in a downward direction from the surface. Initially the fractures do not transect the entire thickness of the caprock. Tensile breaks occuring in the sound ground have a characteristic break of 85° to 90° as measured from the horizontal. Tensile stresses are predominant, and if contemporaneous compressional stresses do exist, they would appear only at the lower edge of the mass of intact conglomerate. This condition is analogous to the flexural stresses developed through loading of a cantilevered beam.

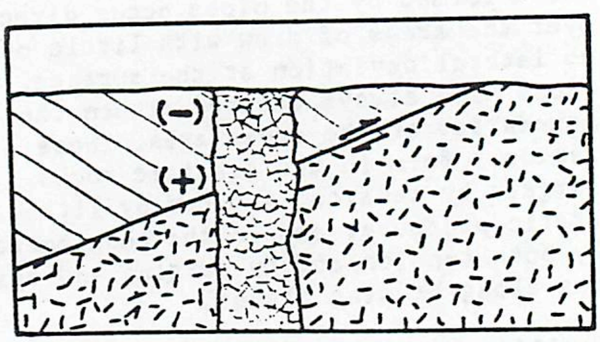

Figure 30. Occurrence of tensional (-) and compressional (+) stresses.

5. Displacement of independent masses of conglomerate increases as a pit develops at the surface. This forces an increased area of breakage along the walls of the pipes (stopes). There is some breakage of rock along the throats of the pipes due to stress relief at the free face of the pipe boundary.

Increased widening and coalescence of pipes occurs with contemporaneous weakening of the caprock. The pipes are probably eventually filled in thier upper reaches by conglomerate. There will be some filling in at lower levels by lateral movement of broken porphyry. An uneven blanket of broken conglomerate is formed over the entire caved area.

6. A lateral component of movement is introduced. This is produced by the shifting of broken conglomerate toward the center of the pit as sufficient amounts of rock are removed through the pipes. Conglomerate is crushed on its way to the pipes, and the material is further reduced in size by the action of weathering. Continued breakage of the caprock into unsupported and unattatched masses results in further rupture of prophyry at depth, through shear. Boundaries of the pits expand in this manner.

7. Faults occasionally limit the lateral growth of the pits by releasing large masses of caprock. Eventually, incipient tension fractures develop into escarpments as failure occurs along the faces of existing escarpments.

From Prospect to Production

Site Map

Discovering the copper ore embedded in the earth and rocks of Arizona is no easy task. It takes a team of highly trained geologists, geochemists and geophysicists, along with sophisticated testing methods and instrumentation to locate this hidden treasure.

Once deposits are found, mining companies must blast and dig their way to the source. Working in Arizona's approximately 12 operating copper mines, both open-pit and underground, miners then carefully separate the ore from the waste material. Huge trucks move up to 240-tons of ore, which is dumped into crushers and broken into pieces ranging from the size of a walnut to that of a softball.

It is important to differentiate between sulfide ore and leachable ore. Generally speaking, sulfide ore is composed of minerals containing copper, iron and sulfur, hence the name sulfide. Leachable ore is composed primarily of minerals containing copper oxide.

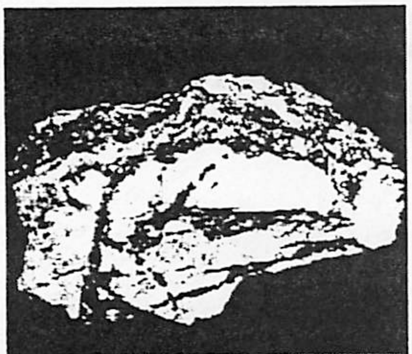

CHALCOCITE
(Sulfide Ore)

Sulfide Ore - A Grinding Process

The next step after crushing for sulfide ore is grinding. The process involves running crushed ore through large, rotating, cylindrical machines called mills until it becomes a fine powder similar to flour or talcum powder. This powder is mixed with water and chemicals to create a slurry that is piped into flotation tanks. Here, particles of copper called copper concentrate, with a copper content of 25 to 30 percent, float up and over the edge of the tanks, while the waste material, tailings, sinks to the bottom for easy removal.

The copper concentrate is then smelted for the purpose of separating the elements - copper, iron and sulfur. The iron is removed from the furnace as slag, the sulfur in the form of sulfur dioxide is processed into sulfuric acid. The copper leaves the smelter in anode form - 99 percent pure. Anode copper is further processed through an electrolytic refinery where impurities are removed, upgrading the purity to 99.9 percent.

Oxide Ores - A Smart Solution

from www.Azma.c r

 Handout 4

Oxide Ores - A Smart Solution

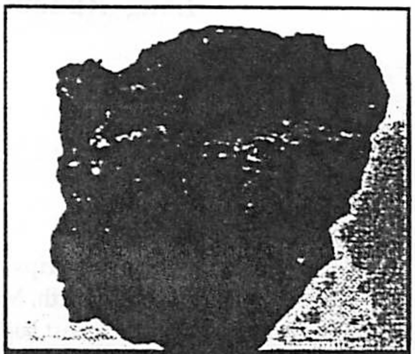
CHRYSOCOLLA
(Oxide Ore)

Extracting copper from oxide ores typically involves spraying the crushed ore with a sulfuric acid solution to dissolve the copper. In *heap leaching,* large piles of oxide ore are placed on impermeable pads and are sprayed with leach solution by a sprinkler system. The leach solution percolates down through the heap over time, picking up copper as it travels along. A central drainage system collects the run-off at the bottom of the heap.

The method used for recovering copper from the leach solution collected at the bottom of the leach heap is the SX/EW or *solvent extraction electrowinning* process. The solvent extraction (SX) part of the process includes a process of ion exchange between two solutions. During the ion exchange, a lighter organic solution floats on top of the heavier leach solution, much like oil floats on water. The copper atoms in the leach solution are extracted by the organic solution in a chemical exchange in which atoms go where they have the greatest chemical affinity. Once the leach solution is "emptied" of copper atoms, it is recycled back to the heaps for further leaching. The copper exchange is reversed in another tank that strips the copper from the organic solution and has a copper concentration approaching eight percent.

The eight percent solution is then pumped into tanks containing an electrolytic bath. Here, copper is attracted out of the solution to cathode starter sheets by applied electric current. This refining process is known as the electrowinning (EW) portion of the SX/EW process. Cathodes are the end of this process, producing a 99.9% pure product with no smelting.

Long Runout Landslides in the Solar System

conducted by
Jim Head

Introduction

In the fine tradition of LPL field trips we will examine in detail the El Capitan long runout landslide, review other large landslides on earth, Mars, and Luna, and discuss several emplacement mechanisms. The El Capitan long runout is the closest such avalanche to LPL, however we have made previous excursions to large landslides in southern California and near the borders of Yellowstone National Park. One of the largest terrestrial landslides is the Siadmurreh in Iran, which I propose Mike should send us to next year.

The El Capitan Landslide

The El Capitan landslide is located in southeastern Arizona between Winkelman and Globe near State Route 77 (Figure 1). The source of this slide is the south side of El Capitan mountain, approximately 1.8-3 km north of and 1500m above its proximal end. The distal end lies 3.8 km southward and 300m below. The slope on which it slid is 6-8 degrees near the proximal end but only 1-2 degrees in its lower half. The slide came to an abrupt halt, plowing into underlying lake sediments, compressing them into folds and sandstone dikes. The slide event probably dates to the Pleistocene.

The slide block consists of Escabrosa megabreccia underlain intermittently by lower Martin megabreccia. The slide block now is 3.8 km long with of width of zero at the proximal end increasing to 1.5 km at the distal end. Exposures in many areas resemble outcrops of the Martin and Escabrosa Formations. Note that stratigraphy is preserved. The lower Martin Formation is more thoroughly shattered than the Escabrosa--a general upward coarsening. Clastic dikes are present. The beds thinned considerably during the slide from 120 m in the source region to 5 m (locally 35 m) thick. Reconstructing the event, it appears the total volume of the El Capitan landslide was 40 million cubic meters.

Long Runout Landslides

Table 1 reports data from long runout landslides in the solar system. Included for comparison is the great pyramid at Giza. The peculiarity of long runout landslides is that they travel horizontally much farther than they should if they behave like ordinary, small avalanches. Typically, landslides runout a distance 1-2 times the vertical drop. It is as if the large landslides have a low coefficient of friction. This oddity is shown in Figure 2, which shows a relationship between volume of the slide and a depressed effective friction coefficient.

Table 1

Slide	Volume (10^6 m^3)	Drop (m)	Runout (km)	Minimum Velocity (km/hr)
El Capitan	40	1200	6.8	?
Blackhawk	283	1300	9	120
Siadmurreh	20,400	1000	15.6	335
Sherman	-	-	5	185
Valles Marineris	10^5	-	60	?
Tsilokovsky	10^6	-	80	?
Pyramid at Giza	0.4	100	100	10^{-8}

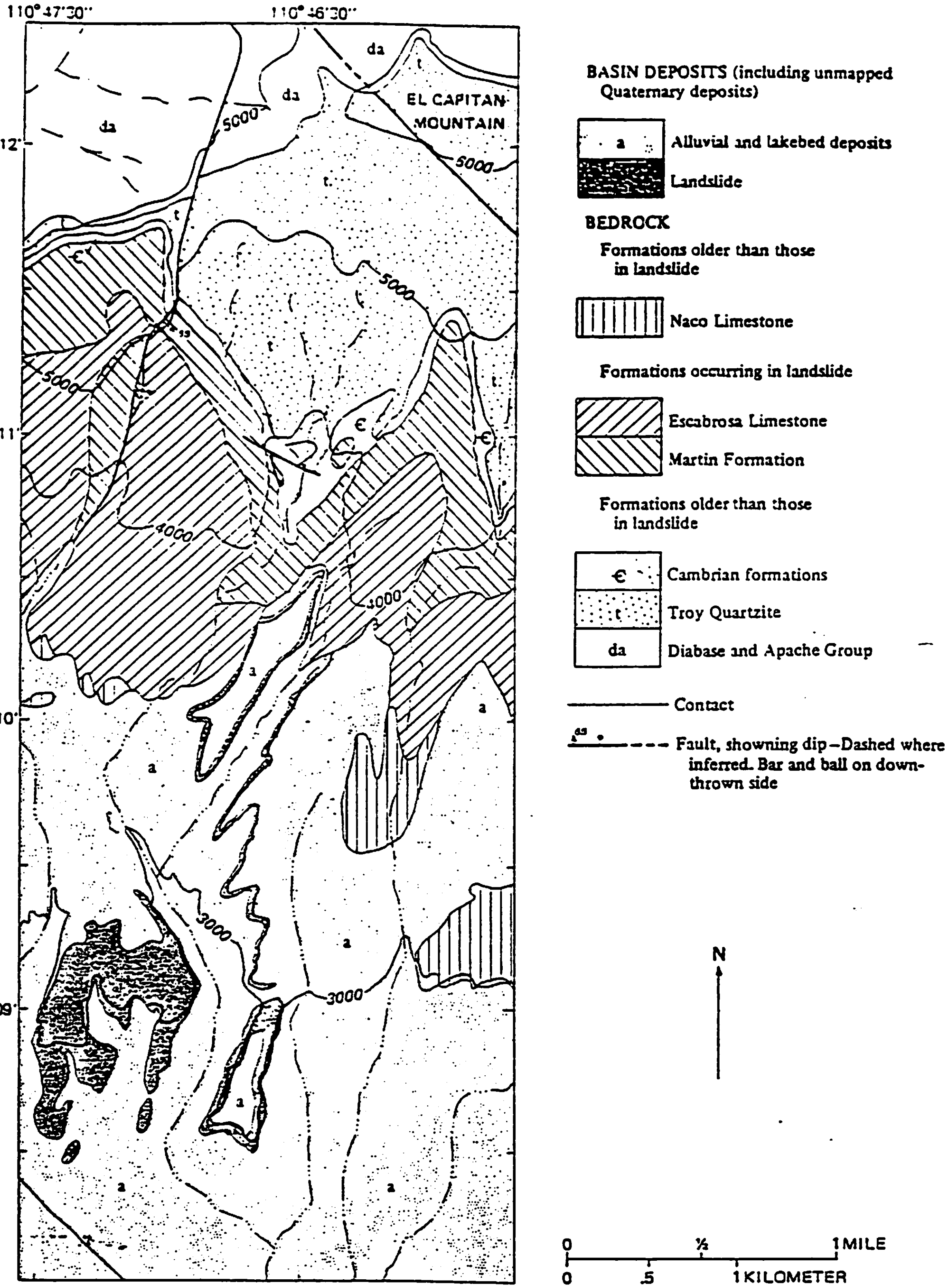

Figure —El Capitan landslide and its source area on El Capitan Mountain. Reduced from geologic map of El Capitan Mountain quadrangle (Cornwall and Krieger, 1977).

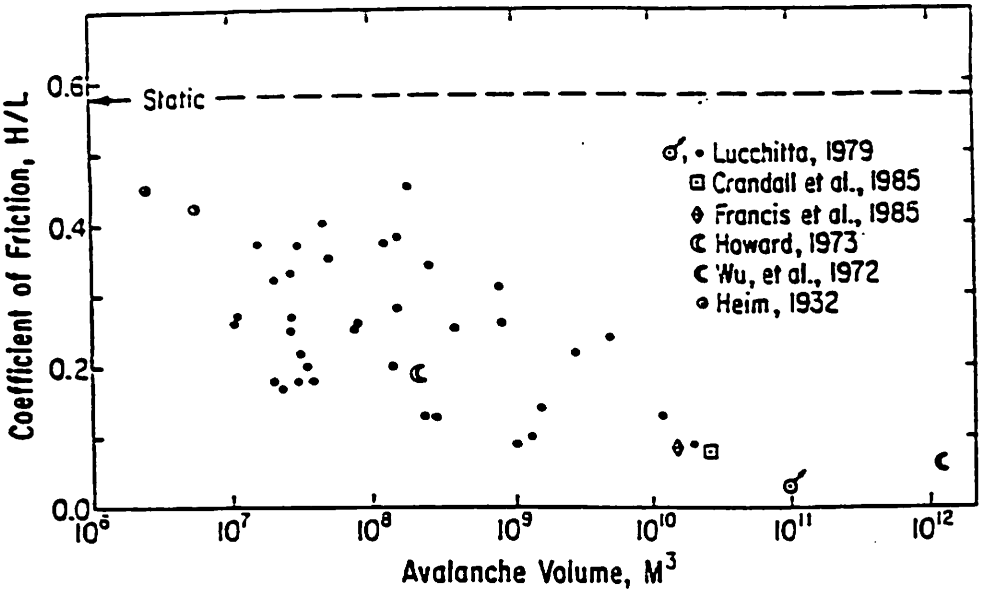

Figure 2. Coefficient of friction, H/L, plotted versus avalanche volume for many terrestrial rock avalanches, Martian avalanche (Fig. 1, center), and two lunar rockslides. Extraterrestrial points fit easily within scatter of terrestrial data, indicating probable similarity of mechanism.

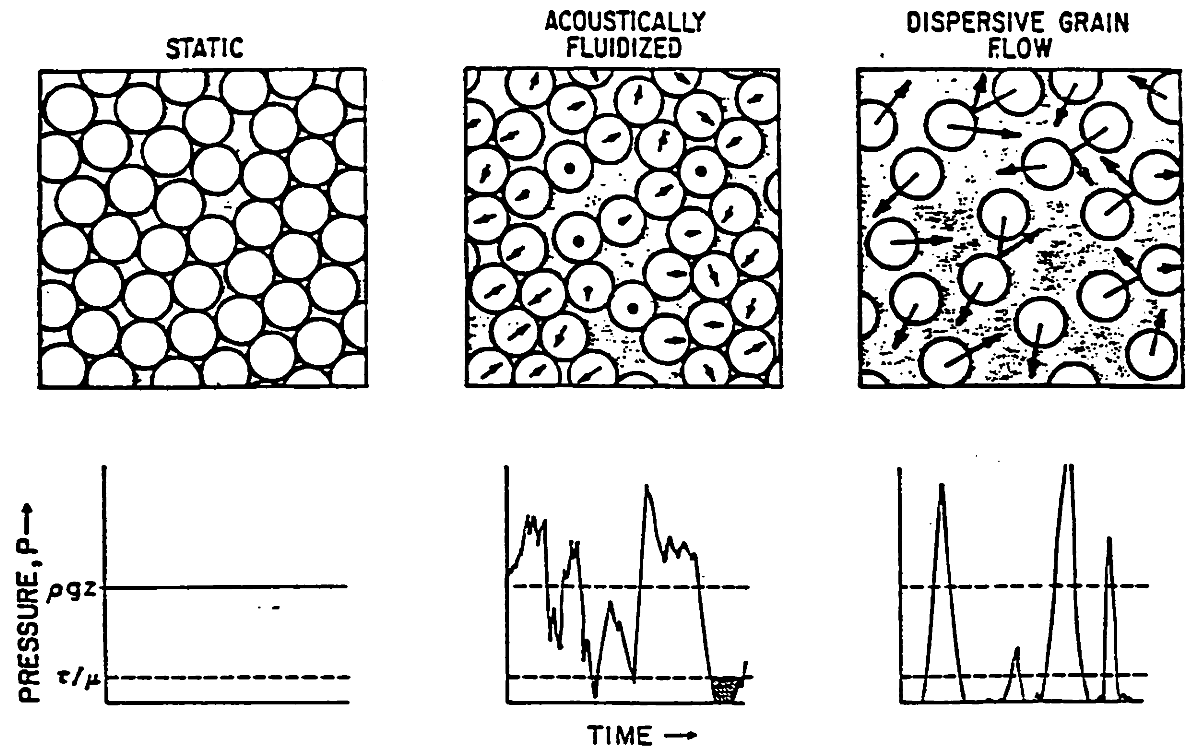

Figure 3. Schematic illustration of relation between static rock mass, acoustic fluidization, and Bagnold dispersive grain flow. Pressure in static rock mass is constant with time; overburden is supported by elastic deformation of rock fragments. Dashed line in this frame is pressure at which sliding may begin, τ/μ, where μ is coefficient of friction. In acoustically fluidized debris, rocks seldom lose contact, but pressure fluctuates about mean overburden value, occasionally becoming low enough for sliding to occur (shaded area on pressure-time plot below). Rock fragments undergoing dispersive grain flow are seldom in contact and their impacts produce large, rare, excursions in pressure. Adapted from Melosh (1983).

Emplacement Mechanisms

A larger number of emplacement mechanisms have been proposed for long runout landslides. These mostly rely on providing a lubricant to allow the slide to have a low effective friction coefficient. They include:

Slide traps an air cushion and floats like a hovercraft (Shreve).

Slide traps a water cushion and glides like a boat.

Frictional heat drives water from the material, generating a water cushion, as before.

These are insufficient hypotheses because of the identification of long runout landslides on Mars and Luna. To resume:

Friction melts rock at the bottom of the slide, which then glides like a boat on a lava lake.

This is contraindicated by the lake of melt glass in well-exposed long runout landslides. Finally:

The slide acts like an energetic gas (Bagnold grain flow).

Acoustic waves from the grinding and crushing of rock cause pressure variations large enough to lift the overburden (acoustic fluidization, Melosh).

The hypothesis of Johnson and Grundy (1993) that these enigmatic deposits are the result of particularly ambitious LPL grad student April Fool's pranks is summarily dismissed.

Figure 3 illustrates the last two mechanisms. The fatal flaws with the energetic gas model is that the collisions between rock fragments dissipates energy too quickly, and it does not explain why small landslides do not runout. Acoustic fluidization does not suffer from these flaws and is to date the favored hypothesis. Far less energy is dissipated because the pressure is transmitted by elastic waves, not rock collisions. The acoustic energy is primarily lost through the bottom of the slide. In small slides the surface area-to-volume ratio is large and acoustic energy is lost rapidly. Large slides lose a proportionally smaller amount of acoustic energy to leakage. The self-generating acoustic waves retain sufficient magnitude to reduce the overburden to the point that the material slides. As the flow spreads out, the surface area-to-volume ratio increases until the acoustic energy is dissipated rapidly and the slide comes to a halt. Figure 4 illustrates the mechanism, in particular the distribution of acoustic energy in the slide.

Planetary Connection

Figures 5 and 6 show spacecraft imagery of long runout landslides on Mars and Luna. It was the recognition of these events in airless and waterless environments that showed air/water lubrication hypotheses to be inadequate. A dramatic and largely accurate description of a long runout landslide in Valles Marineris can be found in *Green Mars*, pp. 111 *et seq.* The author avoids critical details that would prove a particular hypothesis, unfortunately. At this point, acoustic fluidization is the most plausible hypothesis.

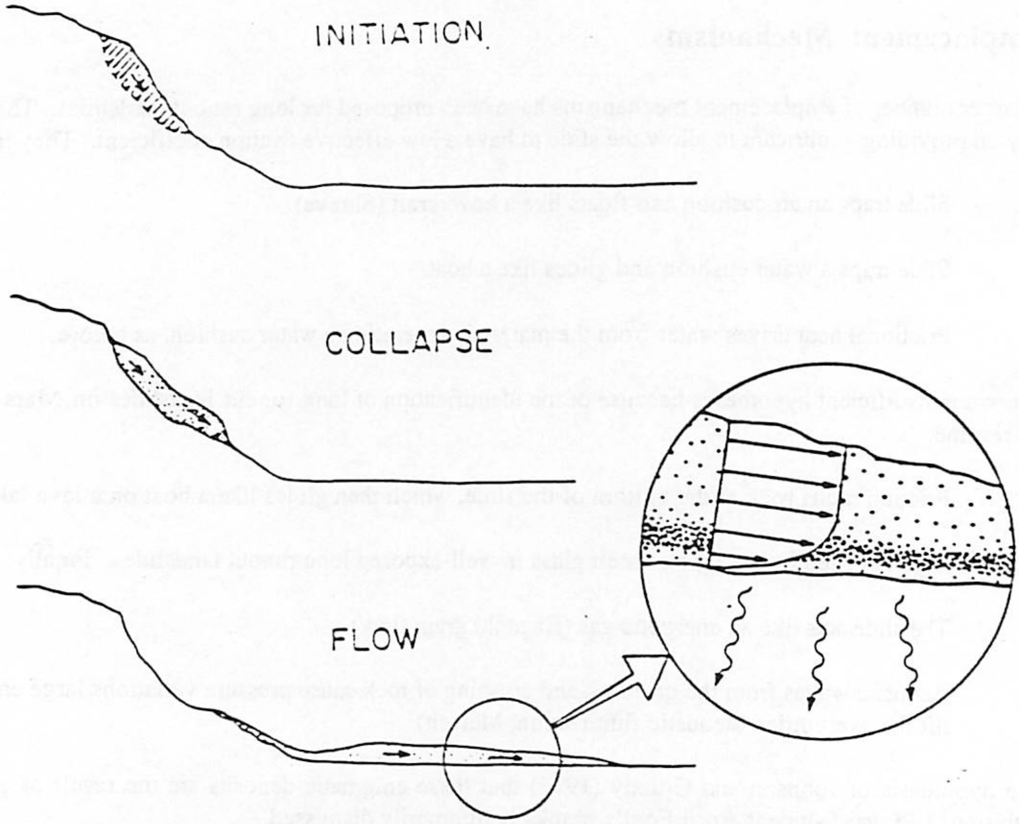

Figure 4. Schematic illustration of events in large rock avalanche on hypothesis of acoustic fluidization. After initiation, rock debris moves down steep slope, increasing its acoustic energy content. If this energy becomes large enough, rock mass may fluidize and continue to flow down low slopes. Inset illustrates velocity profile expected for highly non-Newtonian flow. Stipple density represents acoustic energy density as largest in basal layer where it is generated. Wavy arrows denote loss of acoustic energy to substrate. After Melosh (1983).

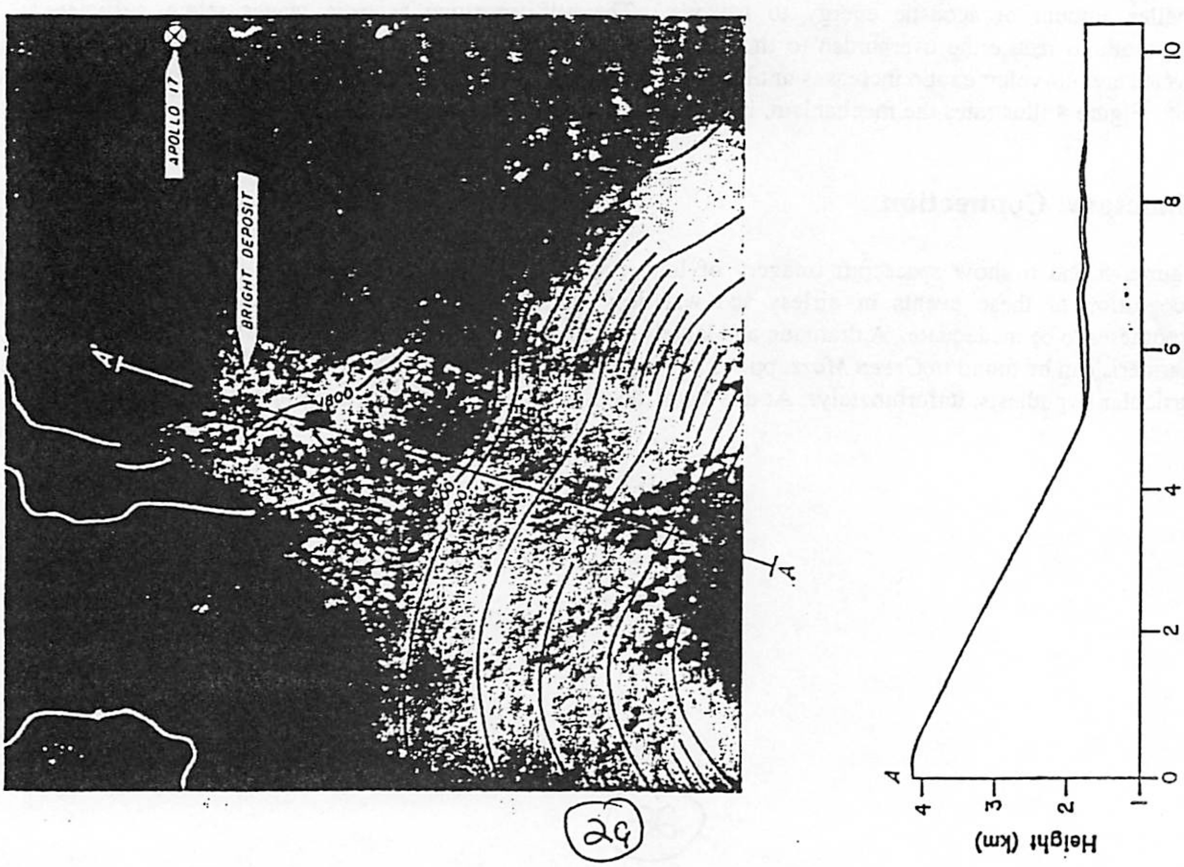

Fig. 6. Apollo 15 photo of the Apollo 17 landing site. The bright deposit overlies a dark plain and appears to be an avalanche from the massif to the south. Contours are in meters; A–A', line of profile shown; C, buried crater; R, ridge; B, bright margin; and M, moat.

1053

Howard, Science 180

26

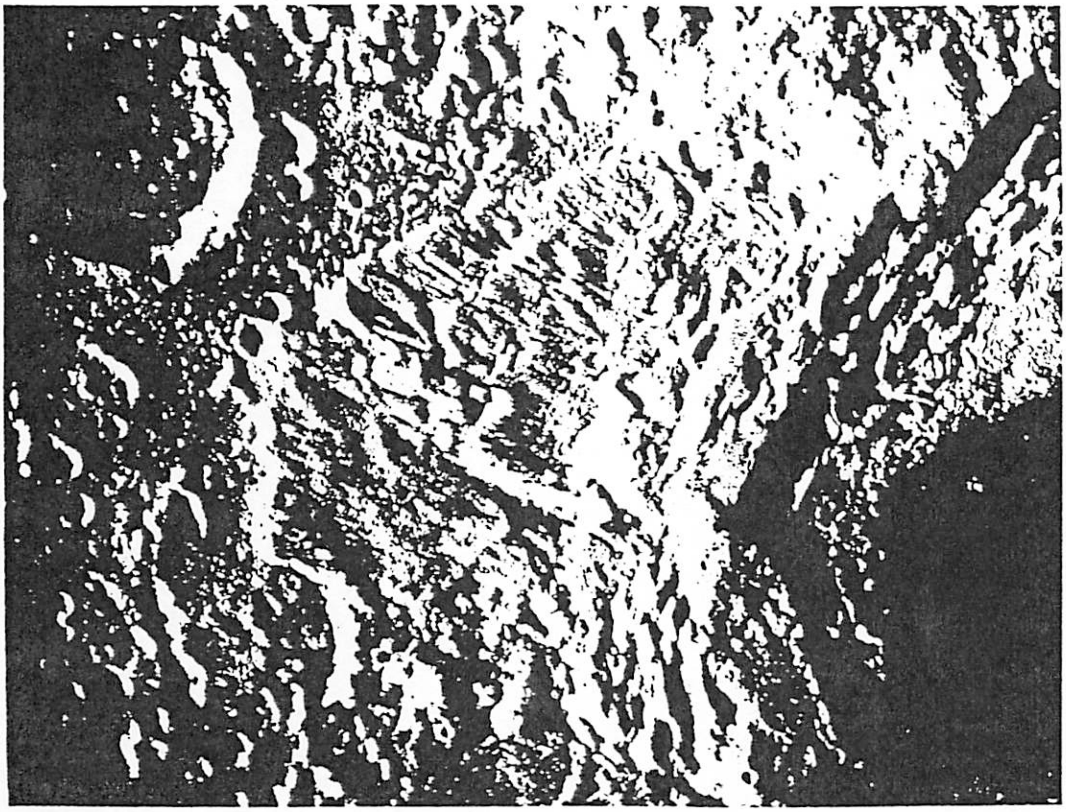

Figure 5 Large rock avalanche deposits on three planets. Left top photo (K642-108 by A. Post) is of Sherman landslide that flowed 5 km across glacier after 1964 Alaskan earthquake. Top right photo (Viking Orbiter mosaic 14A27-32) depicts rock avalanche on Mars that traveled 60 km across floor of Valles Marineris. Left bottom photo (AS17-2608) shows lunar landslide that slid 80 km from farside crater Tsilokovsky.

REFERENCES

Bagnold (1956) The flow of cohesionless grains in fluids, Phil. Trans. Royal Soc. London, 249, 235-297.

Howard (1973) Avalanche Mode of Motion: Implications from Lunar Examples, Science 180 1052-1055.

Krieger (1977) Large Landslides, Composed of Megabreccia, Interbedded in Miocene Basin Deposits, Southeastern Arizona, USGS Professional Paper 1008.

Lucchitta (1979) Landslides in Valles Marineris, Mars, JGR 84 8097-8113.

Melosh (1987) Mechanics of large rock avalanches, Rev. Engineering Geology VII, 41-49.

Melosh (1986) The Physics of Very Large Landslides, Acta Mechanica 64, 89-99.

Shreve (1968) The Blackhawk Landslide, GSA Special Paper 108, 47p.

Yarnold and Lombard (1989) A Facies Model For Large Rock-Avalanche Deposits Formed In Dry Climates, in Colburn *et al.* ed. Conglomerates in Basin Analysis: A Symposium Dedicated to A.O. Woodford, Vol. 62, 9-31.

A Bungee Jump Through Time

(A Little Geology of the Salt River Canyon)

by
Moses Milazzo

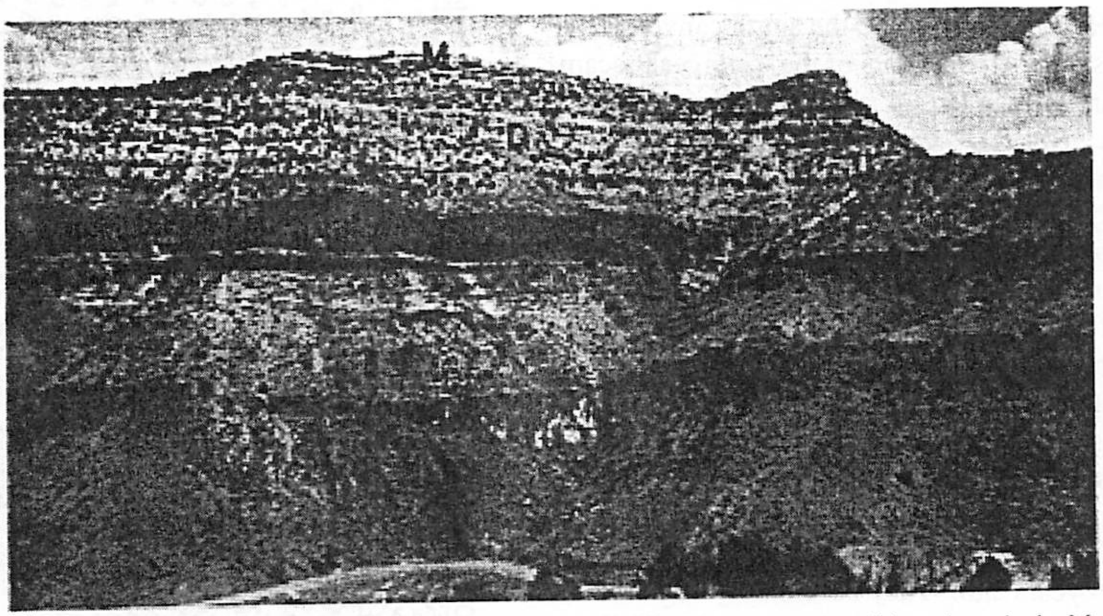

(fig. 1) View from Hieroglyphic Point at the Salt River Canyon. Dark sills of Precambrian diabase intrude the Mescal Limestone. Devonian (D) and Missiapian (M) limestones of the Paleozoic age form the upper wall above the highest diabase. (Peirce, 1967)

(Bring your own bungees, get life insurance, get death insurance, and notify your next of kin.)

A little background

The Salt River lies within the Transition Zone, just south of the Colorado Plateau. At its east end, the Salt River Canyon shows Colorado Plateau-like flat sedimentary strata and monoclinal folds. At the west end, the Canyon's structures are Basin and Range in nature, with Tertiary volcanic and sedimentary rocks bounded by normal faults. (Davis, et al. 53)

Hieroglyphic Point

At Hieroglyphic Point, the south canyon walls consist mostly of units of the Younger Precambrian Apache Group, and Precambrian diabase. (fig. 1)

The view of the canyon wall as seen by a bungee jumper from Hieroglyphic Point is summarized below. A geologic column is given in figure 2.

Before you jump, take a look at the classic example of below-the-surface spheroidal weathering in one of sills near the pull-out. These spheroidal rocks will soon (geologically speaking) be exposed to the surface.

Also notice the Petroglyphs, thought to have been chiseled into the desert varnish about 1000 years ago. They have barely begun to show new deposits of desert varnish. (Halka, et al)

As you fall, the first rocks you will see are light-colored more clearly stratified rocks, which are Paleozoic. (The Devonian Martin Limestone and the Mississippian Redwall Limestone seen in figure 1). If you have time, notice the diabase sills which have intruded and vertically expanded the Mescal Limestone. The Mescal Limes stone is the lighter-colored segments, while the diabase that has been forcefully injected between the layers of limestone are dark.(Peirce, 33)

As you near the bottom, hope your bungee will hold.

The Apache Group rests on granite, forming the lower two thirds of the north canyon wall. (Halka, et al., 152)

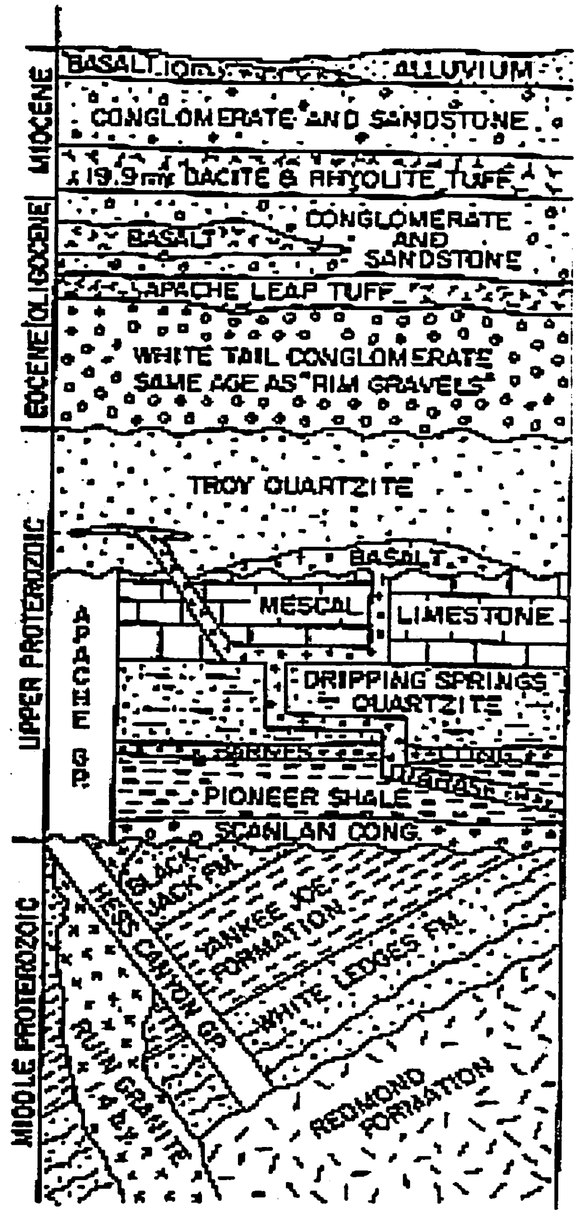

(fig. 2)Geologic column for the Salt River Canyon. (Davis, et al.)

While you are returning to the top, we'll review Spheroidal weathering and Intrusive and Extrusive Volcanism .

Spheroidal Weathering

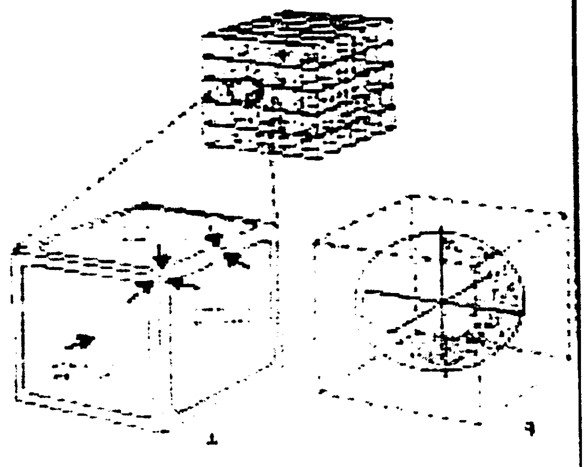

(fig. 3) Geometry of spheroidal weathering. (Ferry)

Spheroidal wreathing is a process that results in the formation of nearly spherical rocks and boulders. In order for spheroidal weathering to take place, several conditions must exist.

1) An unlayered, homogeneous rock with high feldspar content and mineral crystals that are approximately the same size.

2) Rain.

3) A network of planar fractures or joints upon which the rainwater acts, rounding corners. As the corners become rounded, the surfaces break off. (figs. 3,4)

You are most likely going to see granite undergoing spheroidal weathering. (Ferry)

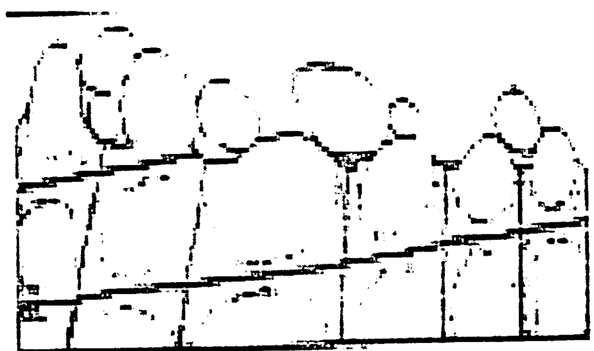

(fig. 4) Stages in the exposure of weather boulders. (Ferry)

Intrusive and Extrusive Volcanism

(in the rocks we'll be seeing.)

Intrusive Volcanism

Diabase Sills and Dikes: The Apache Group's size was doubled by the intrusion of these rocks. Sills are coplanar with the surrounding strata. Dikes follow cracks or faults across the stratigraphy. Sizes of both kinds of intrusive rocks range from a few centimeters to hundreds of meters. (fig. 5)

Extrusive Volcanism

Basalt Flows: Near the top of the Apache Group, occur Upper Proterozoic flows. In the uppermost stratigraphy, interspersed with pyroclastics and river sediments, occur Tertiary flows.

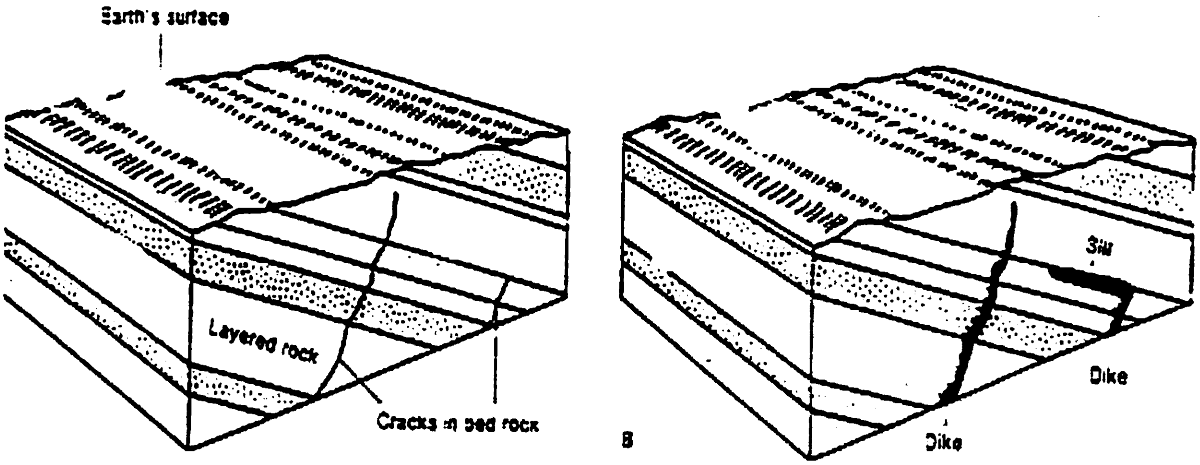

(fig. 5) Cracks in planes of weakness before intrusion of magma (A). Intrusions between layers are sills, intrusions across layers are dikes. (Reid, Chabot)

References:

Chronic, H., Roadside Geology of Arizona, pp. 152-153, 1983

Davis, G. H., Showalter, S. R., Benson, G. S., McCalmont, L. S., Cropp, F. W. III, Guide to the Geology of the Salt River Canyon Region, Arizona. *Arizona Geological Society Digest* 13: pp. 48-97, 1981

Ferry, J. M., Landforms of Spheroidally Weathered Rock, in *Landforms of Arizona*, pp. 415-427, 1984

Reid, B., Chabot, N., The History, Geology, and Stratigraphy of the Salt River Canyon, Intrusive and Extrusive Volcanism on Earth, the Moon, Venus, and Mars, Spheroidal Weathering, and Their Effect on the Rise of the English Parliamentary System in *Fire and Ice, PTYS 594a Practicum,* University of Arizona pp. 55-62, 1996

Basic Geology of the Colorado Plateau

Jason Fields

Millions of years ago, the Four Corners area was radically different. Due to the movement of tectonic plates, that area was then much closer to the equator. It was also much lower in elevation, forming a seabed on the west coast of Laurasia instead of the high arid plateau we know it as today.

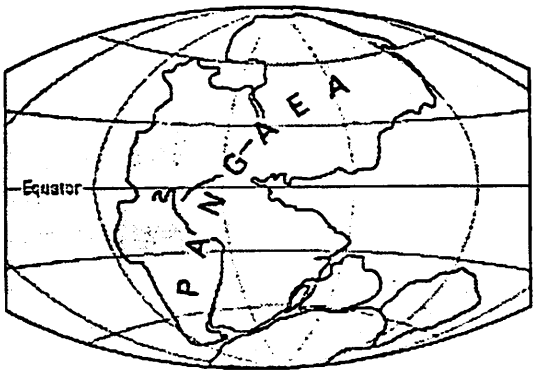

PERMIAN
225 million years ago

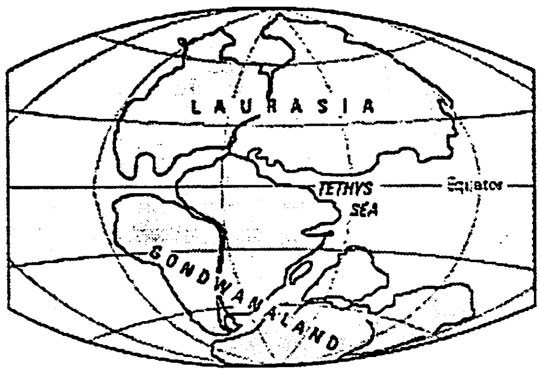

TRIASSIC
200 million years ago

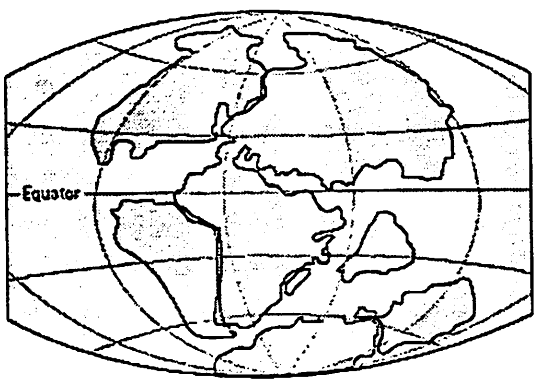

JURASSIC
135 million years ago

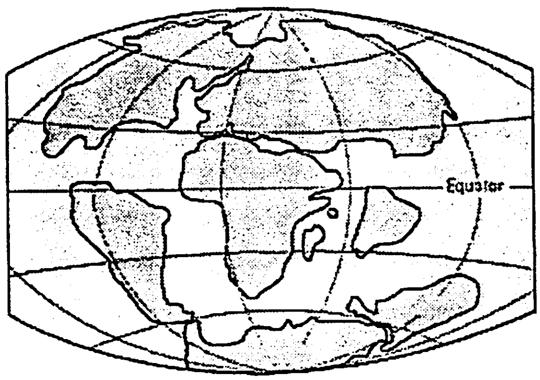

CRETACEOUS
65 million years ago

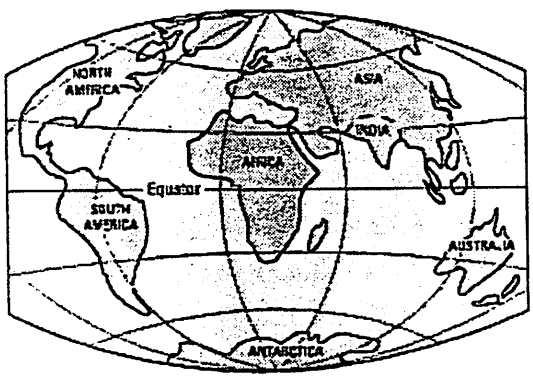

PRESENT DAY

As the North American plate moved to the northwest, it began to subduct the Pacific Plate about 100 million years ago, forming the Rocky Mountains.

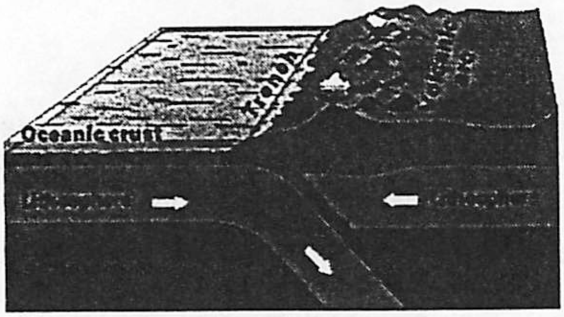

Oceanic-continental convergence

One area where mountain building should have occurred but did not is the Colorado Plateau. This section of the earth's crust is a relatively thick, flat, and stable area and was resistant to mountain forming. As a result, the entire area, shaded below, began to rise intact, in some places to 10,000 feet above sea level.

With the area steadily rising, river gradients became dramatically steeper, aiding the canyon-forming process. The greatest and most rapid uplift took place approximately 5.5 million years ago. Since the area was once a seabed, most of the rock is sedimentary and readily carved by water.

The Colorado Plateau is so-named because the Colorado River and its tributaries drain almost the entire region. An interesting effect of the canyon carving done by these rivers is isostatic uplift or isostacy. Due to the buoyancy of the earth's crust, the uplift is actually aided when rock is carried off the Colorado Plateau by the scouring action of the rivers.

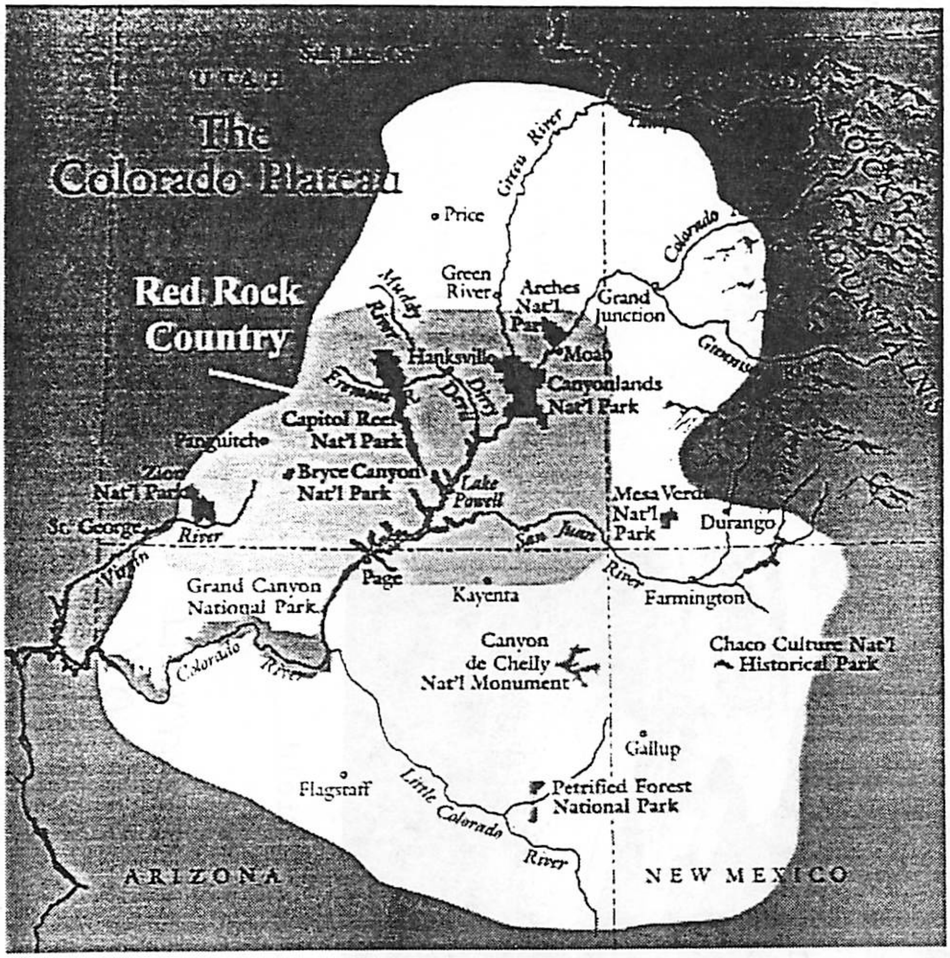

Dramatic colors in the rock are caused by different elements: oxidized iron is found in the red rocks, green and blue is due to unoxidized iron, black rocks have carbon in them, manganese produces several different dark colors, and green usually denotes copper. Also, due to the arid climate and relative lack of plant life, our view of the rock formations is enhanced. We have these sets of circumstances to thank for the many amazing and colorful geological formations on the Colorado Plateau.

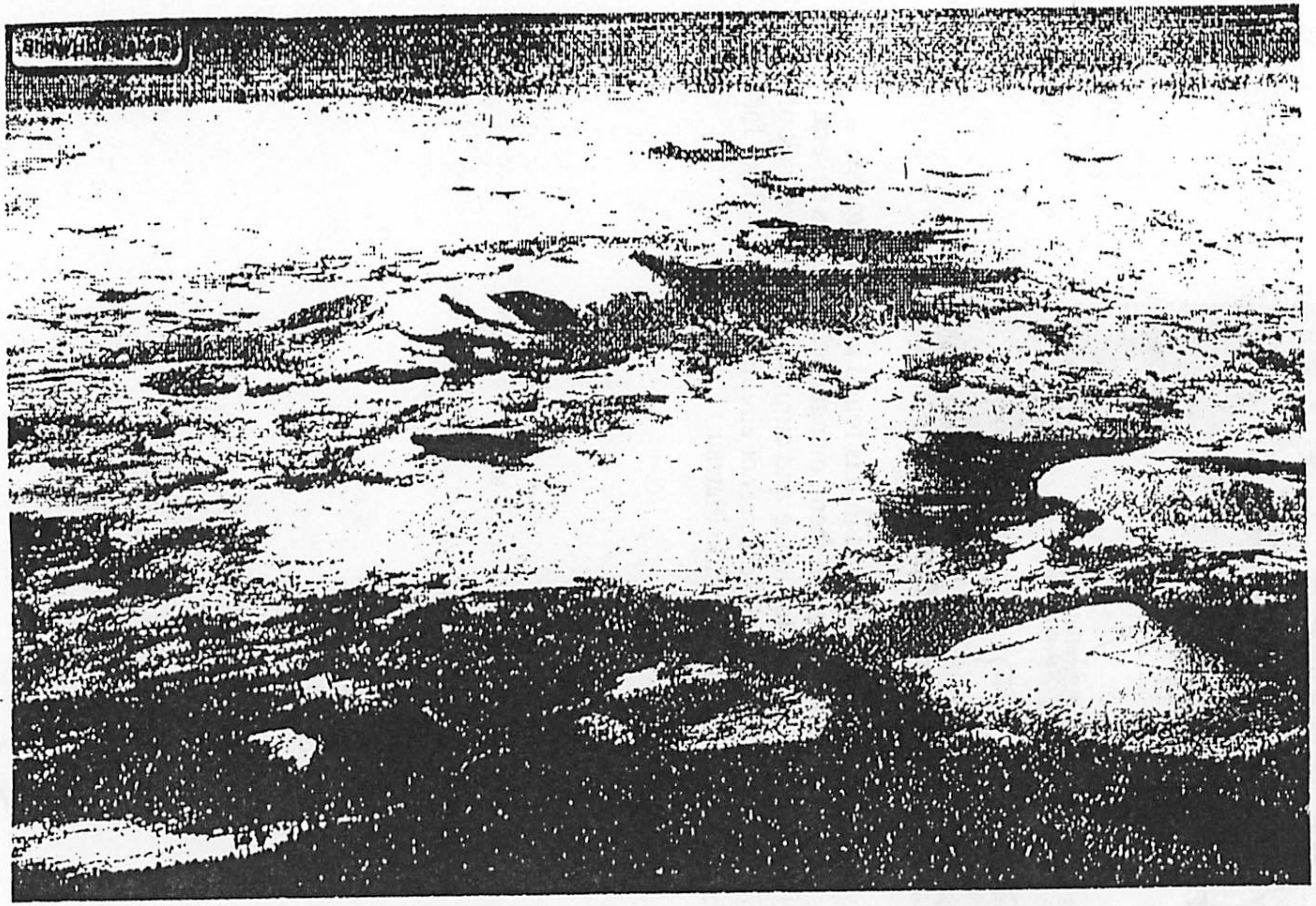

Fig 3 - Aerial view of Springerville Volcanic Field

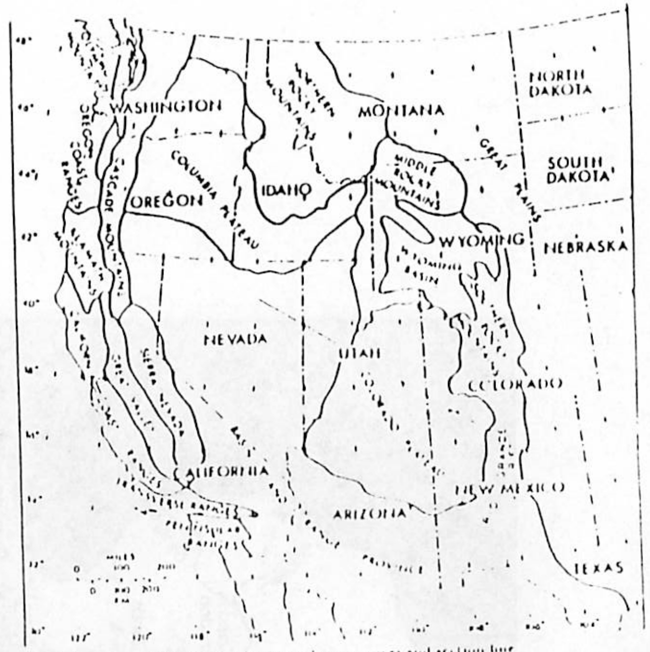

Fig 1 - Physiographic provinces of Western US

Fig 2 - Plateau Margin Volcanism

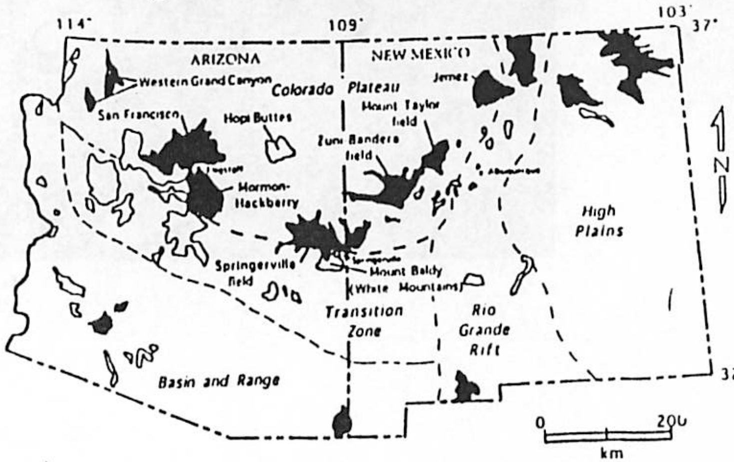

Fig. 1. The Springerville volcanic field is located along the southern margin of the Colorado Plateau, in central east Arizona. Physiographic provinces of the area delineated. The Mogollon Rim is a topographic escarpment which defines the boundary between the Transition Zone and the Colorado Plateau, south of the SVF. Shaded areas indicate volcanic fields ... n 5 m.y. ... ed areas ... olcanic f... 6 m.y. ... Wolfe et al. 1983]. The Jemez lineament ... be comp... olcanic f... ssociate... s extend ... the ... 1984] is ... through the Mount Taylor, Zuni Bandera, and Springerville fields

(W) "PLATEAU MARGIN VOLCANISM AND THE SPRINERVILLE VOLCANIC FIELD"
PAUL WITHERS

1) Thompson, G.A. & M.L. Zoback; Tectonophysics v61 (1979) 149-181
2) Connor, C.B et al; JGR v97 #B9 (1992) 12349-12359
3+4) Condit, C.D et al; http://www.geo.umass.edu/faculty/condit.html
5) Sheridan in 'Landscapes of Arizona', ed. Smiley et al (1984)
6) Wolfe in 'Landscapes of Arizona', ed. Smiley et al (1984)
7) Condit, C.D. et al; JGR v94 #B6 (1989) 7975-7986

...se ...ic... we... als... the main sources for the text of this

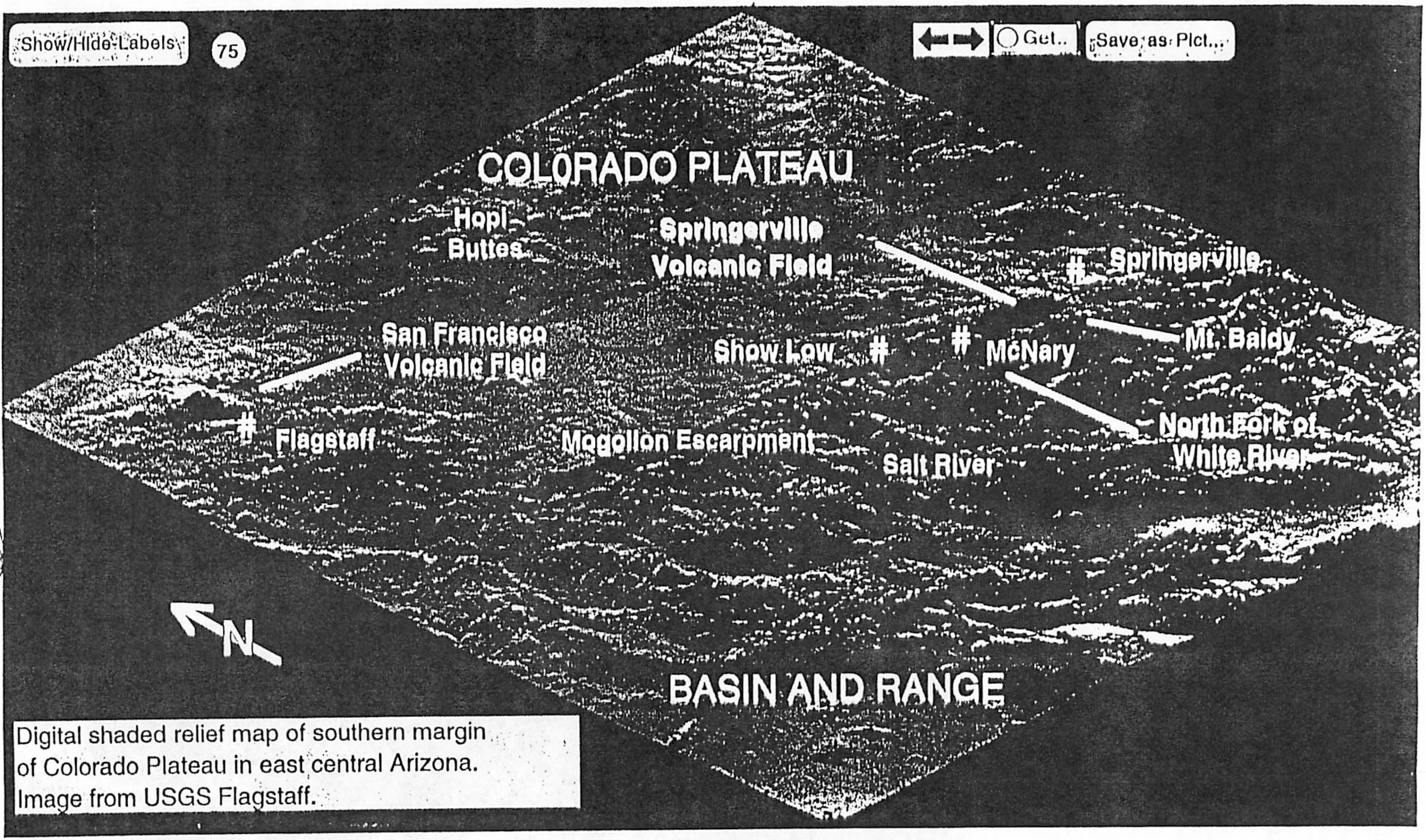

Fig 4 - Plateau Margin Topography

Points to Remember:
Cool lithosphere prevented deformation of the Colorado Plateau.
Plateau then uplift by heating and crustal thickening.
Crustal thickening leads to stresses and volcanism around Plateau Margin.
Low effusion rate of basaltic lava formed cinder cones in Springerville Field
These are small, steep sided and easily eroded.
Vents migrated eastward due to motion of plate over fixed source in mantle.
This field likely to be extinct but others still active.

Fig 6 Aerial View of
Cinder Cone and [illegible]

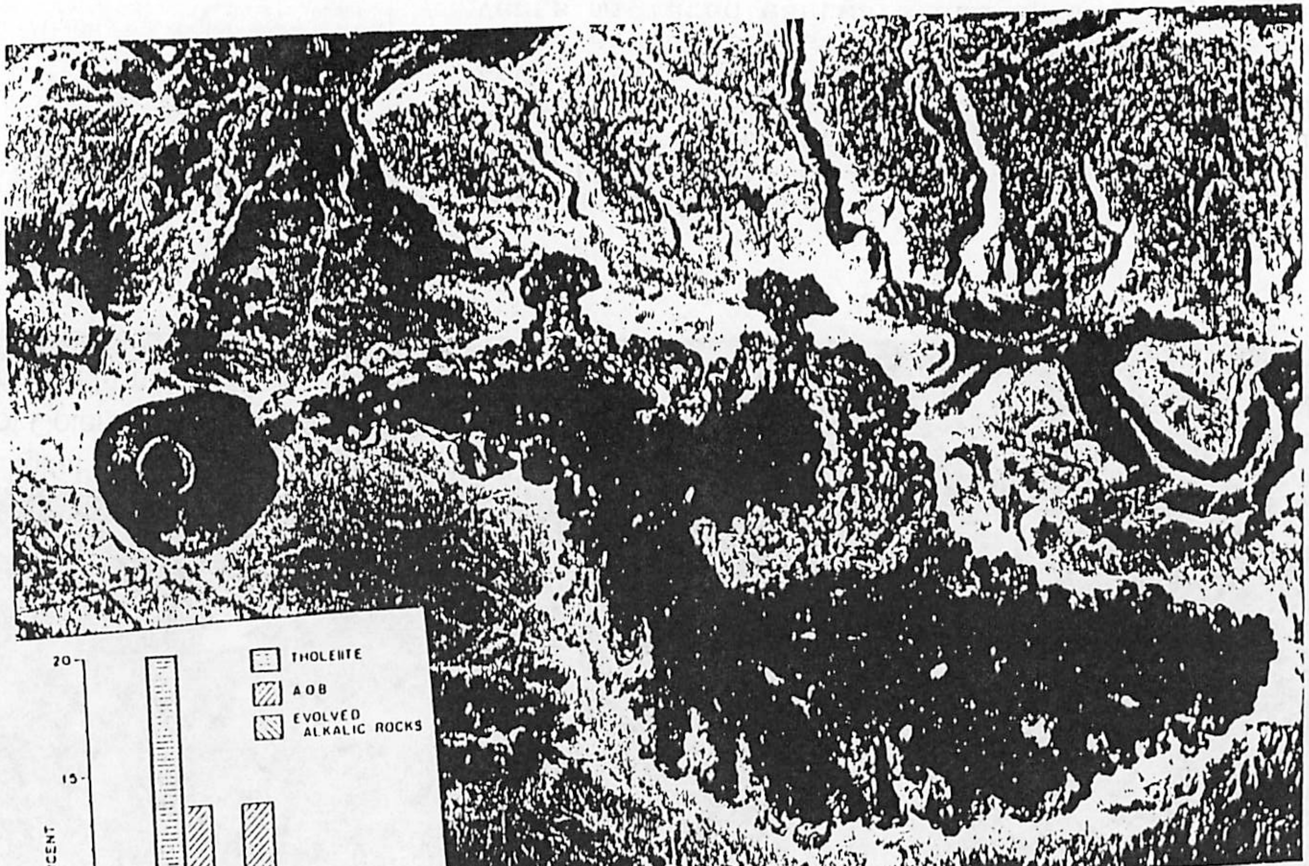

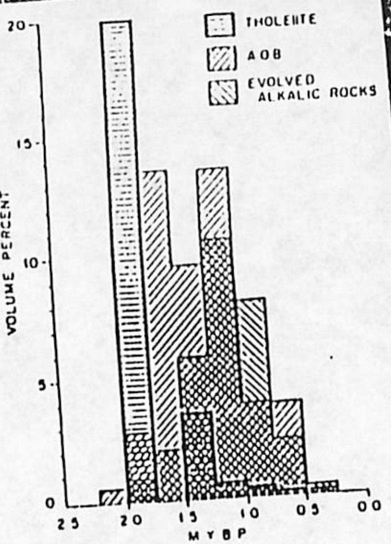

Fig. 1. Estimated volume effusion rates (volume percent, as estimated from areal percent) for three rock types through time, in 250,000 year intervals. AOB are alkali olivine basalt (sensu stricto). Hawaiite, mugearite, and benmoreite are classified as "evolved alkalic rocks".

Fig 7 - Estimated volume effusion rates
Hawaiite = Evolved alkalic rocks

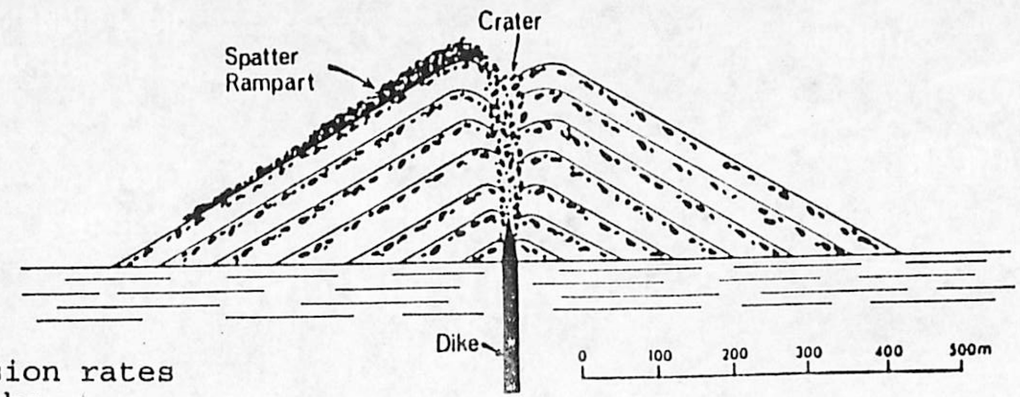

Fig. 5 Schematic diagram of a cinder cone. Bedding of cinders at the flank of the cone is at the angle of repose (30^{o}). A small welded spatter rampart is on the left side of the diagram.

15

The Little River That Could

The Hydrology and Geomorphology of the Little Colorado

Fred Ciesla

1. Introduction

Throughout history, visitors to the Little Colorado River could have been greeted by any one of the many personalities that the river cared to show. More often in the past than the present the Little Colorado could be as impressive as its big brother that winds through the Grand Canyon. At other times it is difficult to see a river at all.

The Little Colorado is contained completely within Arizona, with its headwaters located in the White Mountains in the east part of the state. It then flows towards the west staying in the north of the state, running diagonally across the Navajo Reservation. Eventually it meets up with the *other* Colorado at Cape Solitude in the Grand Canyon.

2. Hydrology of the River and Grand Falls

Nowadays, the river is in its declining years, due to its for irrigation for the growing population, thus extending the amount of time that the river is in its more dormant stage. However, as winter gives way to spring, the river can roar again and become as impressive as it was when the first Europeans set eyes on it.

Colorado comes from the Spanish, meaning reddish. This is by no means a misnomer, for when the Little Colorado is running at full volume, the water is colored red by the soil and silt it carves out. In addition, Carrizo Creek, Clear Creek, and the Zuni River dump their own stained waters into the flow. Most of this soil is topsoil eroded from the Hopi and Navajo farmlands.

One of the most interesting features of the Little Colorado is the Grand Falls, or as it is affectionately called, "The World's only Dusty Waterfall." This waterfall is 185 feet high, and is surprisingly broad, reminding some viewers of Niagara Falls in New York. This spectacle was formed when an ancient lava flow made its way into the river, changing the Little Colorado's flow from a northward direction to more eastward. This lava flow came from nearby Merriam Crater, a volcanic cone located between the river and the San Francisco Peaks. The river made its way around the lava tongue and eventually formed a horseshoe around it to join its own channel 60 miles down stream. Where the river rejoined itself, it excavated a canyon along a break between the basalt and the limestone and sandstone walls. This is what became the Grand Falls.

Like the river, its impressiveness depends on the season. For most of the year, the falls is nothing but a dry terrace. During times of high river volume, the falls can be deafening as the water, or more precisely mud, pours down the staircase of the falls, striking the sandstone at the bottom.

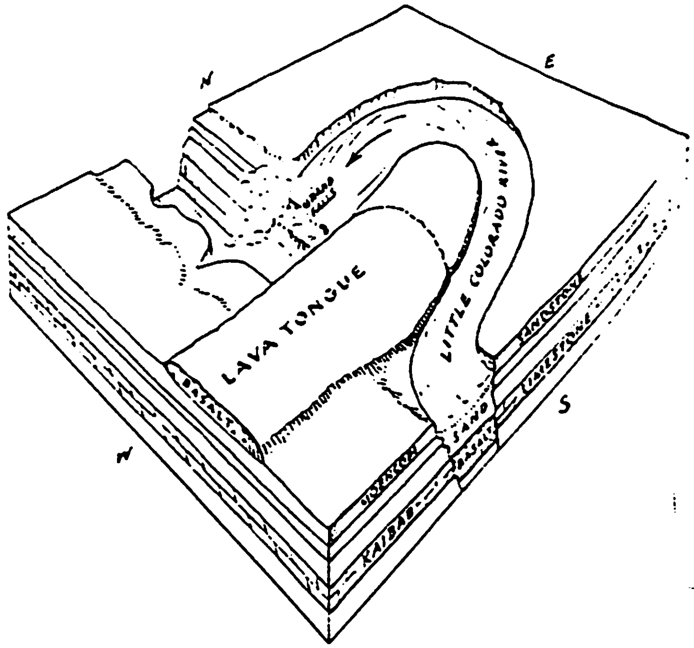

Diagram showing how a lava flow blocked the Little Colorado and forced the river out of its channel to cause the Grand Falls.
(After Museum of Northern Arizona, Flagstaff)

3. Geomorphology and Other Stuff

During times of high river volume, the water can reach over the banks of the river and flood the surrounding land. After times of low river volume it can sometimes be difficult to distinguish dry river bed from this surrounding area. Given the chance to examine the areas closer, you can tell the difference by looking at the alluvium. Flood plain sediments tend to be finer grain due to the fact that once the water reaches over the banks of the river while channel sediments are more coarse. This is because flood waters do not have the same power and current as does the river, and therefore the finer grains can settle out. Using this principle allows one to examine the history of the Little Colorado by looking at the layering of the land.

Richard Hereford of the U.S. Geological Survey used this idea and examined deposits of the river and found that over the past 100 years the major geomorphological processes have been largely dependent on the climate. In the beginning of the century, the major process was erosion, which gave way to a period of aggradation, which recently gave way to another period of erosion. The erosion periods were linked to warming trends, which have affected most of North America. The aggradation period, in turn, corresponded to a period of low precipitation. This theory disproved the theory that humans had been responsible for the changes.

References

Ferry, Phillip (1957): **The Little Colorado Runs Dry** _Pacific Discovery_ 10(3, May/June), p.18-23.
Hereford, Richard (1984): **Climate and Ephemeral-Stream Processes: Twentieth-Century Geomorphology and Alluvial Stratigraphy of the Little Colorado River, Arizona.** _Geological Society of America Bulletin_ 95, 654-668.

Stratigraphy of the Chinle Formation, Painted Desert National Park, Arizona

or

the rocks confide in me

by ®

Intro

This presentation will be about the rock types and ages of the Chinle Formation, specifically those found in the Painted Desert National Park. I will then tell you why anyone cares about stratigraphy and what these rocks can tell you about the palæoenvironment. But first...

A Crash Course in Stratigraphy (a la Steno)

a) The rocks on the bottom are the oldest
b) Sedimentary rocks are generally put down in horizontal layers
c) Sometimes are layers are eroded off before another is deposited, otherwise known as an unconformity.

The Stratigraphy of the Chinle Formation

(from oldest to youngest/bottom to top)

<u>Moenkopi Formation</u> (Early and Middle Triassic) - sandstone
  unconformity - erosional surface
<u>Chinle Formation</u> (Late Triassic)
  Shinarump Member - yellow sandstone w/ gravel beds
  Lower Red Member - layers of mudstone, sandstone, and conglomerate
    200-300 feet thick
  Mesa Redondo Member- mud and siltstones 160 ft
  Monitor Butte Member
  *Petrified Forest Member - three subunits
    lower- blue and gray mudstones 300 ft
      brown sandstone
      blue shale
    Sonsela sandstone - 10-50 ft log-bearing
    upper - gray-red less sandstones
      painted desert sandstone #1
      painted desert sandstone #2
      painted desert sandstone #3
      black forest tuff
      purple red shale
  *Owl Rock Member - pale red calcareous siltstone and limestone
    unconformity
<u>Bidahochi Formation</u> (Pliocene)

* - These are the only layers cropping out in the park.

Correlation of Stratigraphic Layers

Correlation is the determining the relation between sedimentary deposits that are not visually continuous. Why would you want to correlate? Correlation can determine the extent of a particular kind of deposit. Thus, one can determine the size of a palæolake or determine the route of a palæoriver. On a larger scale, one can find connections between palæocontinents.

How do you correlate?

1) Visually - color, rock type, texture
2) Thin section - compare on microscopic levels
3) Compare rare minerals - zircon
4) Fossils (see *B*)

Zircon ($ZrSiO_4$) has small amounts of Uranium.

$^{238}U \rightarrow {}^{206}Pb$ $t_{1/2} = 4.5$ Ga

$^{235}U \rightarrow {}^{207}Pb$ $t_{1/2} = 0.7$ Ga

Palæomagnetism

Once you have determined the extent of a formation you can use it for different kinds of sampling, such as palæomagnetism. A large undeformed formation is perfect for these kinds of measurements. The basic concept behind paleomagnetic sampling is that when fine sediments that contain small grains of metal such as iron are deposited, they line up along the north-south axis of the magnetic pole. These samples can be used to determine the Apparent Polar Wander (APW) of the region. That is, either the locality was rotating with respect to the local paleomagnetic pole, or the north pole was wandering.

In this case the Chinle formation extends over most of western North America. Bazard and Butler took samples from the Chinle Formation in several localities in Arizona and New Mexico. Their basic results showed a change from counterclockwise to clockwise rotation of the supercontinent, Pangæa.

References

Bazard, D. R., and R. F. Butler, (1991) Paleomagnetism of the Chinle and Kayenta Formations, New Mexico and Arizona, Journal of Geophysical Research, 96, B6, 9847-9871.

Murray, P. A. (1990) Stratigraphy of the Upper Triassic Member (Chinle Formation) in Petrified Forest National Park, Arizona, USA, Journal of Geology, 98, 780-789.

Riggs, N. R., T. M. Lehman, G. E. Gehrels, and W. R. Dickinson, (1996) Detrital Zircon link Between Headwaters and Terminus of the Upper Triassic Chinle-Dockum Paleoriver System, Science 273, 97-100.

Roadifer, J. E. (1966) Stratigraphy of the Petrified Forest National Park, Arizona, Ph. D. Thesis, Department of Geology, University of Arizona.

(Murry)

		Painted Desert Area	Rainbow Forest Area
	BIDAHOCHI FORMATION (PLIOCENE)		
CHINLE FORMATION	OWL ROCK MEMBER		
CHINLE FORMATION	UPPER PETRIFIED FOREST MEMBER	PURPLE AND RED SHALE	
		BLACK FOREST TUFF	FLAT TOPS SANDSTONE # 4
		PAINTED DESERT SANDSTONE # 3	FLAT TOPS SANDSTONE # 3
		PAINTED DESERT SANDSTONE # 2	FLAT TOPS SANDSTONE # 2
		PAINTED DESERT SANDSTONE # 1	FLAT TOPS SANDSTONE # 1
CHINLE FORMATION	SONSELA SANDSTONE		
CHINLE FORMATION	LOWER PETRIFIED FOREST MEMBER	BLUE SHALE	RAINBOW SANDSTONE
		BROWN SANDSTONE	NEWSPAPER SANDSTONE

FIG. 2.—Stratigraphic nomenclature of Petrified Forest National Park, after Billingsley (1985).

Zircons (Riggs et al.)

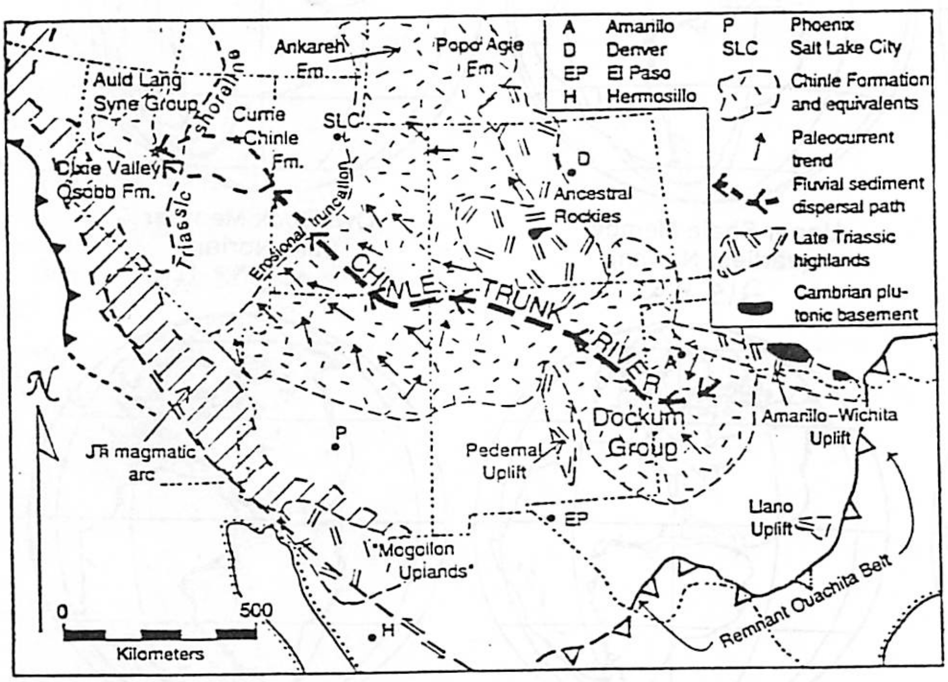

Fig. 1. Late Triassic paleogeographic map showing the proposed location of the Chinle-Dockum trunk river.

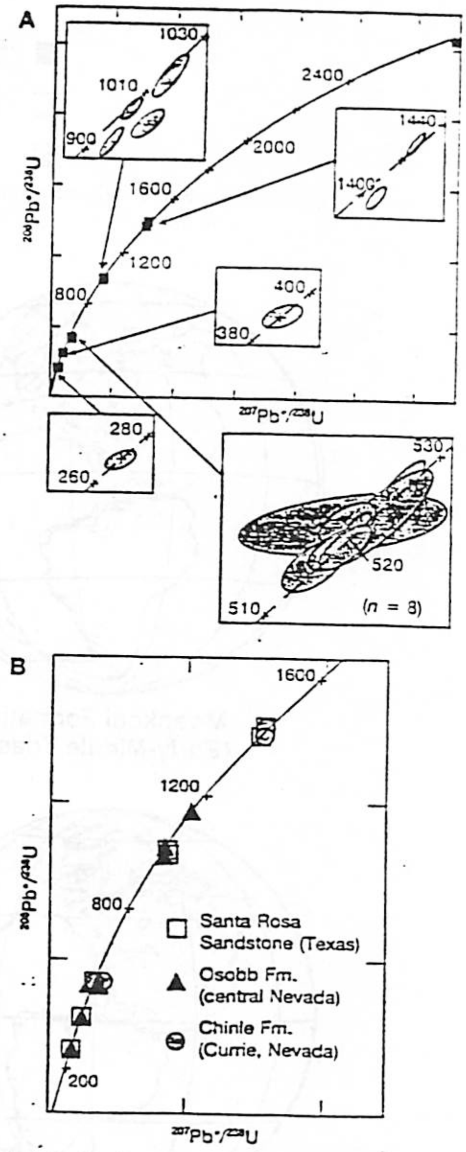

Fig. 2. (A) Concordia diagram showing zircon populations in the Santa Rosa Sandstone. Error ellipses are shown at the 95% confidence level. (B). Concordia diagram comparing congruent zircon populations of the Santa Rosa Sandstone (Dockum Group, Texas), Chinle Formation (Currie, Nevada), and Osobb Formation (Auld Lang Syne Group, Dixie Valley, Nevada).

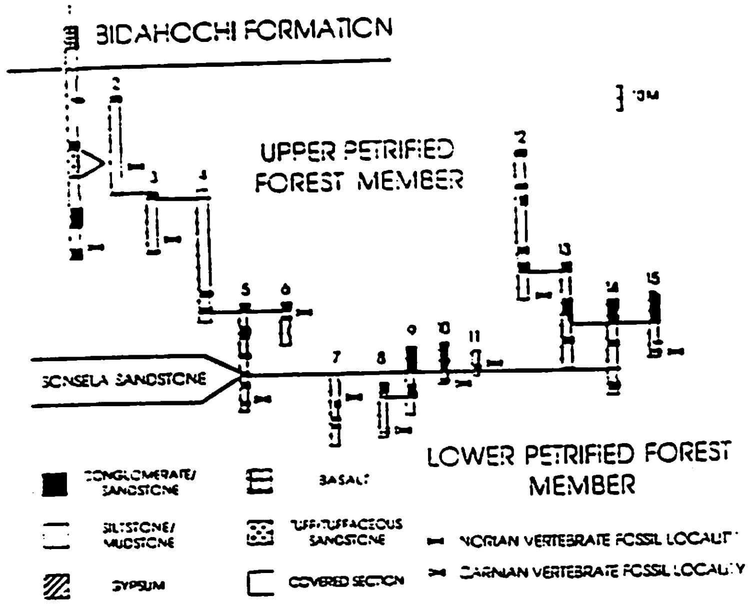

FIG. 6.—Correlation of the Painted Desert, Blue Mesa, and Rainbow Forest areas. Sections locations as in figure 1.

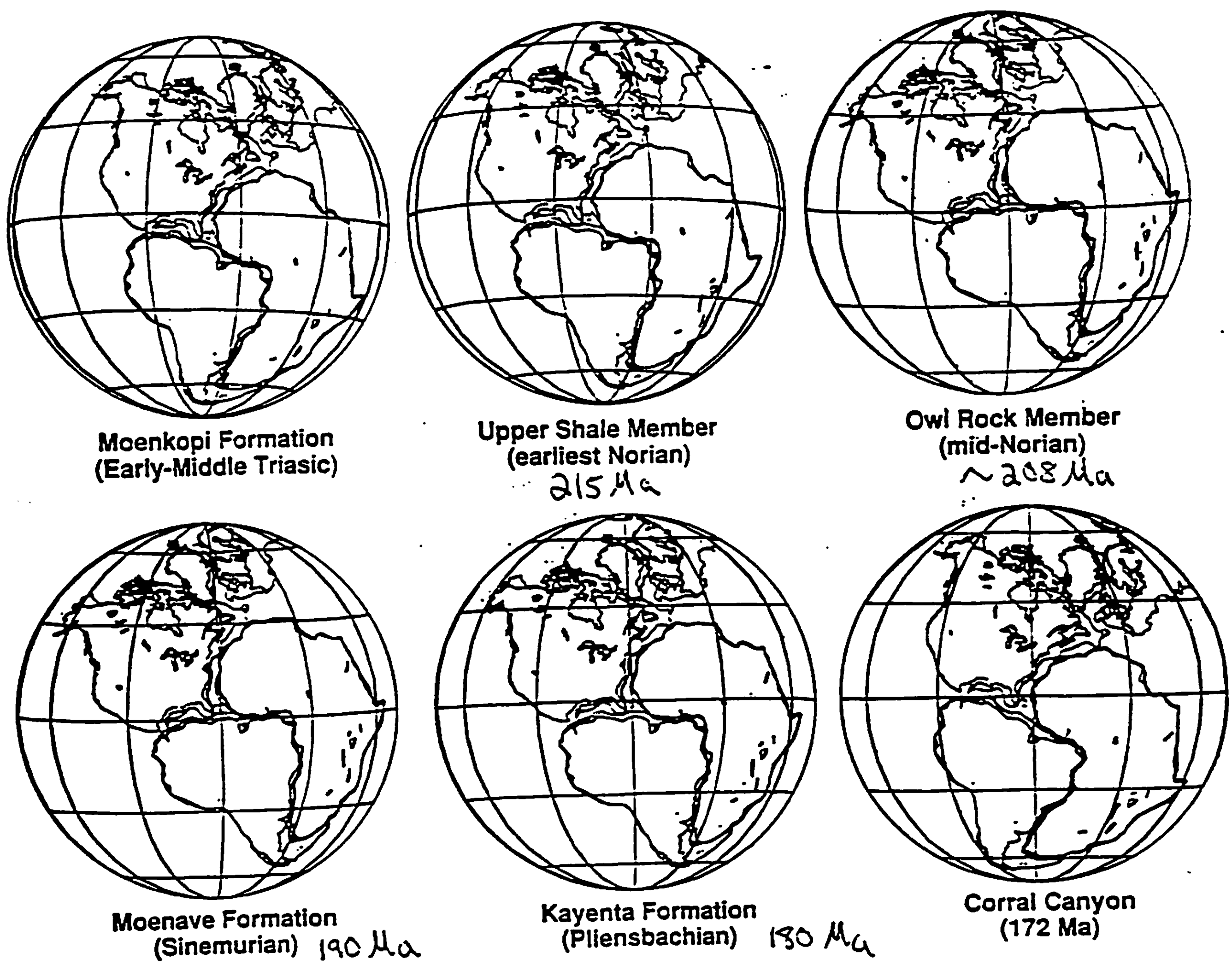

APW (Bazard & Butler)

Fig. 16. Paleogeographic reconstructions for North America, Greenland, Eurasia, Africa, and South America based on selected Late Triassic-Middle Jurassic North American paleomagnetic poles. The orthographic projections were generated by rotating the North American paleomagnetic pole indicated by the label to the geographic pole. Greenland, Eurasia, Africa, and South America were positioned relative to North America using the reconstructions of *Ziegler et al.* [1983] as given by the software *Terra Mobilis*™. Paleolongitudes are arbitrary in these reconstructions.

Palæoecology of the Pætrified Foræst

❀ Bærbæræ Cohæn ❀

Petrified Forest National Park was established as a national monument in 1906 and as a national park in 1962. It occupies an area of 146 square miles (378 square km). The park includes sections (Blue Mesa, Jasper, Crystal, and Rainbow forests) mostly filled with fossilized leaves, plants, and broken logs. Other features include petroglyphs (such as Newspaper Rock) and ancient Indian Pueblo ruins.

The Petrified Forest wood occurs as prone logs, some upright. A few logs appear to be buried in place, but most of the prone logs occur in channel deposits with preferred orientation (paleoflow direction). Others have a random orientation, suggesting they were deposited in overbank floodplains. These were probably transported some distance before burial, as they lack bark and limbs. Some trunks are 2 m (6 ft) in diameter and exceed 30 m (100 ft) in length.

Petrified wood forms by the gradual mineral replacement of the organic material as it lies buried underground. Sometimes the original cellular structure is obliterated and what remains is simply a cast of the original log; other times, growth rings, bark, knots, and even cellular structure are preserved with remarkable fidelity.

Ash, S.R. and Creber, J. T. (1992) Palaeoclimatic interpretation of the wood structures of the trees in the Chinle Formation (Upper Triassic), Petrified Forest National Park, Arizona, USA. *Palaeogeog., Palaeoclim., Palaeoec.* **96**, 299-317.

Ash, S. (1996) Evidence of arthropod-plant interactions in the Upper Triassic of the Southwestern United States. *Lethaia* **29**, 237-248.

Dubiel, R.F. (1993) Depositional setting of the Owl Rock Member of the Upper Triassic Chinle Formation, Petrified Forest National Park and vicinity, Arizona. *Bull. N. M. Mus. Nat. Hist. Sci.* **3**, 117-121.

Gottesfeld, A.S. (1971) Paleoecology of the Chinle Formation in the Petrified Forest National Park, Arizona. PhD dissertation, University of Arizona.

Hunt, A.P. and Lucas, S.G. (1990) Paleontology and biochronology of the Petrified Forest Member of the Upper Triassic Chinle Formation near San Ysidro, Sandoval County, New Mexico. *N. M. J. Sci.* **30**, 17-26.

Lucas, S.G. and Hunt, A.P. (eds) (1989) *Dawn of the age of dinosaurs in the American Southwest* and references therein.

Parrish, J.M. (1989) Vertebrate paleoecology of the Chinle Formation (Late Triassic) of the Southwestern United States. *Palaeogeog., Palaeoclim., Palaeoec.* 72, 227-247.

Scurfield, G and Segnit, E.R. (1984) Petrification of wood by silica minerals. *Sedimentary Geology* **39**, 149-167.

Sigleo, A.M.C. (1977) Organic and inorganic geochemistry of the petrification of wood. PhD dissertation, University of Arizona.

Weibel, R. (1992) Petrified wood from an unconsolidated sediment, Voervadsbro, Denmark. *Sedimentary Geology* **101**, 31-41.

The Fæte of Organic Matærial: Petrifaction or Putrefaction?

While petrified wood occurs throughout the world in a variety of geologic deposits, the petrifaction process is rather complex. Similar environmental conditions could result in coal deposits or total organic decay. The wood silicification sequence can be summarized as follows:

❶ Wood is buried rapidly, as when rivers overflow their banks, or when forests are covered by volcanic ash. The subsequent environmental conditions require plant degradation to be at a minimum, such as in stagnant, poorly-drained basins, swamps, and bogs.

❷ Silica-rich waters, which result from silicate weathering or clay mineral modification in surrounding or overlying strata, percolate over an extended period of time through sediments containing wood. The sediment mineral and trace element contents indicate that silica mineralization takes place within the chemical and pH range of most surface waters.

❸ Silica is deposited along the outer cell walls of the wood. The most probable mechanism is hydrogen bonding between the hydroxyl functional groups in cellulose or lignin and the hydroxyl groups in the silanol molecule. This is why there aren't petrified bones--animals don't have cell walls.

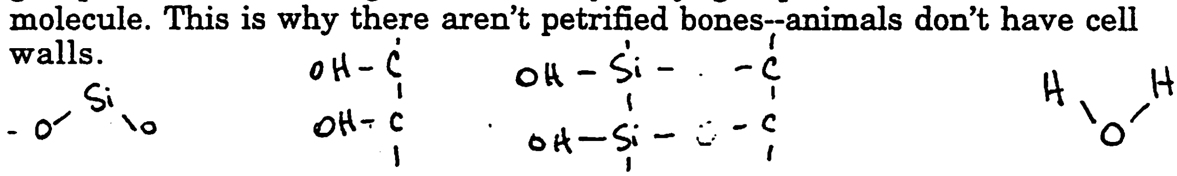

Silicic Acid + Cellulose ➡ Polymerized silicon + water

Iron hydroxide also hydrogen bonds, so wood often has traces of ferrous iron, making it yellow, brown and red. Black and purple take their hue from carbon or manganese

❹ When the organic surfaces are fully cemented, the accumulation of silica proceeds until all of the open space is filled with siliceous material. This material is almost pure, cryptocrystalline α-quartz (chalcedony or agate).

❺ Organic material degrades and is sometimes later removed from the sample. Silicification proceeds from to the inside of the wood sample.

❻ Final lithification involves loss of water and often a transformation from one form of silica to another (opal➡chalcedony➡quartz).

Silicification is thus an impermeation or permineralization process. The term replacement is valid only in those cases where the original plant or animal decayed entirely after burial and the void, or mold, was later filled by mineral matter.

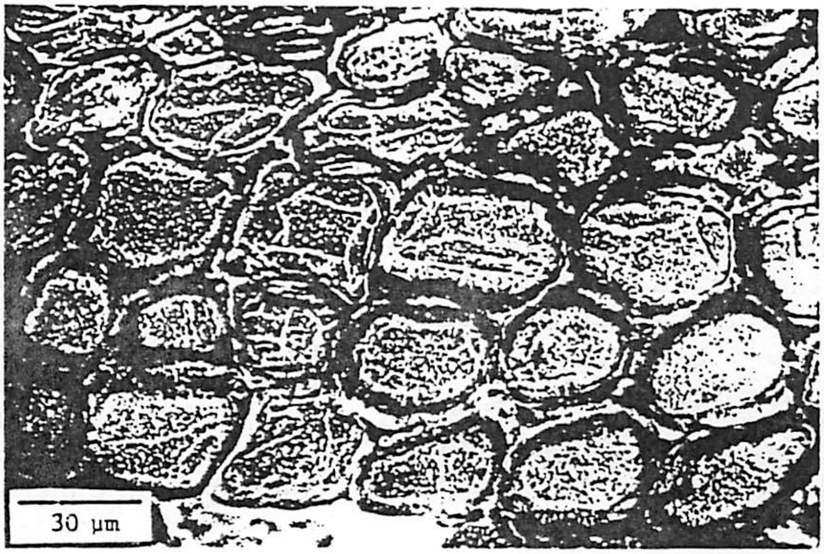

Chalcedony. Cell walls of transversely oriented fibres; lumina filled with finely crystalline chalcedony showing "gel-like" cracking (optical, thin section).

The mineralization process tends to deplete the wood silica in most elements. Notable exceptions are uranium and antimony, which are highly enriched in the petrified wood relative to the surrounding sediments. This is because uranium and antimony are adsorbed onto organic matter and then precipitated by a reduction and/or complexing reaction. Wood can extract 40% of the uranium in a uranyl sulfate solution; lignite and bituminous coal can extract up to 98%!

Fossil Wood as Palæoenvironmæntal Mærkers

The inorganic chemical analysis of the Petrified Forest wood gives us insight into the particular conditions there. The distribution of variable valence elements suggests an anoxic environment such as the bottom muds of a swamp or pond. The total lanthanide concentration of the clay separates point to an intermediate to slightly acidic pH typical of decaying organic material. The major element chemistry of montmorillonite and the mineralized wood indicate that the chemical weathering of primary silicate minerals such as plagioclase may have influenced the chemistry of silicification.

Typically fossil woods in the Petrified Forest do not show annual ring growths, but rather contain irregular growth interruptions similar to those found in trees now growing in the humid tropics. The late Triassic fossil forests probably lived in conditions that permitted continuous growth. The paleomag data indicate that the Chinle was deposited at 18°N latitude--definitely tropical. Some workers have suggested that monsoons were the dominant weather pattern. However, fossil wood evidence does not bear this out.

Other Læte Triassic Flora and Fæuna

Plants

Over 70 well-characterized species of plants occur in the Chinle, representing nearly all major groups. The lower Chinle is dominated by conifers (evergreens), represented by needle and scale leaf fossils. Ferns are the most important element of the of the upper Chinle. The most common ferns had large (20 cm) fronds and have been well-preserved. Other species have been identified only by petrified stems. Spores, pollen, and amber have also helped to identify Chinle plants.

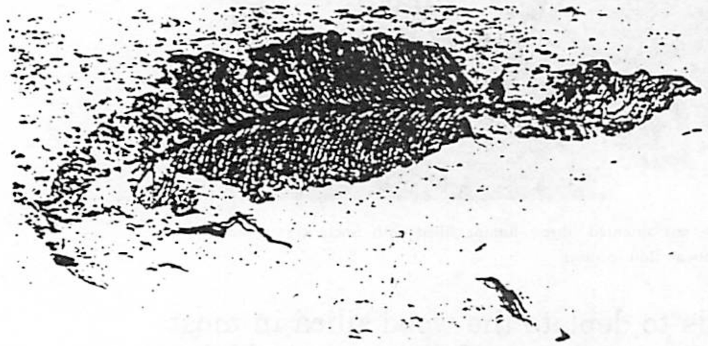

Invertebrates

Invertebrate remains are moderately diverse in the Chinle formation. They are mostly bivalves and gastropods (freshwater mollusks). The distribution of these fossils provides clues about drainage patterns and stream capture events. Insects are represented by tunnels in the petrified wood and by feeding patterns on fossil leaves. Spirochete worms and ostracods (both parthenogenic!) are also found. These fossils indicate permanent water bodies with high electrolyte concentrations (brackish). In 1944, K.E. Caster described a very interesting trace fossil--an early horseshoe crab track made in the Newspaper Sandstone. The occurrence of this track suggests that during this interval of Chinle time, the Petrified Forest area was not very distant from the sea, since the horseshoe crab was an inhabitant of salt or brackish water.

Vertebrates

The vertebrate deposits of the Chinle are among the best in the Triassic of North America. Many sharks, fishes and amphibians are represented, but the most varied and abundant vertebrates are the reptiles. Two types of alligator-like animals appear with short jaws and straight teeth, suggesting carrion feeding. They are well-preserved because of their heavy bone armor, which suggests a rather sedentary life. Another Triassic swamp-dweller was a short-limbed, heavy-bodied, rhinoceros sized reptile, which had a horny beak instead of teeth and ate roots and tubers. Some probable upland dwellers have been reported as well, including herbivorous and carnivorous dinosaurs. Although many small vertebrates must have existed during Chinle time, preservation of skeletal remains is limited to large vertebrates. Reptile tracks have also been found in the channel sandstones interbedded with the Tepees sediments.

Diatremes in the Hopi Buttes Volcanic Field

Andreas Ekholm

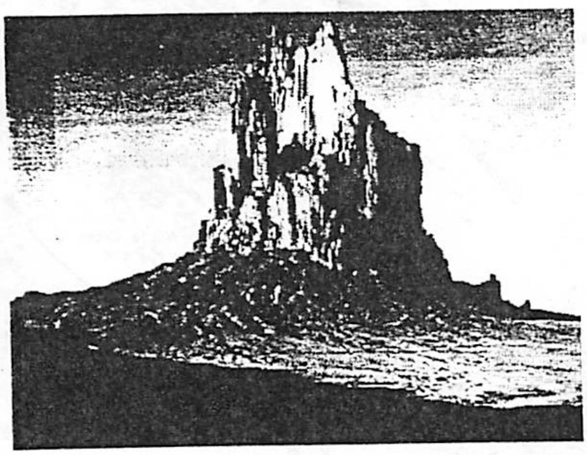

Cover picture: Ship Rock, New Mexico.

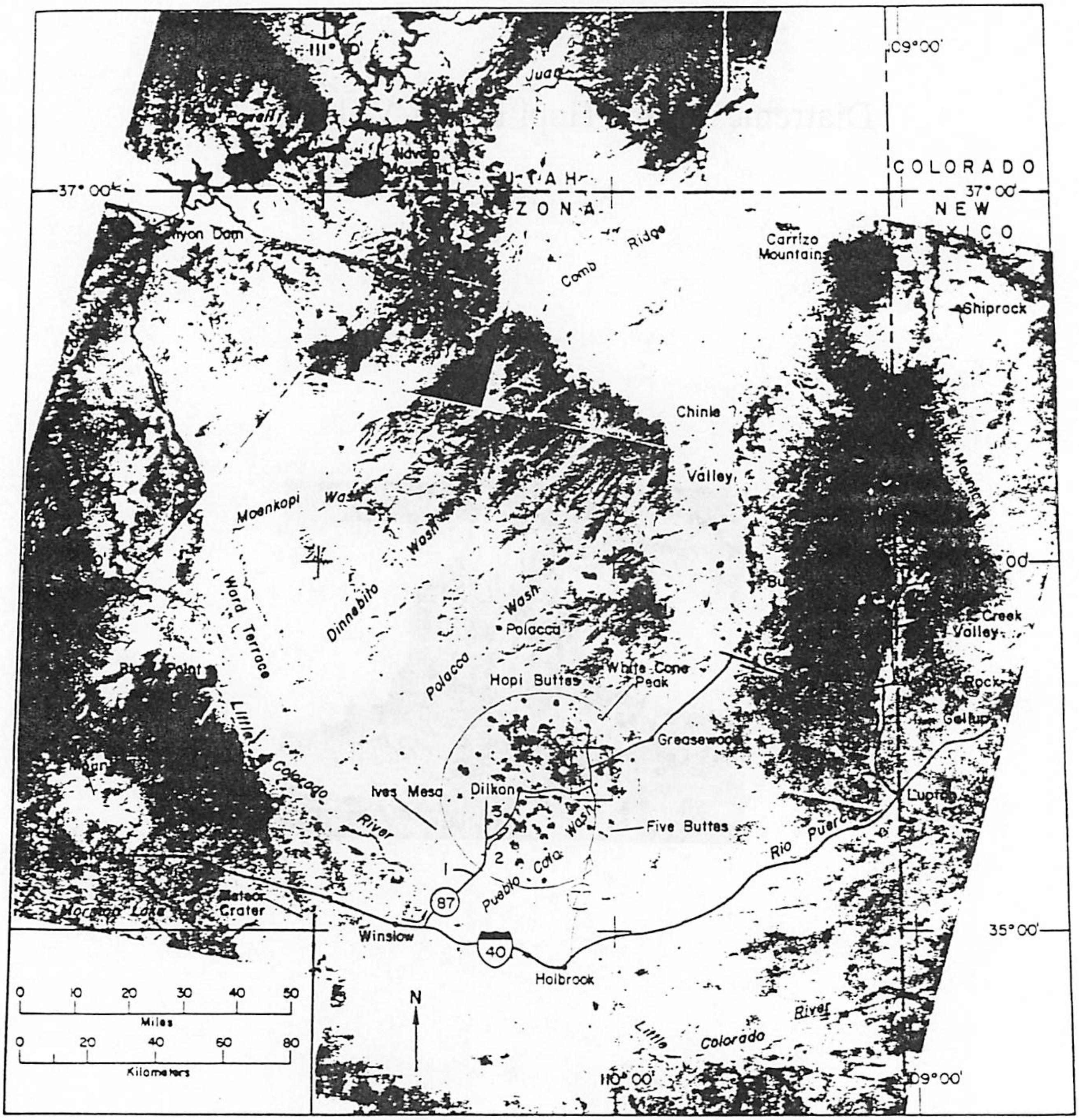

Figure 1. ERTS photomosaic of northeastern Arizona. The diameter of the area enclosed by the circle is 60 km. The small square inside the circle shows the location of the area depicted in Fig. 4.

Introduction

The Hopi Buttes volcanic field covers a roughly circular area ca 65 km (40 miles) in diameter north of Holbrook in northeastern Arizona (Fig. 1). It consists of about 200 extinct eruptive vents of the maar/diatreme type (these terms are defined below, as well as in the Glossary), many of which are aligned along a set of fractures striking northwest and northeast. The vents were active during the Pliocene (2-12 My ago), shortly after the Hopi Lake (which covered approximately the same area) had disappeared (White 1991).

Volcanic plugs

The type of volcanic structure found in the Hopi Buttes is known as a volcanic plug. Volcanic plugs are roughly circular, funnel-shaped structures consisting of solidified magma and/or fragmental volcanic and wallrock materials that have been preserved in the feeding conduits of extinct volcanoes. Because they are typically more erosion-resistant than the surrounding rocks, these formations often become exposed as buttes - isolated hills rising from the surrounding flat, eroded plains (Fig. 2). Volcanic plugs originating in explosive eruptions of highly gas-charged magma are called *diatremes.* They are identifiable as plugs largely or completely consisting of fragmental material.

Explosive eruptions - diatreme formation in the Hopi Buttes

An explosive eruption occurs when rising magma comes into contact with a water source; in the Hopi Buttes, this source is believed to have been wet sediments formed in the Hopi Lake. The water source is incorporated into the rising magma, which thus becomes increasingly gas-rich. Eventually, it reaches a level where the pressure of the overlying rocks is equal to the partial vapor pressure of the magma. The magma then boils, letting the dissolved gases escape through fractures to the surface. The pressure on the upper layer of

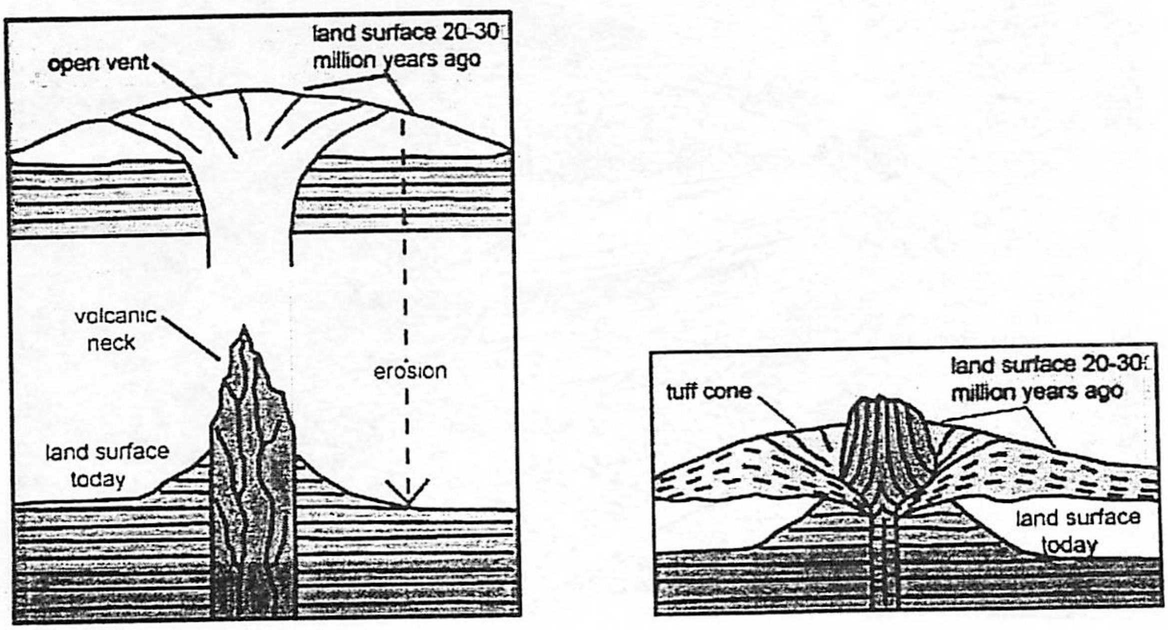

Figure 2a,b. Graphical depiction of the erosion process.

magma thus decreases, allowing underlying magma to boil, releasing more gases, which further decreases the pressure, etc.

As the gas rushes upward towards the surface, it widens the fractures through spalling (the pressure of the gas tearing loose rock fragments) into a central vent, and at the surface forms a crater - a *maar* (Fig. 3).

When the explosive activity ceases, the walls of the crater collapse, filling the vent with fragmental material from the eruption. If the water source is depleted before the eruption ceases, actvity transforms into quiet upwelling of lava, forming a lava dome capping the diatreme.

One of the few maars observed in eruption is the Nilahue maar in the Riñinahue volcanic field in southern Chile. It erupted for about 3.5 months during the summer of 1955. Initially, there were violent gaseous discharges for about 20-30 minutes, interrupted by periods of quiescence. Ejecta - mainly fresh lava and pieces of older rock - was thrown 5-8 km (3-5 miles) into the air and rained down over an area extending more than 200 km (125 miles) from the volcano. The quiet periods slowly grew longer, until activity completely ceased. Stratigraphic evidence suggests that most of the Hopi Buttes vents were similarly short-lived.

When the Hopi Buttes fell silent, the area thus consisted of a plain with low lava domes and numerous maars. This landscape was then eroded down to what we see today - exposed diatremes standing high above the plain, some capped with lava domes, and maars surviving to the present day, overlying still unexposed diatremes below the ground.

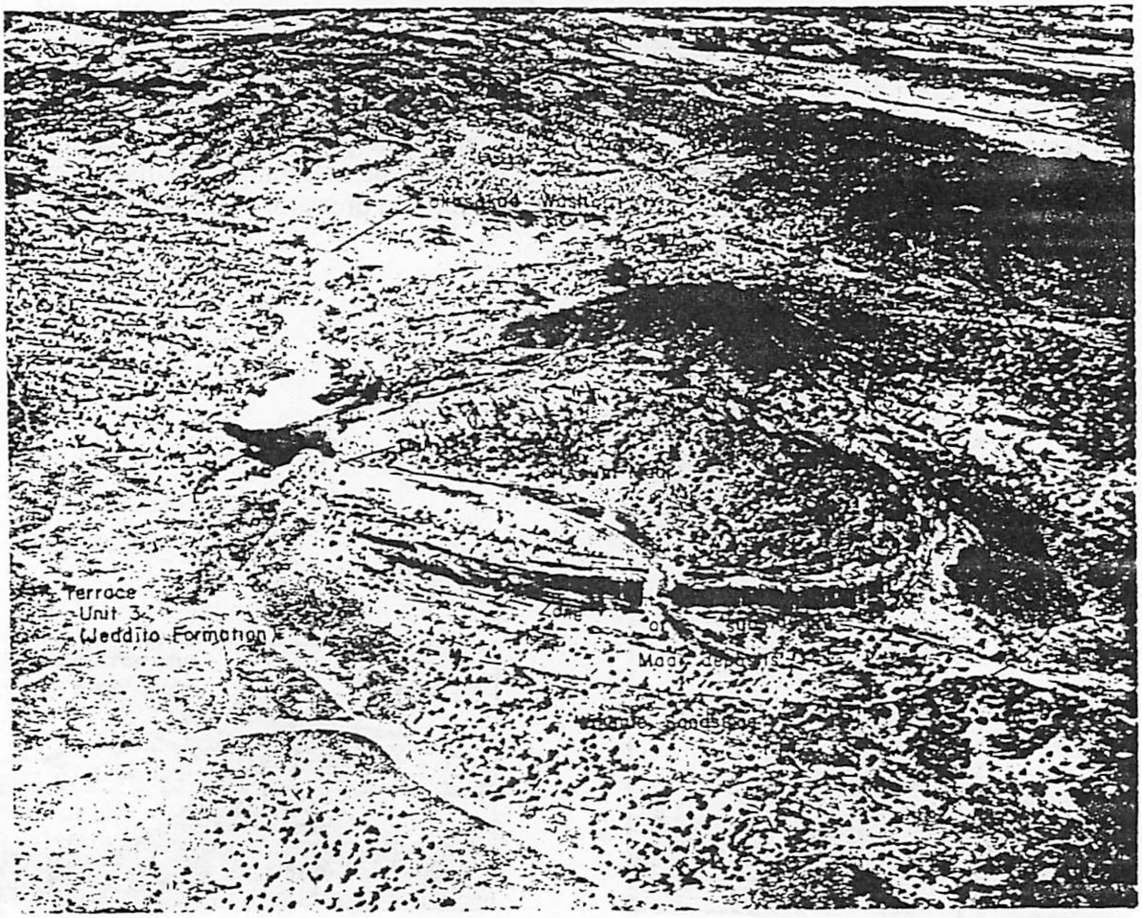

Figure 3. The Coliseum maar in central Hopi Buttes.

Composition of the diatremes

The Hopi Buttes diatremes consist of highly erosion-resistant, basaltic pyroclastic rocks - mainly breccia, agglomerate, tuff and monchiquite. Chemically, the rocks are characterized by a relative deficiency in silica and a greater abundance of several minor elements, including uranium and thorium. The late Eugene Shoemaker conducted several investigations of the uranium deposits in the Hopi Buttes diatremes (e.g. Shoemaker et al. 1962), and concluded that except for a few small, localized high-grade (400-500 ppm U_3O_8) deposits, the uranium content of the rocks was too low for mining to be economically feasible. (Luckily so, who knows how many diatremes would have been left today otherwise.) About one third of the exposed diatremes contain low-grade (a few tens of ppm; 100-200 ppm is considered ore-grade) uranium deposits in carbonate rocks.

Occasionally diatremes contain kimberlite - an ultramafic igenous rock originating deep in the mantle. What's interesting about kimberlite is that it sometimes contains diamonds, something that has been exploited, e.g., by the famous South African diamond industry.

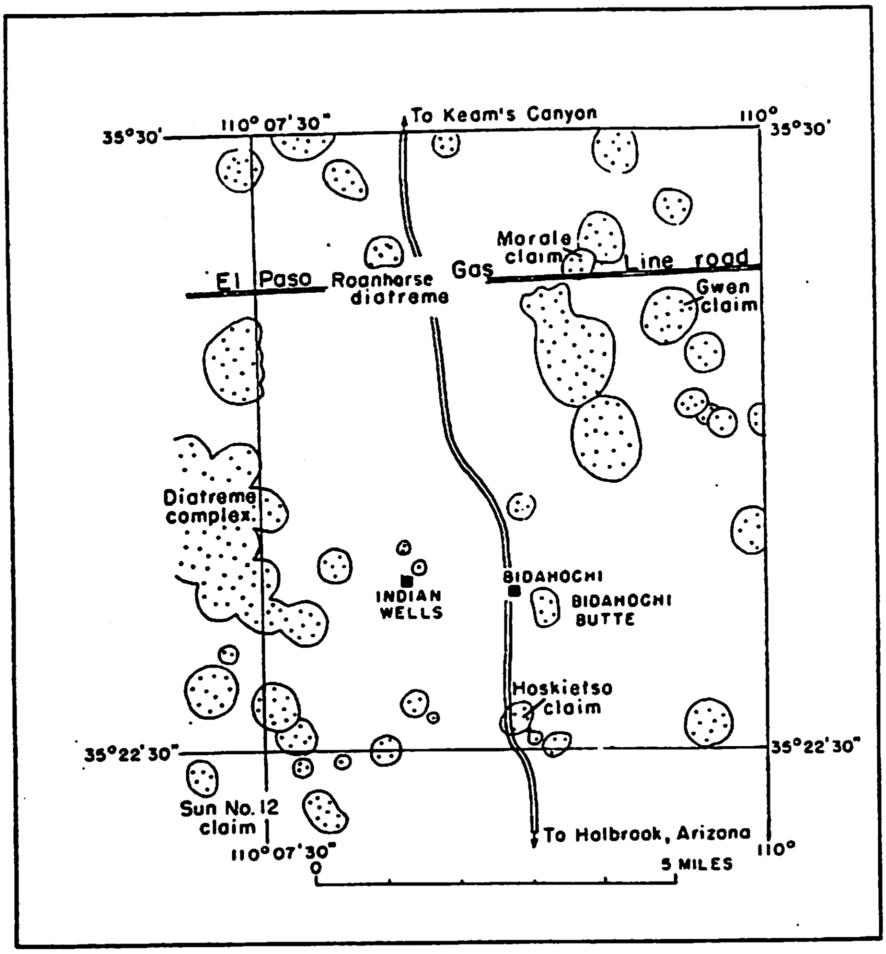

Figure 4. Map showing the locations of diatremes in a part (see Fig. 1) of the Hopi Buttes.

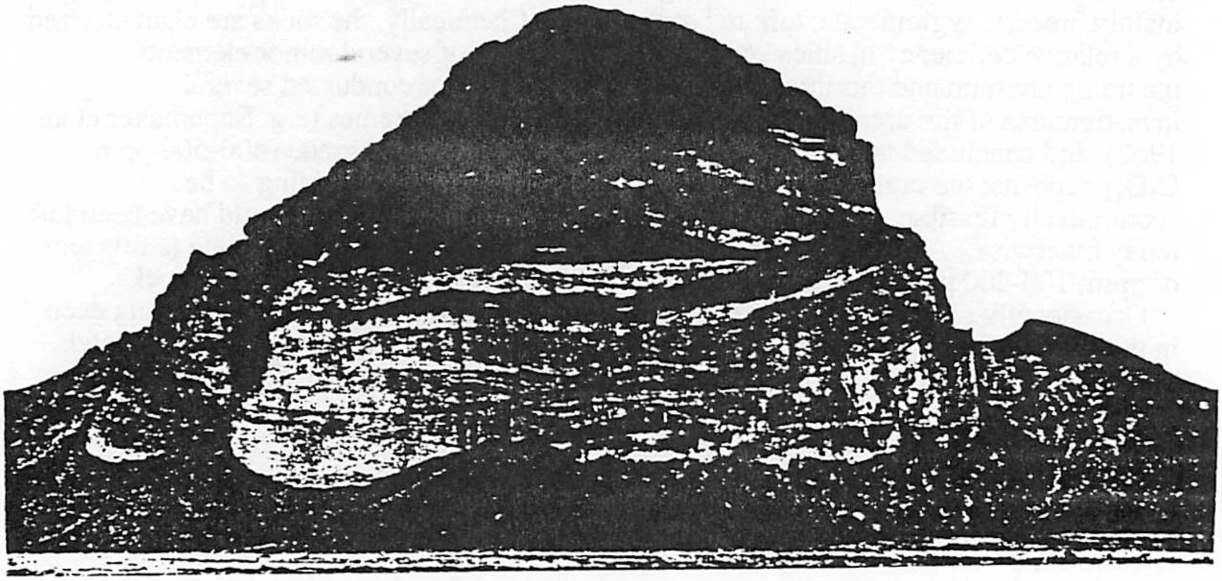

Figure 5. The diatreme at Hoskietso Claim.

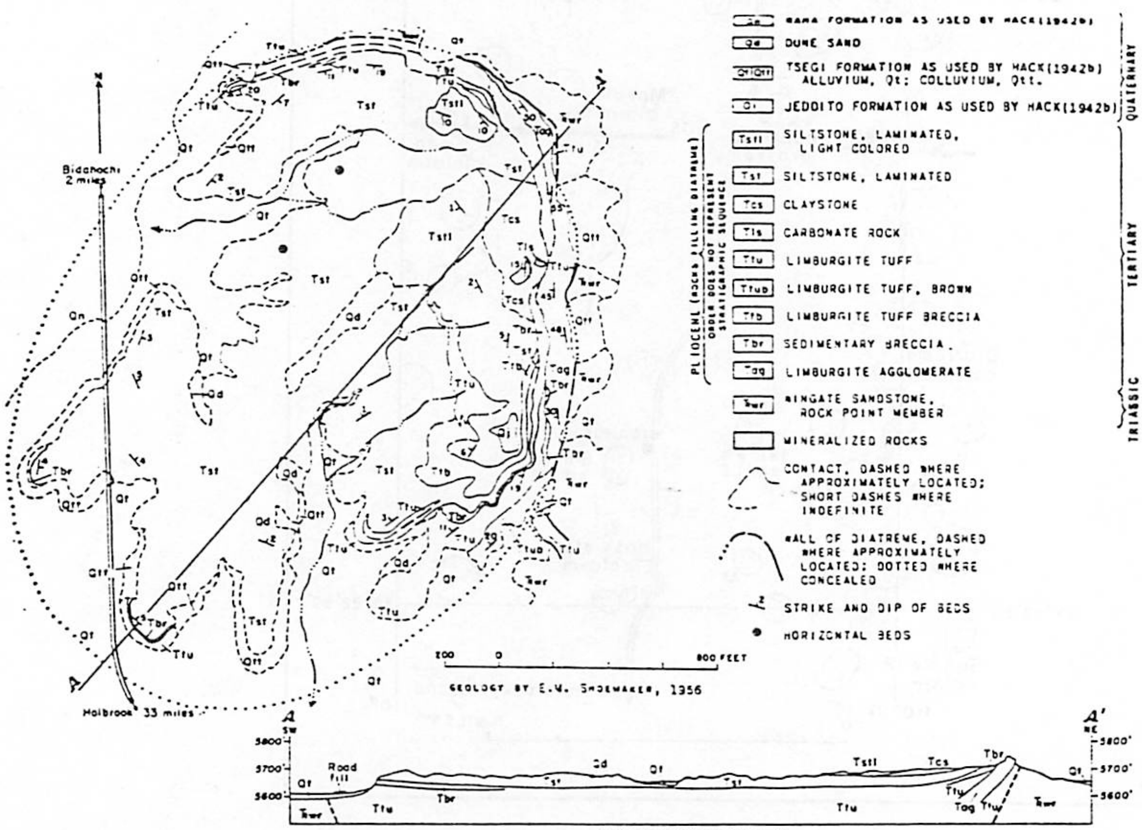

Figure 6. Geologic map and section of the diatreme at Hoskietso Claim.

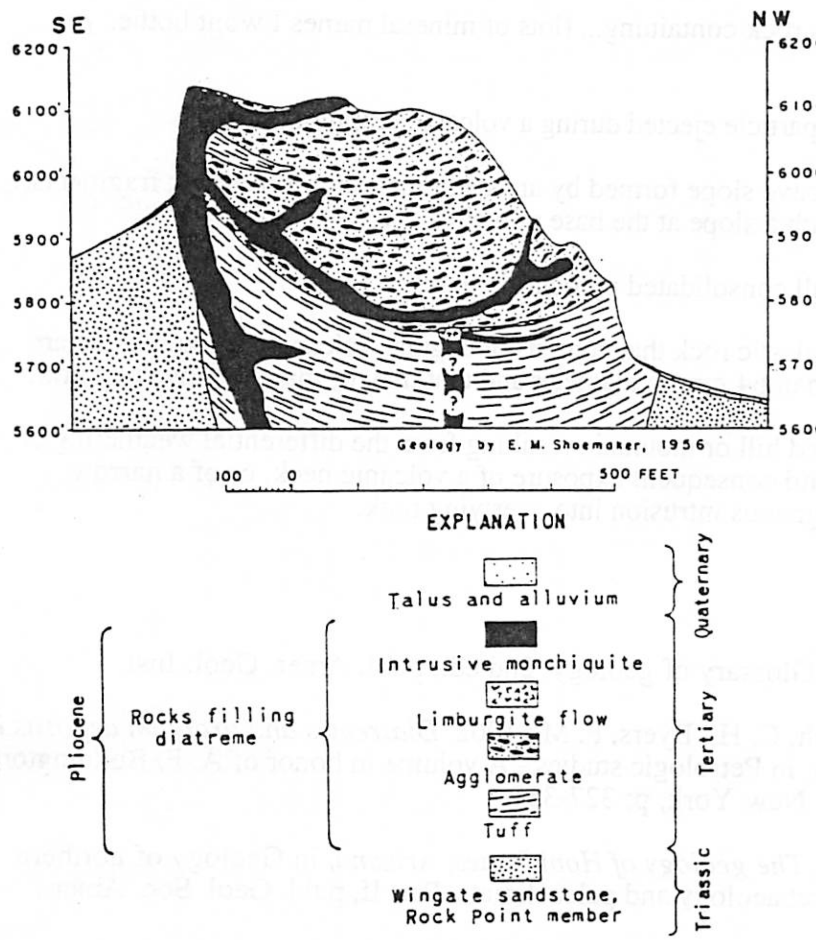

Figure 7. Cross section of diatreme southeast of Hoskietso Claim.

Glossary
(from Bates & Jackson 1980)

agglomerate - A chaotic assemblage of coarse angular pyroclastic materials.

diatreme - A breccia-filled volcanic pipe that was formed by a gaseous explosion.

maar - A low-relief, broad volcanic crater formed by multiple shallow explosive eruptions.

mesa - An isolated, nearly level landmass standing distinctly above the surrounding country, bounded by abrupt or steeply sloping erosion scarps on all sides, and capped by layers of resistant, nearly horizontal rock (often lava).

monchiquite - An igenous rock containing... (lots of mineral names I wont bother you with).

pyroclast - An individual particle ejected during a volcanic eruption.

talus slope - A steep, concave slope formed by an accumulationof loose rock fragments, especially such a slope at the base of a cliff.

tuff - A general term for all consolidated pyroclastic rocks

volcanic breccia - A pyroclastic rock that consists of angular volcanic fragments that are larger than 64 mm in diameter and that may or may not have a matrix.

volcanic butte - An isolated hill or mountain resulting from the differential weathering or erosion and consequent exposure of a volcanic neck, or of a narrow, vertical igneous intrusion into overlying rock.

References

Bates & Jackson, 1980, Glossary of geology, 2nd ed., publ. Amer. Geol. Inst.

Shoemaker, E. M.; Roach, C. H.; Byers, F. M.; 1962, *Diatremes and uranium deposits in the Hopi Buttes, Arizona,* in Petrologic studies - A volume in honor of A. F. Buddington, publ. Geol. Soc. Amer., New York, p. 327-355.

Sutton, Robert L., 1974, *The geology of Hopi Buttes, Arizona,* in Geology of northern Arizona with notes on archaeology and paleoclimate, Part II, publ. Geol. Soc. Amer., Boulder, p. 647-671.

White, James D. L., 1991, *Maar-diatreme phreatomagmatism at Hopi Buttes, Navajo Nation (Arizona), USA,* Bulletin of Volcanology, 53, p. 239-258.

THE ANASAZI: A BRIEF HISTORY

Elisabetta Pierazzo

The settlers whose evolution would lead to the Anasazi culture first crossed a land bridge from Asia into Alaska about 12,000 years ago and followed the Rocky Mountain chain south. They were nomadic hunters and gatherers, called by the archeologist the ***Archaic people***. Remains of their dwellings date back to 9000 B.C. (near Wendover, Utah). The transition toward a warm, dry climate, much like that of the present-day Southwest, caused dramatic changes in animal and plant population. By 6000 B.C. there was less dependence on big game hunting, for the larger animals had migrated, and the Archaic became more domestic, beginning to build baskets and crafting sandals from native materials. By about 5500 B.C., two distinct Archaic traditions had evolved within the Southwest: the Cochise Culture, found south of the Mogollon Rim (Hohokam and Mogollon Groups descend from them), and the Oshara Culture, found to the north and east of the Cochise, on the Colorado Plateau (direct ancestors of the Anasazi). By about 2000 B.C., both Archaic traditions began gardening by nurturing wild plants, even building crude water control systems for them. About the time of Christ, basket making began to proliferate, altering the Archaic way of life so drastically that the early A.D. years are known as Basketmakers. These people are the earliest group of Anasazi.

The original Anasazi homeland is the high tableland of the Colorado plateau, encompassin the Four Corners region of Colorado, Utah, Arizona, and New Mexico.

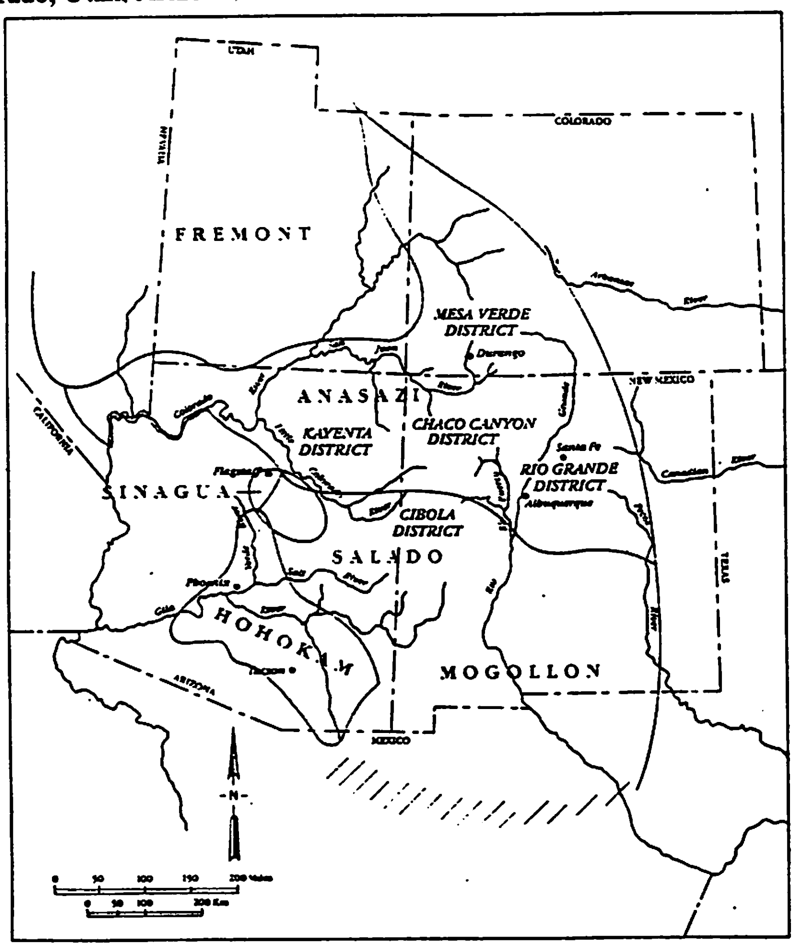

The Anasazi were never politically unified, spoke at least six mutually unintelligible languages, and it is unlikely that they were ethnically homogeneous. Their name comes from and English language corruption of a Navajo Indian work for the many abandoned stone ruins of the Four Corners.

It is a matter of debate whether the original Navajo term meant *"the ancient ones"* or *"enemies of our ancient ones"*.

Since the Anasazi, like most native people of North America, had no written language, our knowledge of them is largely inferential and comes from three primary sources: archeological remains, written records of sixteenth-century Spanish explorers, and traditions of their Pueblo Indian descendants.

The Early Basketmakers

The early Basketmakers (1-500 A.D) lived in alcoves or under overhanging cliffs. They were hunters and gatherers whose major big game weapon was an atlatl (AT-lat-uhl), a notched stick about two feet long which acted as an extension of the spearshaft. The hunter rested the end of his spear on the atlatl, thereby gaining distance and accuracy in his throw.

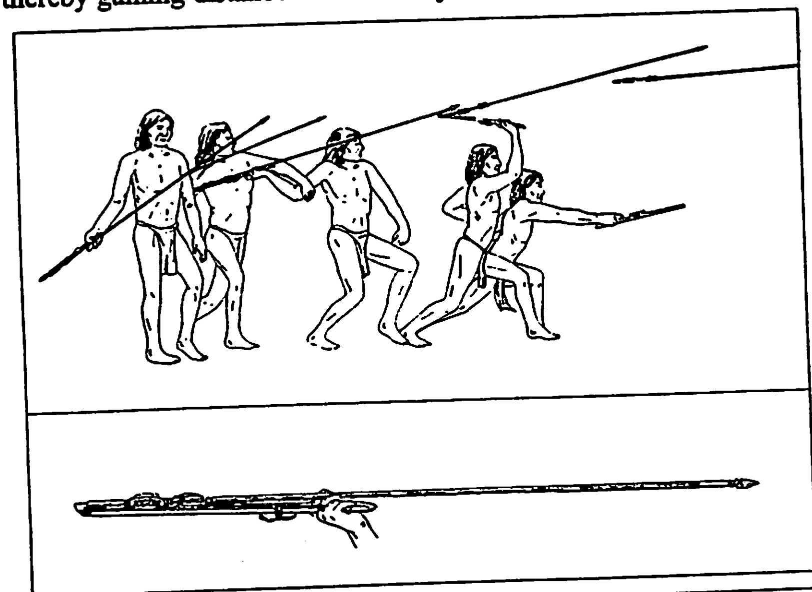

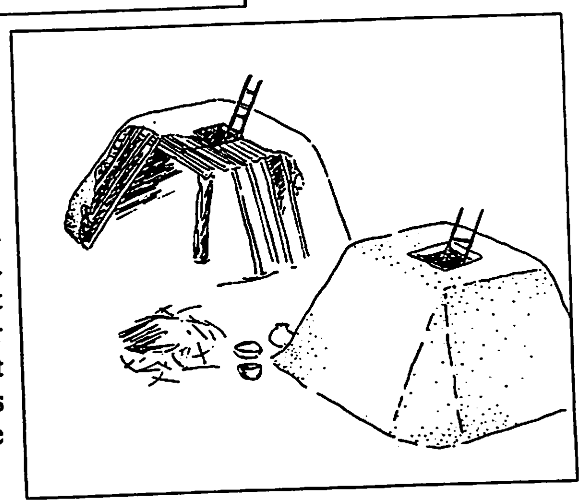

Near the end of the first 500 years, the Anasazi learned to raise corn. Although their farm implements were little more than sharp sticks, farming gradually changed their way of life. It transformed the Anasazi from a nomadic to a sedentary people, making housing more important. The Anasazi moved from cliffs to open areas where they built villages. A village might include a few low, roughly circular houses called "pit houses" that where excavated into the ground, consisting of a shelter of poles and adobe mud, about 15 feet in diameter, built around and above a pit. Entrance to the pithous was usually by way of a ladder placed through a smoke hole in the roof.

The Modified Basketmakers

Between about 500 and 700 A.D. pithouses proliferated and more villages, larger and more widely distributed, were created. Religion may have become more influential, for the people began setting aside special areas of homes or villages for ceremonial events.

Protein-rich beans were addded to the inventory of cultivated foods in about 600 A.D., when crafting of pottery from clay was acquired. With clay pots, women could soak and bake directly over a fire rather than placing hot rocks in a basket of water to "cook" their food. The Anasazi likely learned pottery making from their southern neighbors, the Hohokam or Mogollon. These people fired their pots in an oxygen-rich flame which produced a yellow, tan, or red finish. Anasazi fires were lower in oxygen, and thus created gray pots. Using plant juices or mineral paste as dyes, craftsmen made black designs on gray or white backgrounds, a hallmark of the pottery of the Anasazi on the Colorado plateau.

In the next century cotton and the bow-and-arrow came into general use, in correspondence with the transition to the Pueblo period.

The Developmental Pueblo

Between 700 and 1050 A.D. the transition from pole and mud construction to contiguous flat-roofed adobe houses brought a new name to Anasazi history: the Developmental Pueblo. Initially the dwellings were single story. Later in the period, about 900 A.D., Anasazi architects began designing storied homes with plazas adjoining in a common area. Underground rooms, accessed by a ladder from the living area, where used as ritual rooms and called *kivas*, after their modern Pueblo equivalents. During this period the number of Anasazi communities increased markedly, and expanded into new territories. High risk of agricoltural failure (droughts, untimely rainfall) and continued dependence on hunting promoted the emergence of a pattern of periodic abandonment and reoccupation of canyons and mesa tops, especially in the Anasazi heartland, where many villages were lived in for only about thirty years.

The Classic Pueblo

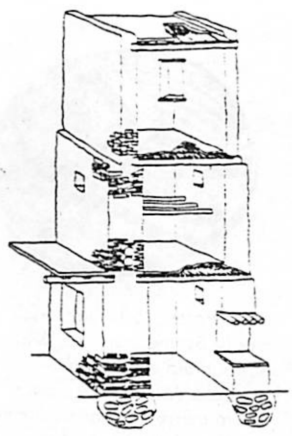

52. The Chaco method for building large, multi-storied houses. The great weight of the upper stories required massive lower walls.

The years 1050-1300 A.D. marked the golden age of the Anasazi. In this period the people crafted their finest, most advanced pottery. They developed excellent methods of farming and irrigation, and generally lived a better life than at any other time in their history. There were many more Anasazi communities than ever before, and many were considerably larger than those of earlier times. Some may have had as many as 5,000-6,000 residents, although it is more probable that the upper limit was about 3,000. To accommodate the increasing population, the Anasazi constructed the grand two-, three-, and four-story apartment-like buildings for which they are best remembered. Villages were built under the shallow overhangs of cliffs with several families comprising a community

During this period, the major regional centers for Anasazi culture were 1) the *Chaco District* (950-1150 A.D.), in Chaco Canyon, 2) the *Mesa Verde District* (1100-1300 A.D.), occupying the areas north and west of the Chaco Canyon, and 3) the *Kayenta District* (1100-1300 A.D.), between the Grand Canyon on the west and Canyon de Chelly on the east.

81. Kayenta-style one-handled pottery bowl from Betatakin at the northern end of Black Mesa. Kayenta polychrome. Ht. 4 ½". Late twelfth century. Indian Art Fund, School of American Research.

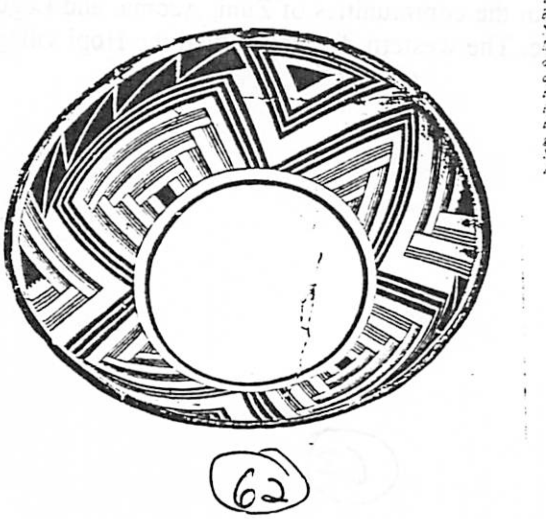

104. Pottery bowl. Mimbres black-on-white, southwestern New Mexico. The tense linearity, fine lines, and use of hachuring as well as black-on-white coloration evidences the strength of Anasazi influence upon the pottery of this southern Mogollon group. Ht. 5". ca. 1100. Maxwell Museum of Anthropology, Albuquerque

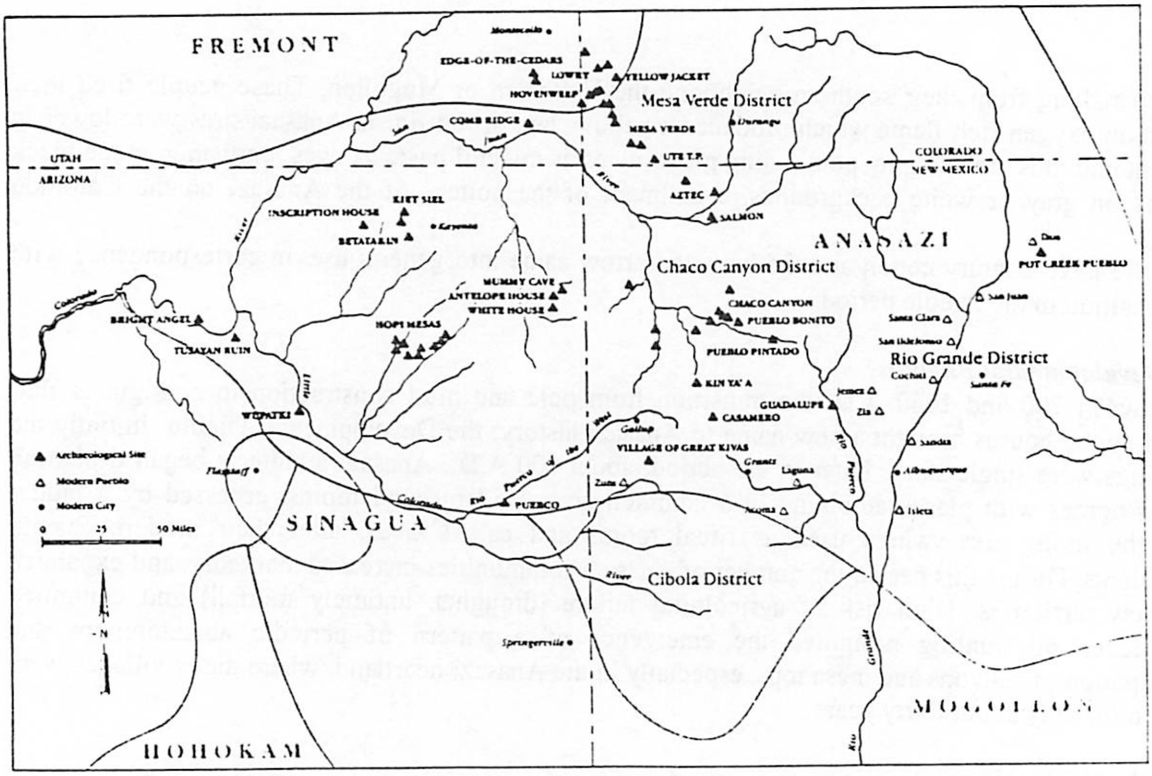

The Pueblo IV Period

This last Anasazi period ends in about 1598 with the first Hispanic settlements, in New Mexico. During this period the culture ceased to advance as it had in the previous 1300 years. It is a period of migrations south and east, lasting several centuries. A portion of the people, the Pueblo Indians, migrated to the upper and middle Rio Grande regions. Other Anasazi moved to existing pueblos in New Mexico and Arizona.

It is possible that, had it not been for arrival of the Spanish in 1540, Anasazi culture might have seen a renaissance. Early Spanish chronicle describe the Anasazi as healthy, industrious, and moderatly prosperous. From the Hispanic perspective, the Anasazi presented a moral and ethical responsibility, for they were a civilized group of souls in need of salvation by conversion to Spanish Catholicism. The influence of Spanish settlers was disastrous to the Indians. Settlers took the Pueblo into slavery, stealed the natives' corn supply and trampling crops they didn't use. The Pueblos were treated so savagedly by the Spanish that a major uprising took place in 1680. The Indians drove the enemy out of their territory for 12 years, but in 1692 the Spanish returned, this time to overwhelm them and occupy.

Today's *Pueblo* are descendants of the Anasazi tradition. After the Spanish invasion, they moved into eastern and western groups. The eastern lived in New Mexico pueblos like Taos and in the communities of Zuni, Acoma, and Laguna in the west central part of the state. The western division settled the Hopi villages of northern Arizona.

82. Pottery bowl, Pinedale polychrome from the White Mountain area of east-central Arizona. The bold asymmetry and iconic forms suggest later Pueblo IV pottery designs while the strong negative patterns and linear precision are reminiscent of western Anasazi Pueblo III wares. Ht. 4 1/2". ca. 1300-1400. Laboratory of Anthropology, Museum of New Mexico, Santa Fe.

History of the Anasazi in Canyon de Chelly

Zibi Turtle

Basketmaker:

Basketmakers appear in the archeological record at Canyon de Chelly between 300 and 420 AD. In Canyon de Chelly alone, ~81 sites had been documented by De Harport (in 1950) who estimated a population of ~100 (again, for Canyon de Chelly, alone). The people were concentrated in the lower sections of Canyon del Muerto and Canyon de Chelly with a few sites in the middle and upper regions of both. Storage bins, graves and artifacts from this period have been found in Mummy Cave, Big Cave, and Battle Cove. Houses were undeveloped, but "cists" were built from slabs of sandstone to store grain.

The Basketmakers depended partly upon hunting and gathering and partly upon horticulture for survival. They hunted deer, jackrabbits, and antelope using atlatls and cultivated corn and squash. Other accomplishments include: expertise in making coiled baskets used, among other purposes, for carrying water and cooking and development of unfired clay vessels (perhaps initially to line baskets).

Modified Basketmaker:

The innovations of the bow and arrow, fired pottery, cultivation of beans and cotton, and domestication of turkeys and dogs, evidence of which appears in the archeological record by ~500 AD, identify the Modified Basketmakers. They occupied the lower canyon (below the junction of Canyon del Muerto and Canyon de Chelly) and the middle sections of both canyons. Only a few sites have been found in the upper canyons, probably due to the lack of land suitable for agriculture. De Harport found only 33 sites from this period in Canyon de Chelly and estimated that its population was ~70.

Pit houses from this period have been found on the plateau as well as in the large caves: Mummy Cave, Big Cave, Antelope House, Tse Ta'a, and Sonic Boom. Pit houses are circular structures, typically 12-25 ft. in diameter and a few ft. deep. The walls and roof were supported by 4 posts and consisted of poles covered by brush and sealed with earth. Pit house floors were made of clay. Early examples had a side entrance and a hole in the roof to provide ventilation, however later these roles became reversed: access was gained through the roof *via* a ladder and a hole in the wall provided extra ventilation, although a stone slab was placed upright between this hole and the central fire pit to deflect the wind. Later these characteristics became important features in the design of kivas.

Developmental and Great Pueblo:

The Developmental Pueblo period is defined by a change in architectural style from separate, circular pit houses to contiguous, rectangular rooms built above ground, which occurred between 800 and 900 AD, and the development of kivas. At Canyon de Chelly the early Developmental Pueblo continued to build pit houses with sandstone slabs supporting upper jacal (wattle and daub) walls. From 850-1050 AD there was little population growth, but the population became concentrated into a few large caves: Antelope House, Tse Ta'a, Sonic Boom, Big Cave, Mummy Cave, and Yucca Cave.

Between 1050 and 1150 AD the population grew rapidly; De Harport found 301 sites in his survey of Canyon de Chelly and estimated that the population had grown to over 500 by ~1150 AD. Construction was begun at the lower White House site in 1050 and at Battle Cove and Ledge Ruin at similar times. Single-story masonry pueblos were also built on the Defiance Plateau during this period. The styles of architecture and ceramics found at the lower White House ruins, Tse Ta'a, and Wild Cherry Ruins from this period have a strong Chaco influence, *e.g.*, rubble core masonry walls, suggesting immigration from the east (the Anasazi sites in Chaco Canyon were abandoned by 1130 AD). The central block and tower in Mummy Cave (which dates to 1284 AD) and some of the walls at Tse Ta'a display the architectural style of the Mesa Verde (or Northern

San Juan) Anasazi -- large sandstone blocks with little adobe mortar -- suggesting a later immigration from the northeast.

By 1150 AD the use of the plateau had ceased (perhaps due to a local drought which lasted from 1140-1180 AD) and the population was concentrated in the cliff villages. De Harport documented 67 Great Pueblo sites in Canyon de Chelly and estimated that they housed ~800 people. However, the population declined rapidly. Antelope house was abandoned by 1270 AD. The last village to be occupied was Mummy Cave which, despite construction in 1284 AD, was abandoned by ~1300AD.

References:

Brody, J.J., *The Anasazi: Ancient Indian People of the American Southwest*, Rizzoli International Publications, Inc., 239pp., 1990.

Dean, Tse Ya'a Kin: Houses beneath the rock, in *House Beneath the Rock: The Anasazi of Canyon de Chelly and Navajo National Monument*, Noble, D.G., Ed., Ancient City Press, Santa Fe, NM, pp. 2-13, 1986.

De Harport, D.L., An Archaeological Survey of Cañon de Chelly: Preliminary Report of the Field Sessions of 1948, 1948, and 1950. *El Palacio*, **58** (2), pp. 35-48, 1951.

Fall, P., The Anasazi of Canyon de Chelly, in *House Beneath the Rock: The Anasazi of Canyon de Chelly and Navajo National Monument*, Noble, D.G., Ed., Ancient City Press, Santa Fe, NM, pp. 34-41, 1986.

Grant, C., *Canyon de Chelly: Its People and its Rock Art*, Univ. of Arizona Press, Tucson, AZ, 290pp., 1978.

Judge, W.J., *The Anasazi: Why did they leave? Where did they go?: a panel discussion at the Anasazi Heritage Center. Dolores. CO*, Southwest Natural and Cultural Heritage Assoc., Albuquerque, NM, 71pp., 1991.

Matlock, G. And Warren, S., *Enemy Ancestors: The Anasazi World with a Guide to Sites*, Northland Press, Flagstaff, AZ, 116pp., 1988.

Mindeleff, Cosmos, The Cliff Ruins of Canyon de Chelly, Arizona, *16th Annual Report of the Bureau of American Ethnology*, pp. 73-198, 1894-1895.

Grant, 1978

Fig. 2.1 SAN JUAN DRAINAGE CULTURAL CHRONOLOGIES

Pecos Classification 1927	Roberts' Classification 1935	Date A.D.
Pueblo III	Great Pueblo	1300 1200 1100
Pueblo II	Developmental Pueblo	1000 900
Pueblo I		800 700
Basketmaker III	Modified Basketmaker	600 500
Basketmaker II	Basketmaker	400 300 200 100

Postulated Basketmaker I

Grant, 1978

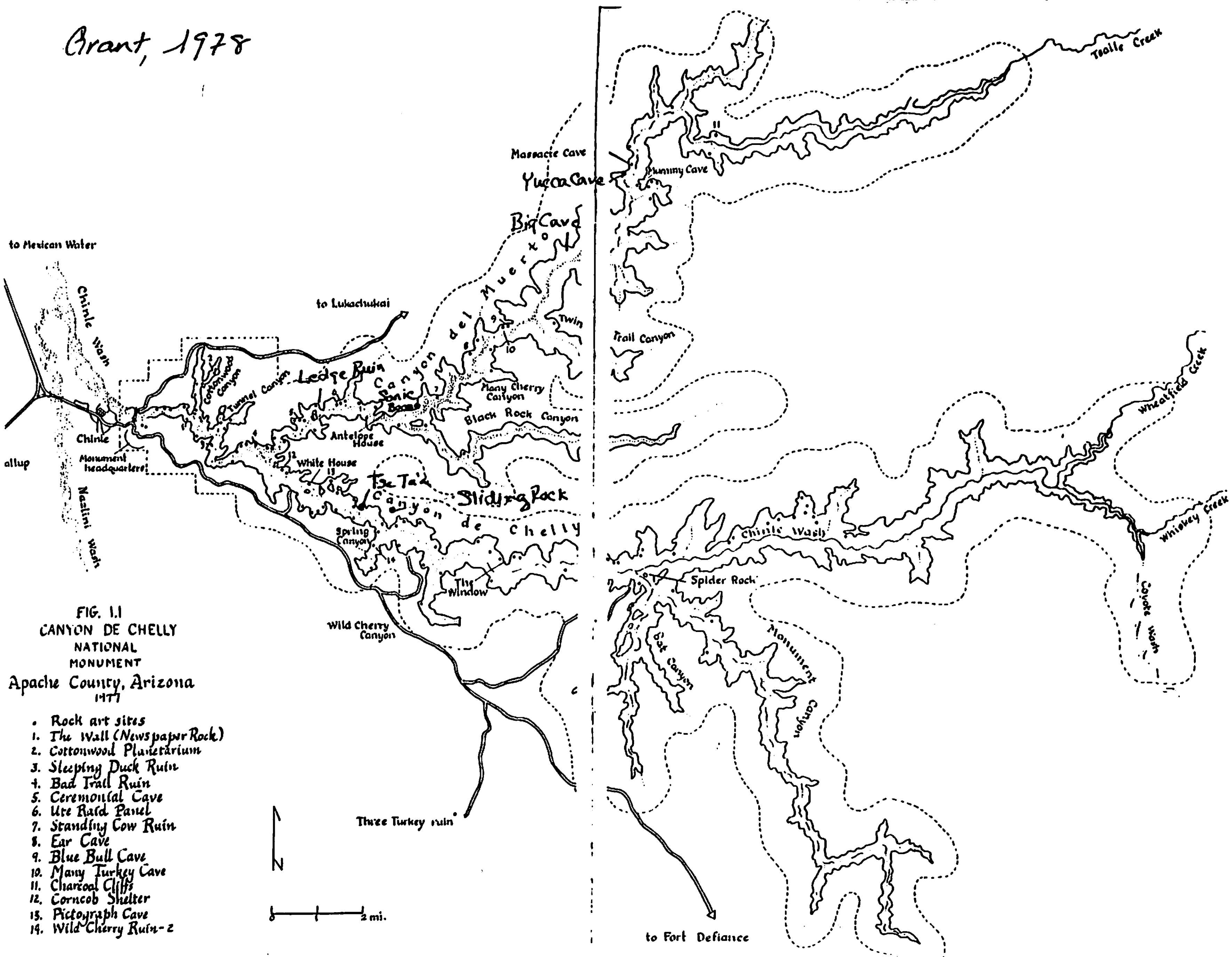

FIG. 1.1
CANYON DE CHELLY
NATIONAL
MONUMENT
Apache County, Arizona
1977

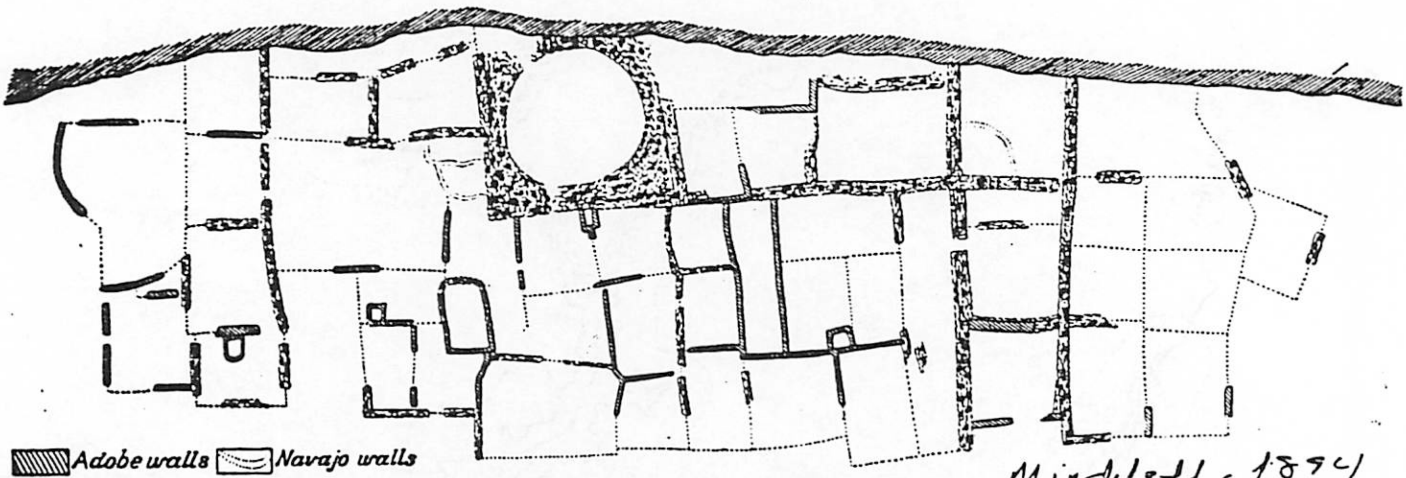

Fig. 14—Ground plan of the lower part of Casa Blanca ruin. Mindeleff, 1894

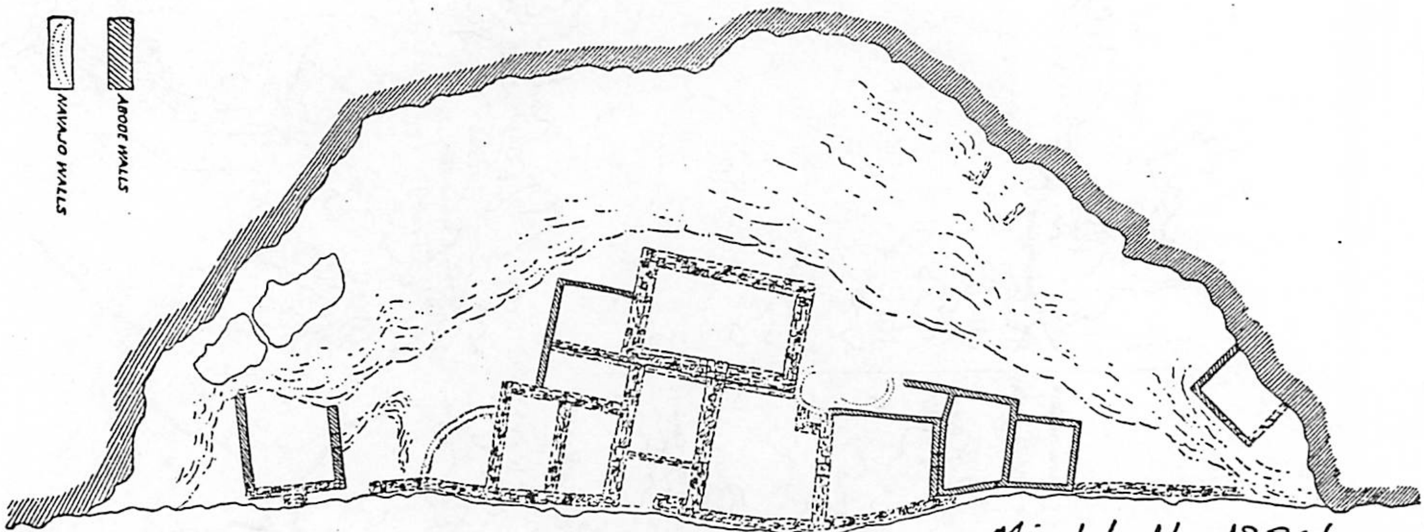

Fig. 15—Ground plan of the upper part of Casa Blanca ruin. Mindeleff, 1894

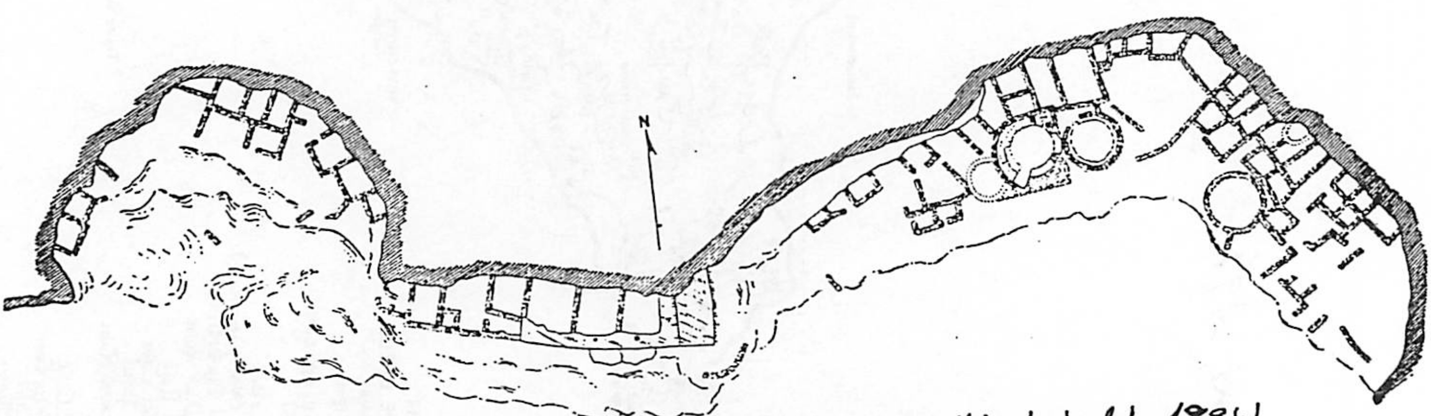

Fig. 16—Ground plan of Mummy Cave ruin. Mindeleff, 1894

Sapping Landforms, Arizona and Mars

Adina Alpert & Ross Beyer

Groundwater sapping is a generic term for weathering and erosion of soils and rocks by emerging groundwater.

Morphologic characteristics:

- Valleys terminate in steep-walled headcuts which are described as cuspate or theater-shaped.
- Sidewalls are near-vertical.
- Main valleys are long, and tributaries are short and stubby.
- Drainage segments are relatively straight with apparent structural control.
- Erosion is sensitive to permeability boundaries rather than to local baselevel.

Characteristic requirements for groundwater sapping:

These are the limiting constraints which make sapping much less common than fluvial erosion.

- a permeable aquifer
- a rechargeable groundwater system
- a free face at which the subsurface water can emerge
- some form of structural or lithologic inhomogeneity, such as jointing or dikes, that locally increases the hydraulic conductivity and along which valleys grow
- a means of transporting material released from the scarp face

Sapping valley networks differ from fluvially eroded networks in:

- morphology
- pattern
- spatial evolution of network
- rate of erosion
- degree of structural control

These valleys grow headward by successive slab failure, aided by processes that break down the debris produced by slope collapse and transport away the disintegrated materials.

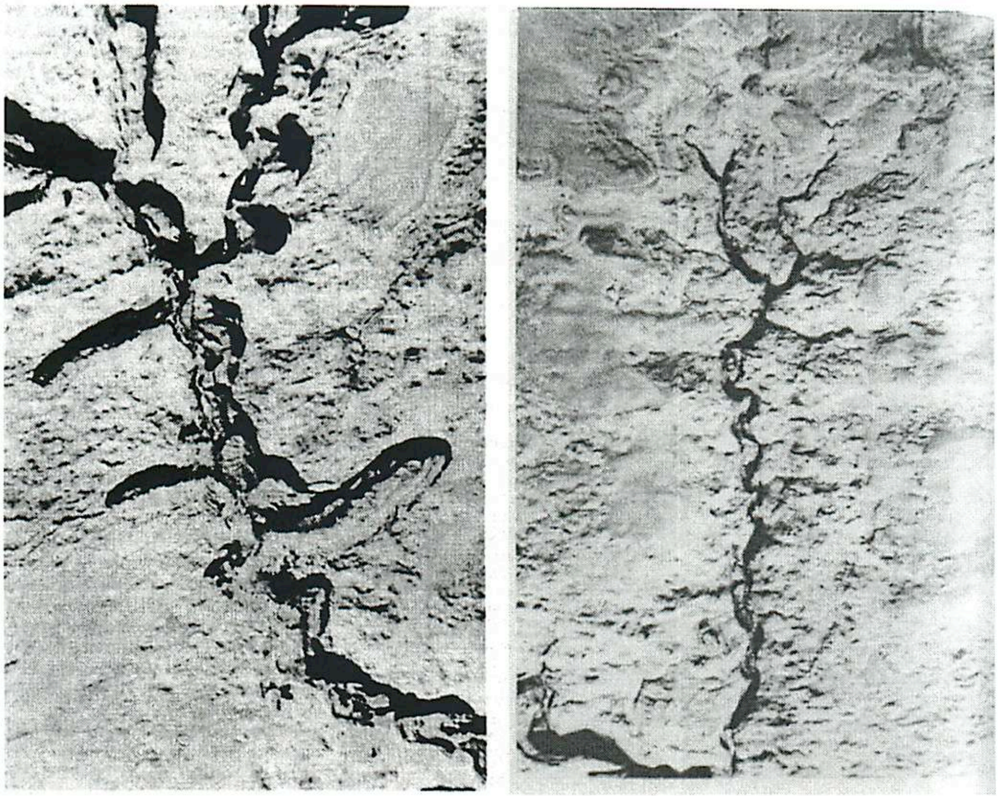

A B

Figure 1 – The development of two morphologically distinct valley types within the Navajo Sandstone. The theater-headed terminations in (A), Iceberg Canyon, indicate development by sapping processes. The canyon is developed within a gently dipping syncline, and ground water is focused toward the canyon walls. The tapered terminations of (B), a tributary to the lower Escalante River from the west, suggest predominant erosion by overland-flow processes. In this region, ground water flows downdip and away from the valley headwalls.

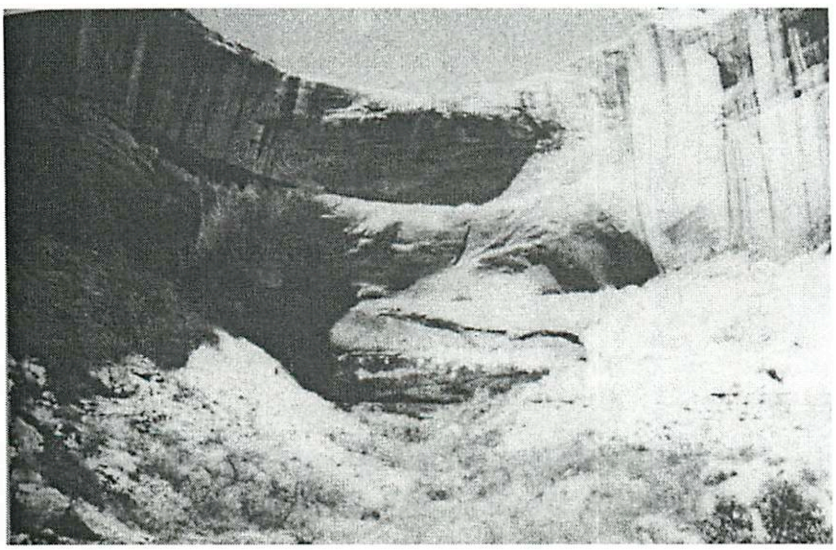

Figure 2 – The theater-shaped headwall of Explorer Canyon.

Terrestrial Sapping

The most extensive sapping valley network is in the Navajo Sandstone of southern Utah.

Fracturing increases the overall permeability of a plateau surface and increases the contribution of precipitation to the groundwater system. The fractures also act at depth to increase the transmissivity of the bedrock, and laterally flowing groundwater exploits major joints. The water subsequently emerges at seepage points along cliff faces, and the canyons migrate headward along joint trends. This process causes the collapse of massive sandstone slabs as sapping undermines steep cliff faces.

Groundwater is sensitive to changes in gradient resulting from regional folding. Therefore, theater-headed valleys are observed to grow in up-dip direction.

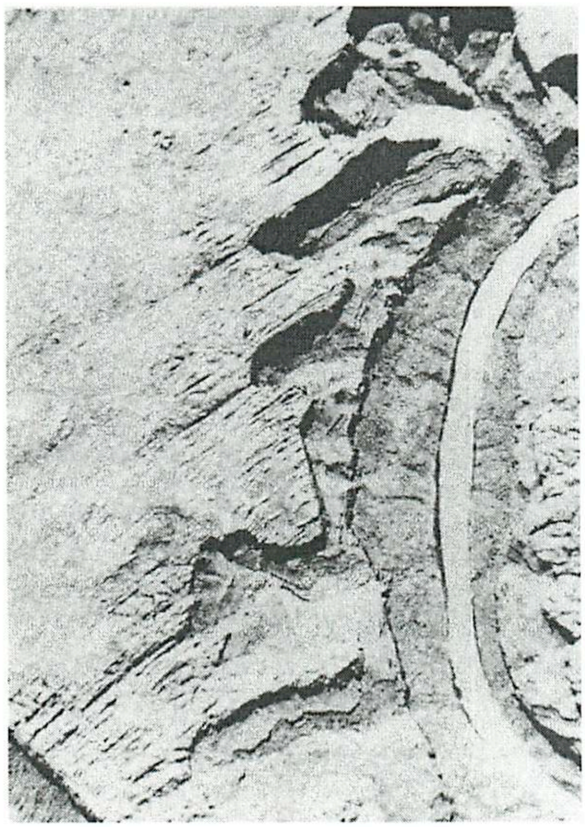

Figure 3 – Aerial photograph of small (1km or less in length) tributary canyons to the Colorado River. The direction of the canyon growth is updip and parallels the strike of joints exposed in the Navajo Sandstone.

Theater-headed valleys are principally found on surfaces with low dip angles (1°–4°). As bed dip or topographic slopes steepen, surface runoff increases and canyon morphology tends toward forms with tapered heads.

Time evolution of a sapping valley:

- The initial growth of the main canyon is more rapid than that of tributary canyons because of its larger subsurface drainage area.
- In time, a network of canyons may result from headward retreat.
- Headward growth rates probably decline as the system enlarges and the drainage area of springheads lessens.
- During more advanced stages, the rate of lateral retreat by sidewall seepage approaches that of headward retreat. Therefore, the valley widens.
- The valley may continue to grow until adjacent tributaries merge. This results in isolated buttes with remnants of the original surface.

Martian Sapping

Some Martian Valley networks show evidence for possible groundwater sapping. It is thought that the Martian regolith is highly permeable and therefore conducive to sapping processes. Similarly, many Martian channels show morphologic similarity to terrestrial sapping channels. Even though most of the characteristics that we list above as indicative of sapping can be applied to some Martian valley systems, there are a few important caveats to the sapping hypothesis that need to be taken into consideration.

What is the source of the Martian groundwater and was it capable of maintaining a constant head over time scales long enough to form the features we interpret as sapping features?

The scale at which the Martian features were observed and interpreted (Viking Images) is many times larger than that of Terrestrial sapping features. Will higher resolution Mars Global Surveyor images change our interpretation or reinforce it?

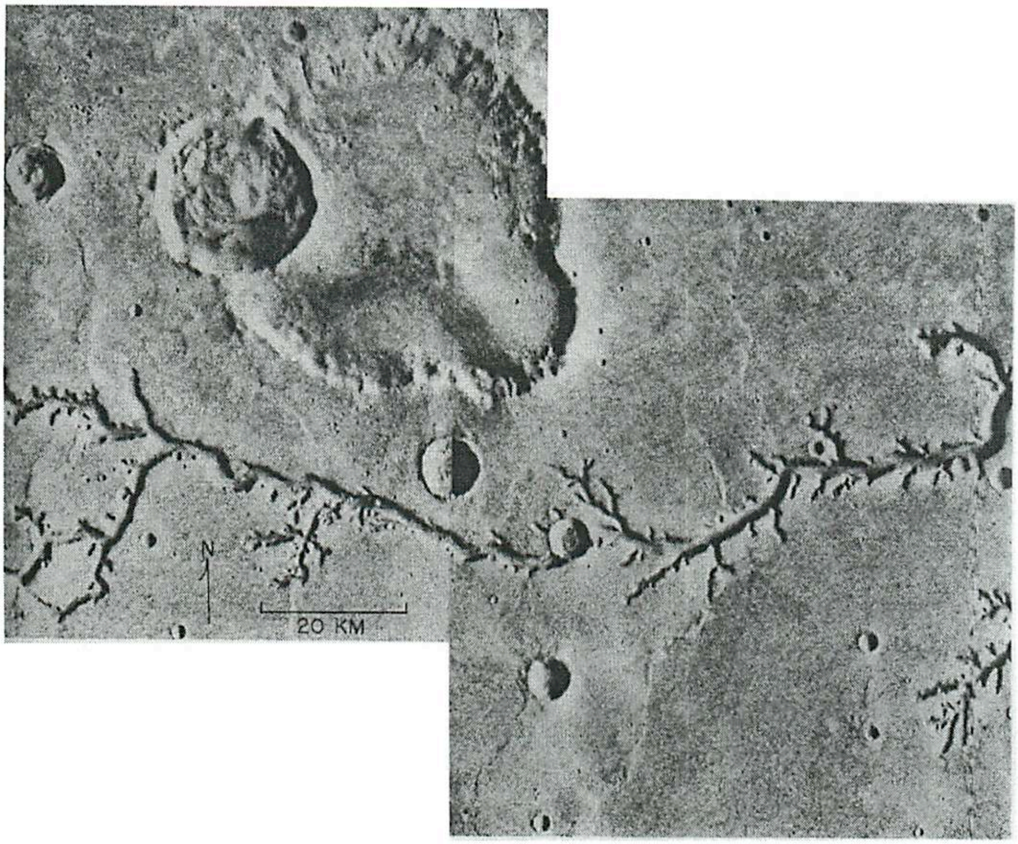

Figure 4 – Viking spacecraft orbital photographs of a portion of Nirgal Vallis, a valley network formed by probable sapping processes on Mars. Compare it to the airbrush map of Canyon de Chelly at the beginning of this booklet.

References

Baker, V.R. *et al.*, 1990, Chapter 11, 'Spring sapping and valley network development,' *Geol. Soc. Amer.*, Special Paper 252. Higgins, C. G. & Coates, D.R., eds.

Baker, V.R. *et al.*, 1992, Chapter 15, 'Channels and Valley Networks,' from *Mars*, Kieffer, H.H., Jakosky, B.M., Snyder, C.W., & Matthews, M.S., eds., University of Arizona Press, Tucson.

Howard, A.D., Kochel, R. C., & Holt, H.E., eds., 1988, *Sapping Features of the Colorado Plateau*, NASA Special Publication SP-491.

Laity, J.E. & Mailn, M.C., 1985. 'Sapping processes and the development of theater-headed valley networks on the Colorado Plateau,' *Geol. Soc. Amer. Bull.* 96:203-217.

Geology and Stratigraphy of the Colorado Plateau and the Canyon de Chelly Region

Peter Lanagan and Jason Barnes

Canyon de Chelly trip, Fall 1998, September 17-19

The Colorado Plateau is a large region of the 4 corners area around Arizona, New Mexico, Colorado, and Utah which has all experienced a similar geologic history. Throughout the majority of its existence, the Colorado Plateau was at a relatively low elevation and was repeatedly covered and uncovered by seawater. The first evidence of these marine transgressions comes from the Cambrian period, but transgressions followed by regressions during the late Devonian, Mississippian, Permian and on into the Jurassic and Cretaceous periods during the Mesozoic Era also occurred. Interspersed with these marine deposits are periods of fluvial depositions indicitive of a continental environment and unconformities indicating times of net erosion of the surface layers. The single event that has most affected the present-day appearance of the Plateau was a time of folding and faulting called the Laramide Orogeny which took place slowly during the late Cretaceous and Early and Middle Tertiary periods. Although most of the features extant on the Plateau were not initially formed during Laramide time, nearly all of these features were affected and altered by this orogeny as existing underlying crustal weaknesses were reactivated by new tectonic stresses. Also during this time the entire Plateau was uplifted relative to the surrounding lands, the entire uplift process adding between 4000 and 6000 feet of elevation to the Plateau region. Smaller features such as the Kaibob, Zuni, and Defiance (into which Canyon de Chelly is cut) uplifts were also created at this time while the basins between them were subsiding. As a result of the fracturing created by the orogeny a rash of volcanism erupted during the first half of the Tertiary period, resulting in the many extrusive basalt features seen across the Plateau. Since the uplift, relentless erosion began wearing away the lower strata and this stepped-up erosion has continued to the present day.

Bibliography :

Baars, Donald L. The Colorado Plateau: A Geologic History, 1983, Albuquerque, University of New Mexico Press.

Blakey, Ronald C., and Rex Knepp, Pennsylvanian and Permian Geology of Arizona in Jenny, J.P., and Reynolds, S.J., 1989, Geologic Evolution of Arizona: Tucson, Arizona Geological Society Digest 17, p1-16.

Dickenson, William R. Tectonic Setting of Arizona Through Geologic Time. in Jenny, J.P., and Reynolds, S.J., 1989, Geologic evolution of Arizona: Tucson, Arizona Geological Society Digest 17, p 1-16,

Kamill, R.J. and Richard, S.M., editors, 1998, Geologic Highway Map of Arizona: Tucson, Arizona Geological Society and Arizona Geological Survey.

Nations, D. and Stump, E. Geology of Arizona. 1996, Dubuque, Kendall/Hunt Publishing Company.

(Dickenson, 1989)

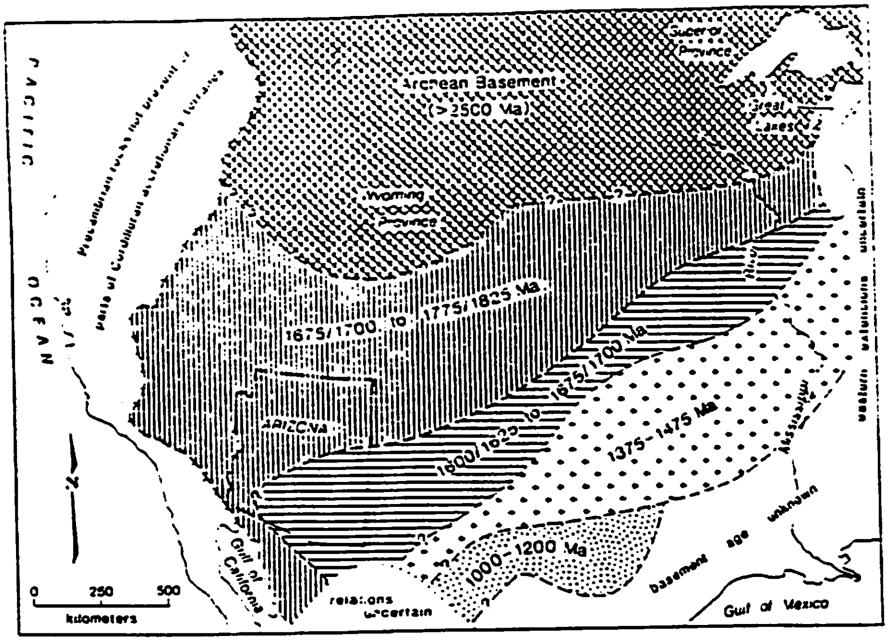

Figure 1. Proterozoic position of Arizona in relation to Precambrian age belts (simplified) of the North American craton. Modified after T. H. Anderson and Silver (1979), Van Schmus and Bickford (1981), J. L. Anderson (1983), Kartstrom and Houston (1984), and Thomas and others (1984).

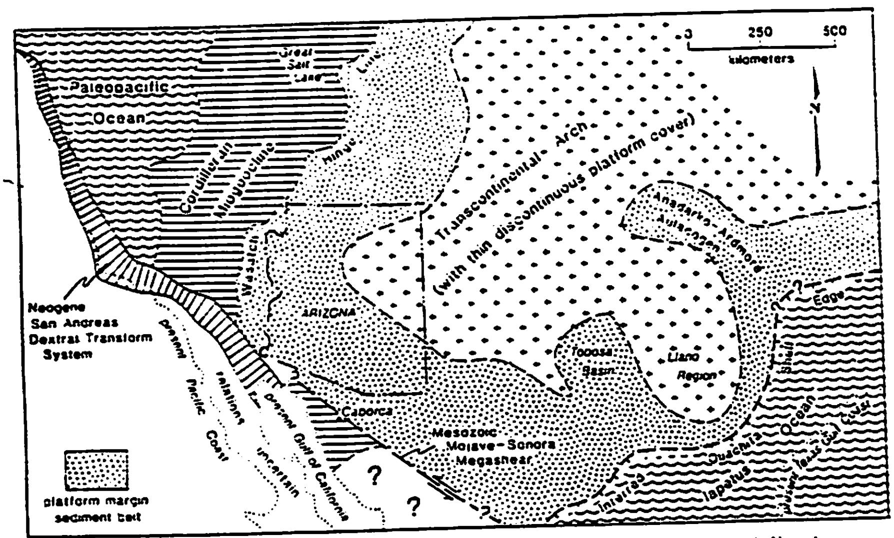

Figure 2. Early to middle Paleozoic position of Arizona in relation to passive continental margins formed by continental rifting in latest Precambrian (to Cambrian) time. Modified after Peiffer-Rangin (1979), Dickinson (1981), Gutschick and Sandberg (1983), and Stewart and others (1984).

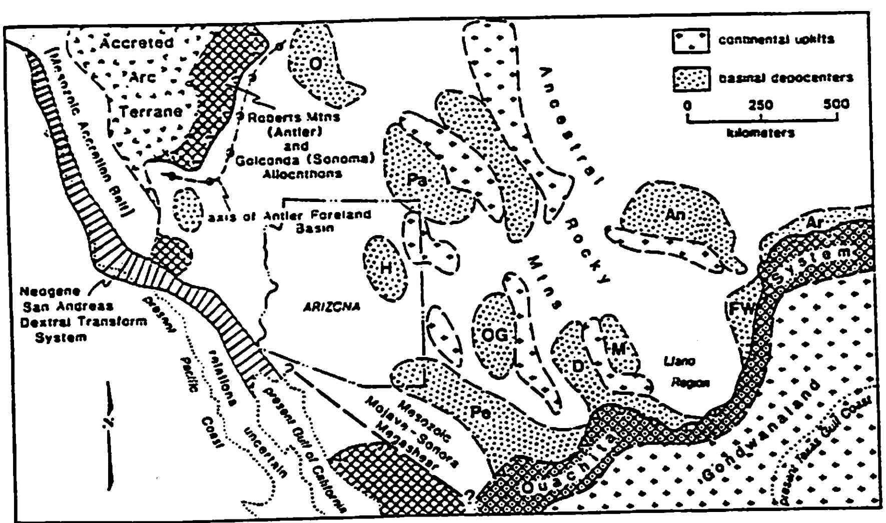

Figure 3. Late Paleozoic position of Arizona in relation to orogenic belts along the Cordilleran and Ouachita continental margins. Modified after Speed (1979), Dickinson (1981), Kluth and Coney (1981), and Dickinson and others (1983). Selected basins: An, Anadarko; Ar, Arkoma; D, Delaware; FW, Fort Worth; H, Holbrook; M, Midland; O, Oquirrh; OG, Oro Grande; Pa, Paradox; Pe, Pedregosa. The Defiance-Zuni uplift extends into northeastern Arizona.

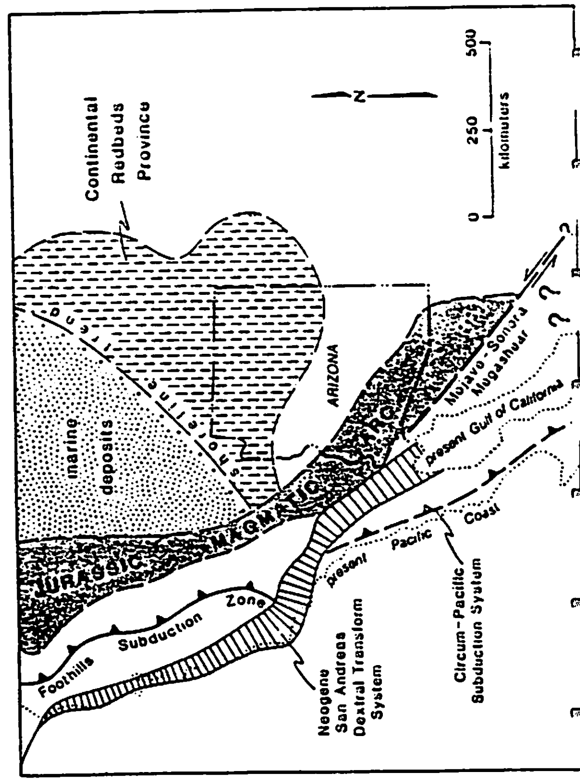

74

Dickenson, 1989

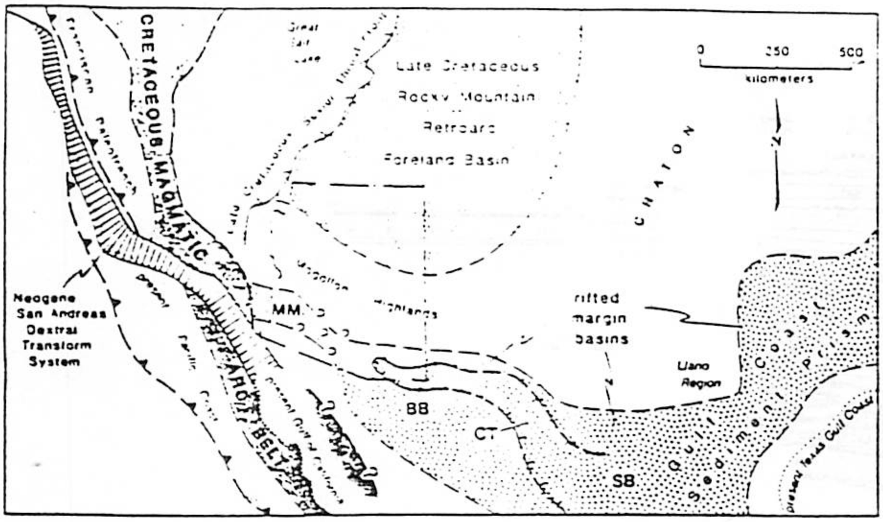

Figure 5. Late Mesozoic position of Arizona in relation to Cretaceous sedimentary basins, the Franciscan paleotrench system, and a Cretaceous magmatic arc delineated by the coastal batholith belt of the Sierra Nevada and Peninsular Ranges. Modified after Dickinson (1981) and Bilodeau (1982). Hachured line denotes Early Cretaceous backarc depocenter (aulacogen) of Bisbee basin (BB) and Chihuahua trough (CT); SB, Sabinas basin; MM, McCoy Mountains Formation and correlatives (see text for discussion).

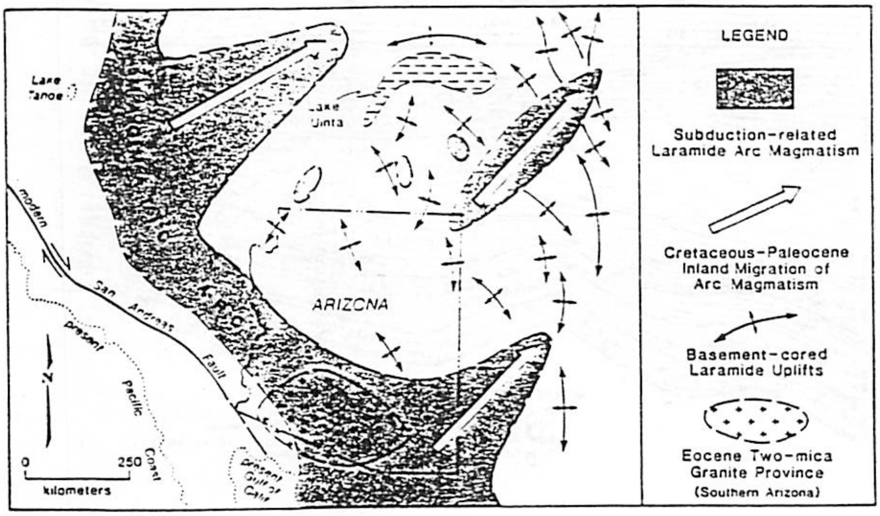

Figure 6. Latest Cretaceous and early Cenozoic position of Arizona in relation to Laramide magmatism and deformation. Modified after Dickinson (1979, 1981), Reynolds (1980), and Keith (1984).

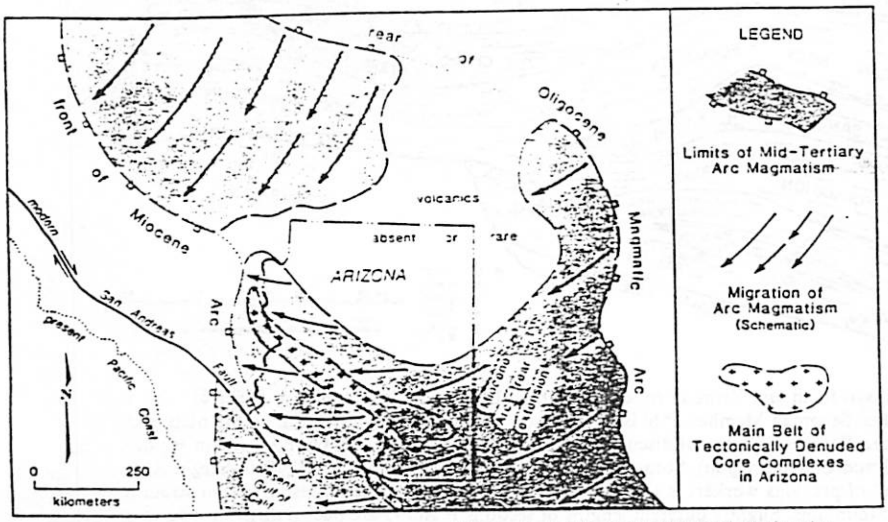

Figure 7. Mid-Cenozoic position of Arizona in relation to migratory mid-Tertiary arc magmatism and associated extensional deformation. Modified after Coney (1979) and Dickinson (1979, 1981).

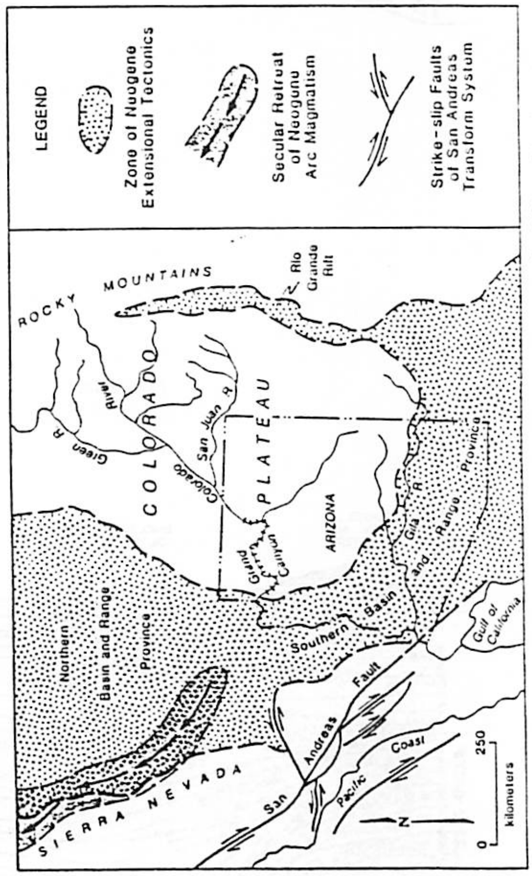

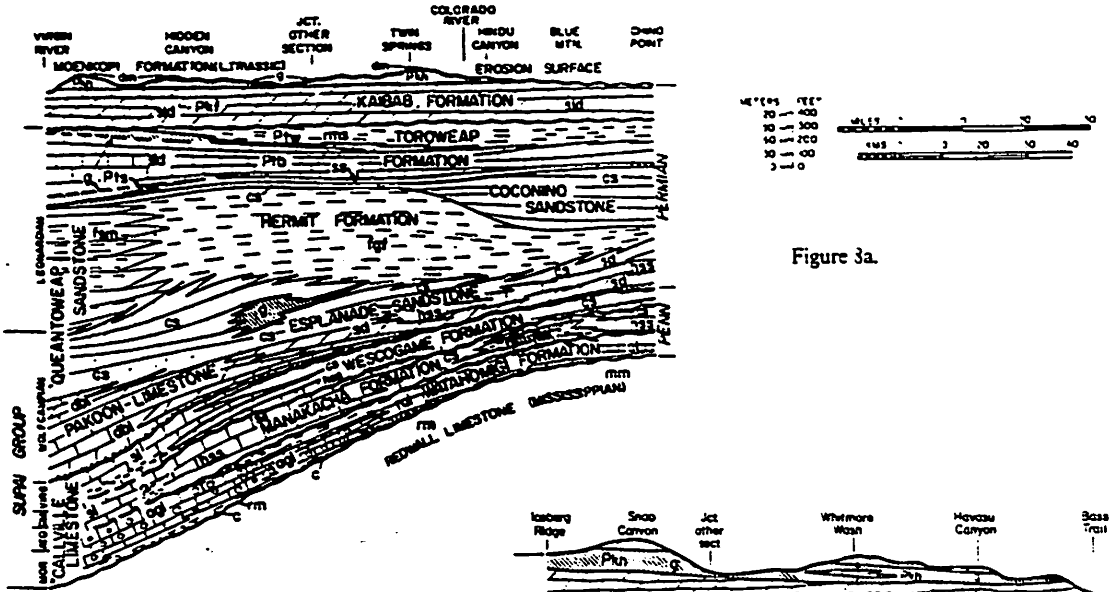

Figure 8a.

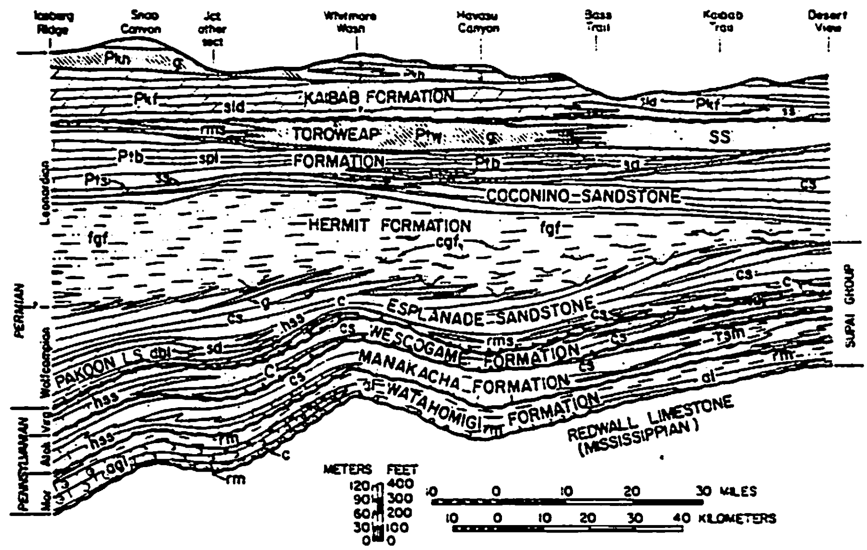

Figure 8b.

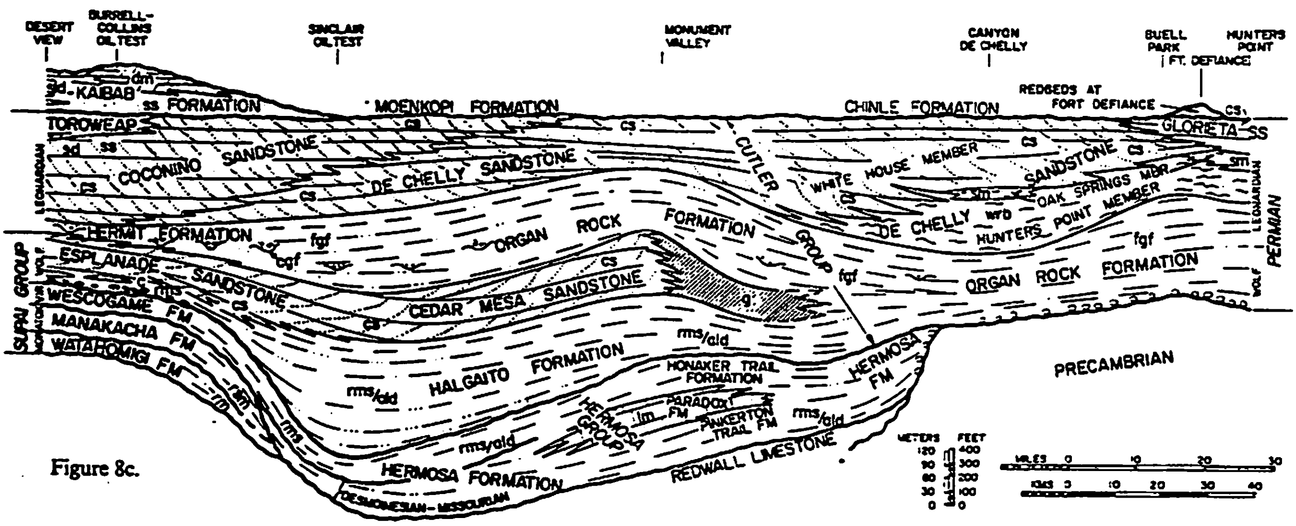

Figure 8c.

Figure 8. Restored lithologic cross-sections of Pennsylvanian and Permian rocks of Arizona. Lower-case letters refer to facies of table 1. Members of Toroweap and Kaibab Formations—Pts: Seligman Member; Ptb: Brady Canyon Member; Ptw: Woods Ranch Member; Pkf: Fossil Mountain Member; Pkh: Harrisburg Member. Sources of data not discussed in text include: Bissell (1969; Grand Canyon region), Brown (1969; Kaibab Formation), Fisher (1961; Grand Canyon region), Sorauf (1962; Grand Canyon region), Steed (1980; Virgin River Gorge). Note that position of "Callville Limestone" of previous workers is shown in Virgin Mountains and that Desmoinesian strata in northwestern Arizona are restricted to the Virgin Mountains. Slightly different lengths of sections F and G are due to different routes of Pennsylvanian and Permian sections.

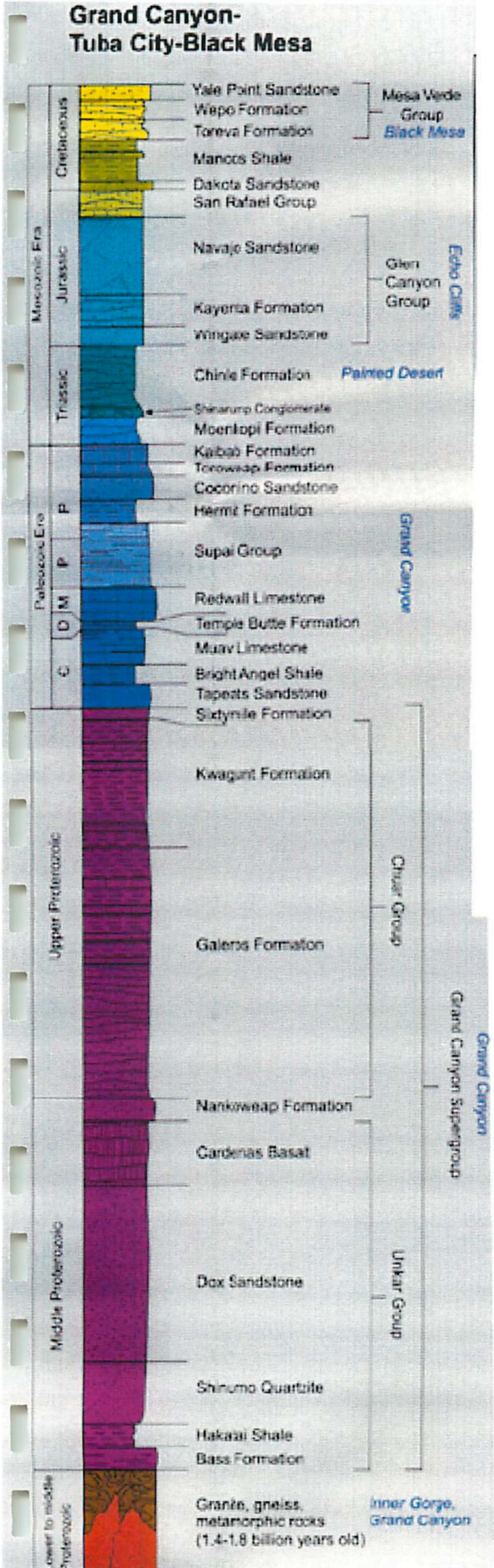

Simplified stratigraphic column from "Geologic Highway Map of Arizona." (Kamilli and Richard, 1998).

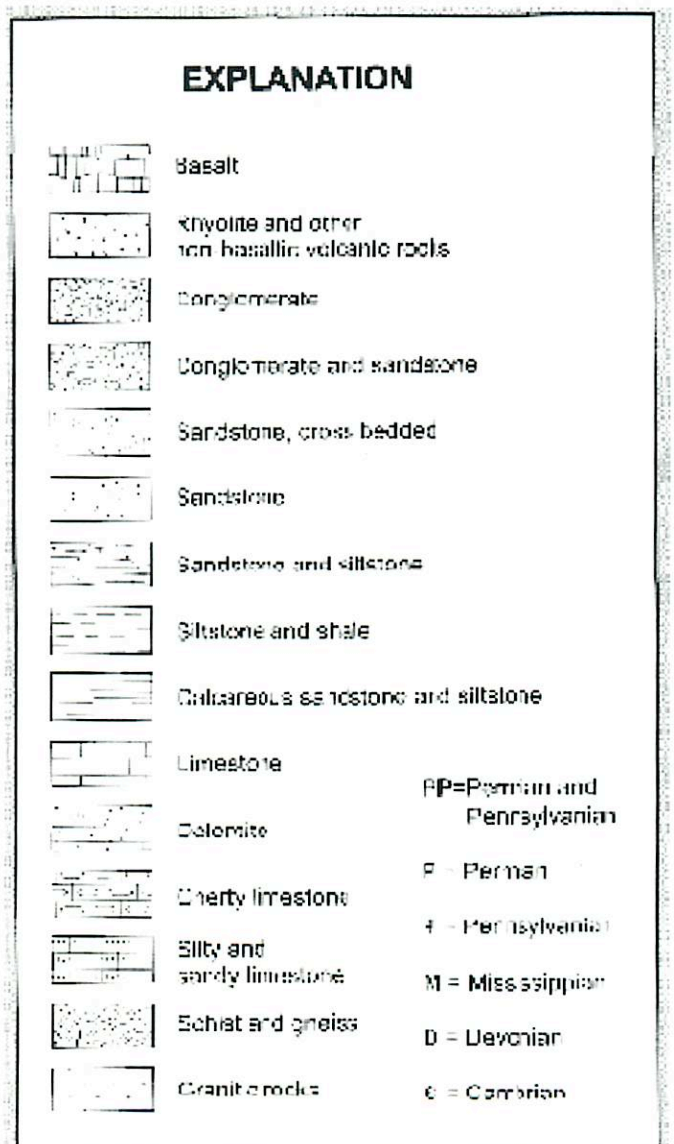

The Navajo People and the Four Corners Melting Pot

with your helpful host, Andy Rivkin

The Navajo (or Diné, as they call themselves) are the 2nd largest Native American tribe in the United States (the Cherokee are the largest), with 225,000 members. They are one of the few tribes whose numbers have increased with time, and did not have a massive population loss with European contact. They are also one of the few tribes whose reservation lands have increased with time.

The Diné are an Athapascan tribe, decended from Canadian tribes and related to the Apaches of Southern Arizona. They are thought to have arrived in the Southwest after travelling over some unknown route for an unknown amount of time. Archaeologists have suggested dates for the migration ranging from 800 A.D. (C.E.) to as late as the 1500s, *after* the Spanish arrival. At this point, however, the Navajo were not a "distinct cultural or political entity" (Bailey and Bailey, 1986), however. At this point. they lived in western New Mexico, an area they call the Dinetah (see Figure 1). The Diné made their living (if such a term is warranted) by hunting, farming, and raiding Pueblo settlements.

After the Pueblo revolt of 1680, Pueblo refugees joined the proto-Navajo in the Dinetah, and an intensive cultural exchange began. The Pueblo intermarried with their hosts, and taught them how to make pottery, weave blankets, and herd animals on a large scale. Pueblo agricultural techniques and religion also made strong impressions at this time. Structures similar to small Pueblo houses were found alongside traditional hogans. By the early decades of the 1700s, the Pueblo had been assimilated, or gone home, and the Navajo became recognizable as a separate cultural group. Nevertheless, there was no central chief, nor would there ever truly be one. Noone controlled the Diné, as numerous Europeans would discover.

With increased farming among the Diné, their settlements became targets for raiding by Utes and Comanches. This spurred the further development of herding among the Diné, which was a much more mobile way of living. Pressed further by the Utes et al., the Navajo abandoned the Dinetah and moved west by 1754, into their current homeland.

However, the Spanish were moving in as well, and conflict was inevitable. Highly mobile, adept at raiding, and desirous of increasing their own flocks and herds, the new Spanish ranches were now obvious targets for young Navajo warriors. A low-level war was waged for decades, oblivious to the change of jurisdiction of the area from Spain to Mexico. In 1846, Gen. Kearney's *Army of the West* captured Santa Fe, and the area now belonged to the United States.

In time, and for whatever reason, the Navajo re-commenced raids on the newly-American settlements. In 1863, Kit Carson led 500 New Mexican volunteers to hunt down the Navajo. They concentrated on destroying crops and orchards, and enlisted the help of Utes and Pueblos, anxious for revenge. In January 1864, they reached Canyon de Chelly, and took a large number of prisoners without a fight. Without crops, and in the middle of winter, the Navajos surrendered. 8,500 Navajo were taken and held prisoner at Bosque Redondo, New Mexico, out of a population of 10,000. Four years later, the Navajo were allowed to return to their homeland.

Since then, the Navajo seem to have benefited by "working within the system". Given their herds back, they traded blankets for more animals. Rather than eat some of their animals, they would hunt deer. Soon their flocks were huge, and their reservation was expanded to accomodate them. There was no assimilationist urge among them since they were doing well, and the government decided to leave well enough alone. Because they had the relative good luck to live in the last place in the continental U.S. that settlers wanted, they managed to keep what they had. Soon they were squatting on Hopi land, and received squatters rights. This is the basis (or among the bases) for the Hopi-Navajo conflict of today.

The Diné supplied many soldiers for the U.S. Army in WWII, the famous "Code Talkers", and are currently one of the more "forward-looking" tribes in America.

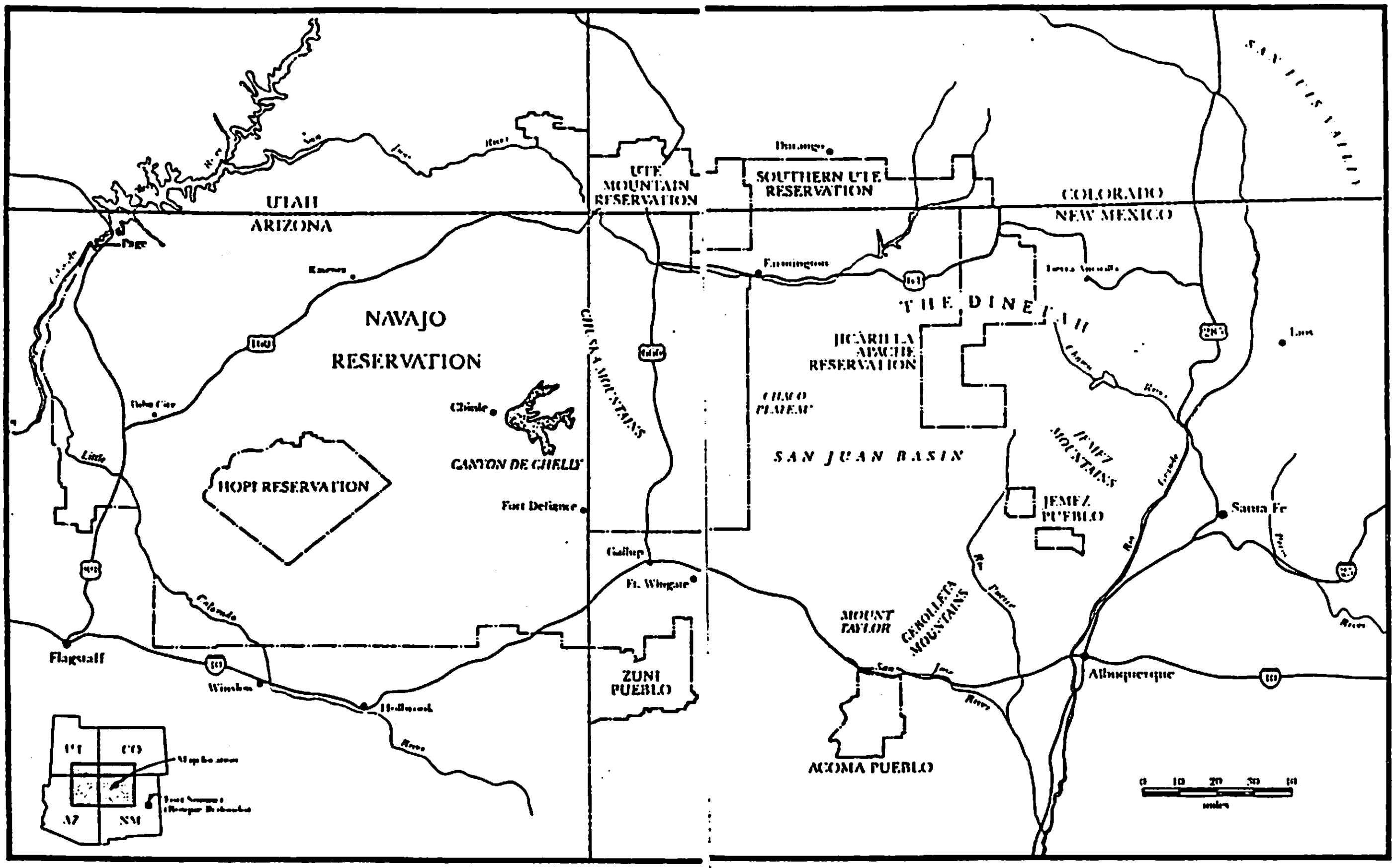

Map 1. Navajo country.

from Bailey & Bailey 1986

Old-fashioned Navajo hogan in Canyon de Chelley.
(Courtesy American Museum of Natural History)

A forked-stick hogan, the type of dwelling used by the earliest Navajos.
(Photograph by Milton Snow, Courtesy U. S. Indian Service)

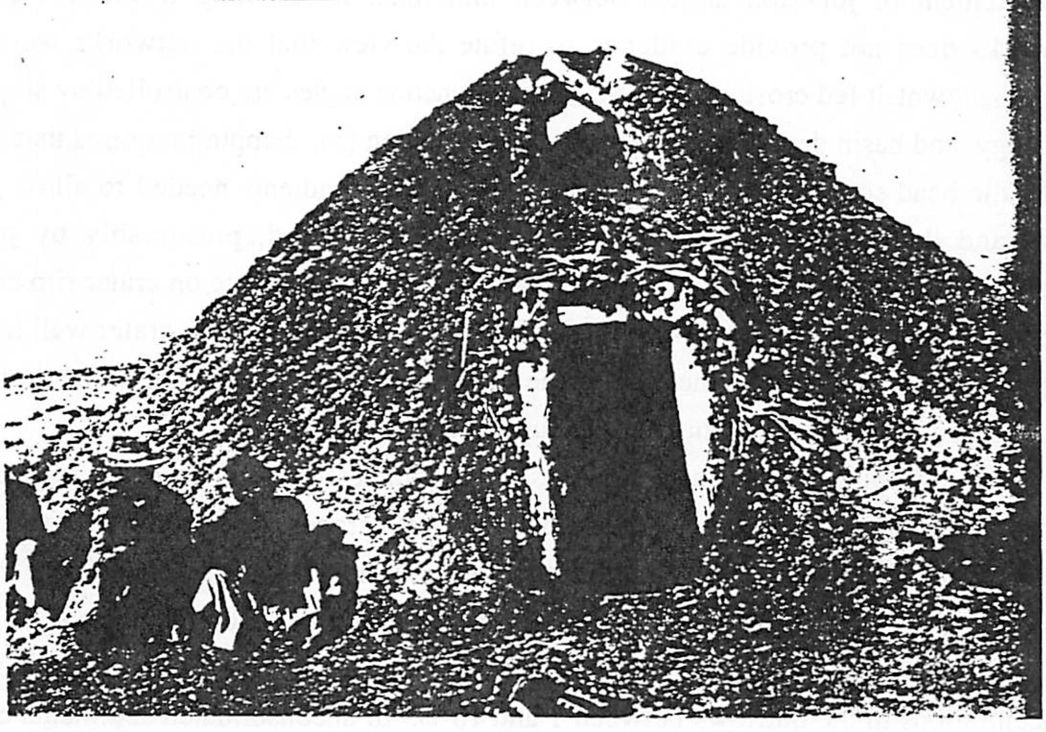

from Underhill, 1956

ARE THE MARTIAN VALLEY NETWORKS REALLY SAPPING CHANNELS ?

JAMES W. RICE, JR.

(Originally published in *Evolution of Martian Volatiles*, LPI Tech. Rept. No. 96-01, p. 37-38, Part I, 1996)

The valley networks bear mute testimony to a drastic climatic change on Mars. These landforms may hold the key to unlocking the paleoclimatic history of Mars, however there is still no consensus among investigators regarding the formation (runoff vs. sapping) of these features. An attempt will be made here to point out some major flaws associated with the sapping hypothesis based on terrestrial analog field studies and laboratory experiments.

It has been argued that the valley networks were formed primarily by groundwater seepage (1). This is based on morphologic characteristics such as U - shaped valleys with theater heads and steep walls, low drainage density, irregular junction angles, and short tributaries. The evidence for sapping is in some cases convincing (i.e., Nirgal Vallis) but, it does not explain many of the dendritic valley systems, e.g. those located in the Margaritifer Sinus region.

Some problems with the sapping model will be discussed below. First of all, the measurement of junction angles between individual intersecting tributaries of the valley networks does not provide evidence to refute the view that the networks were formed by rainfall/snowmelt fed erosion (2, 3, 4). Stream junction angles are controlled by slope, structure, lithology, and basin development stage not precipitation (5). Sapping requires that zones of low hydraulic head somehow be established to support the gradients needed to allow groundwater flow, and that zones of high hydraulic head be recharged, presumably by precipitation. Additionally, some of the valley networks whose channels originate on crater rim crests indicate that the local water table must have intersected the surface high on the crater wall if sapping was involved (4). This would mean that the crater was once filled with water but there is no evidence, such as inflowing channels, to support this condition.

The sapping process also requires large volumes of water in order to produce a *well* developed sapping network. The most efficient process of sapping erosion occurs in unconsolidated sediments where the limiting factor is the transporting capacity of the spring fed flows. Experiments (6) suggests that a minimum of 10 times more water than volume eroded sediment must be discharged in order to form a sapping valley network. This work had sediment concentrations in the outflows between 1 and 10 %. In unconsolidated sediments a ratio of 100 to 1,000 fold is more reasonable. For consolidated rocks, valley erosion is limited by the rate of weathering of the rocks at the sapping face. These weathering processes (solution of cement/melting of ice, salt fretting and or freeze thaw cycles) are very slow and require water to eroded rock ratios of 10^5 or greater.

Field work on channel systems located on the Canterbury Plain, New Zealand (7) indicate that these systems are of a composite origin. These features occupy U - shaped valleys with theater heads and steep walls, have low drainage densities and short tributaries. The above mentioned characteristics are often cited as evidence for sapping but these channels are in fact formed predominantly by surface runoff and subsequently modified by ground water sapping. The smaller channels are being formed by seepage and mass movement, but they stagnate when an armor is formed that cannot be breached by seepage flow.

Finally, drainage system studies have been conducted on Earth and Mars using drainage density and drainage pattern characteristics. The density of drainage may provide information on permeability and texture of materials, thus inferring the identity of materials (8). The patterns which streams form are determined by inequalities of surface slope and rock resistance (9). Therefore, based on terrestrial drainage system studies, this paper will make the first attempt at suggesting what geologic materials and slopes the Martian valley networks may have eroded. Most of the Martian valley networks have drainage patterns that fit the following patterns as described by terrestrial researchers (8, 9), subdendritic and subparallel. These are modifications of the basic drainage systems which are classified as dendritic and parallel, respectively.

Subdendritic drainage develops where rocks offer uniform resistance in a horizontal direction. This suggest nearly horizontal sedimentary rocks, superposed drainage on folded sedimentary rocks of equal resistance, or massive igneous rocks of gentle regional slope at present or at time of drainage inception.

Subparallel drainage implies either pronounced moderate to steep regional slopes or slope controlled by parallel topographic features. This pattern usually occurs in sedimentary, volcanic and metasedimentary rocks that have been faulted and folded.

Another useful drainage system characteristic is that of drainage texture(9). Drainage texture describes the relative spacing of drainage lines using the relative terms; fine, medium, and coarse. Drainage texture is controlled by (1) climatic factors such as the amount and distribution of precipitation and permafrost; (2) rock characteristics, including texture and size of weathered fragments; (3) infiltration capacity; (4) topography; (5) stage and number of erosion cycles. In unconsolidated sediments the drainage texture is directly related to grain size. Fine texture describes a system that has a high degree of ramification of drainage lines. This results in a dense network involving multitudes of small streams. This texture type is typically observed in fairly impervious materials (shale, clay, and silt). The low infiltration capacities of fine grained materials allow for more surface runoff, hence a denser network of surface drainage.

Coarse textures exhibit very little ramification and longer more widely separated valleys. Permeable materials such as sand, gravel, and rocks that weather into coarse fragments exhibit coarse textures. The higher infiltration capacities of coarse grained materials readily absorb precipitation and have fewer surface streams and display coarse drainage texture. Medium texture is the intermediate of the above mentioned textures.

The above mentioned drainage basin characteristics will also be combined with an age reassessment of the valley networks on Mars. This involves examining both the startigraphic age and morphologic preservation "age" of the valley networks. Recent work (10) indicates that many of the valley networks are in fact younger than Noachian. This is contrary to most valley network studies and carries with it important implications to the geologic, climatic and possibly biologic evolution of Mars.

References:

(1) Pieri D.C., (1980) Science 210, 895-897. (2) Jakosky B.M. and Carr M.H. (1985) Nature 315, 559-561. (3) Rice J.W. (1993) MSATT LPI Tech Rept. 93-03, 22-23. (4) Clow G.D. (1987) Icarus 72, 95-127. (5) Schumm S.A. (1956) GSA 67, 597-646. (6) Howard A.D. (1988) NASA SP-491, 71-83. (7) Schumm S.A. and Phillips L. (1986) Geology 14, 326-29. (8) Howard A. D. (1967) AAPG 51 no.11, 2246-59. (9) Zernitz E.R. (1932) Journal of Geology 40 no. 6, 498-521. (10) Scott D.H., Dohm J.M. and Rice Jr., J.W. (1995) USGS Misc. Inves. Series Map I-2461.

MARTIAN VALLEY NETWORK AGE REASSESSMENT

JAMES W. RICE, JR.

(Originally published as Scott, D.H., J.M. Dohm, and J.W. Rice, Jr., Map Showing Channels and Possible Paleolake Basins, U.S.G.S. Misc. Inves. Ser. Map I-2461, 1995)

The geologic ages of valley networks have been difficult to date either by crater counting [*Carr and Clow,* 1981] or by stratigraphic methods based on geologic maps made from Mariner 9 images. To define better the stratigraphic positions of both highland and lowland channels, the valley networks were mapped on Viking photomosaics and topographic maps [*U.S. Geological Survey,* 1989]. These features were then dated by considering its superposition relations with rock units shown on the global geologic maps of Mars (see section Highland and Lowland Channels). This type of study was not feasible prior to completion of these maps made from Viking images.

The channels were assigned a maximum stratigraphic age based on the youngest age of the rocks that they transect. To refine these maximum stratigraphic ages further, we next considered the morphology of the channels and classified them, according to the appearance of their walls and floors, as fresh, subdued, or degraded. For example, a fresh-appearing channel on rocks of Middle to Late Noachian age was assigned an Early Hesperian age, although it might well be younger. In places, an upper age limit can be estimated for some channels where they have been partly overlapped by rocks of known stratigraphic position.

A detailed examination of the age relation between Martian terrains and the channels that transect them was made possible by the completion of the global geologic maps of Mars [*Scott and Tanaka,* 1986; *Greeley and Guest,* 1987; *Tanaka and Scott,* 1987] and the availability of other geologic maps 1:5,000,000, 1:2,000,000 and 1:500,000 scales. We have mapped and documented more than 1,600 highland and lowland channels longer that about 30 km in all of the 120 Viking 1:2,000,000-scale photomosaic quadrangles of Mars. These data, including the paleolake boundaries, were compiled at 1:15,000,000 scale on topographic maps [*U.S. Geological Survey,* 1989] and their ages established from the global geologic maps. (We have not studied the small linear grooves around the rims and walls of some craters, because (1) most are so small (less than 30 km long) and so numerous that they would lend a strong statistical bias to the data and (2) their ages and origins are uncertain, most having probably formed long after the cratering event.)

Each channel in both highlands and lowlands was assigned a maximum age based on the age of the youngest material cut by the channel. This very conservative method showed that 25 percent of the highland channels are younger than Noachian (Plate 1,

Figure 12A) *[NOTE: for figures and plates please refer to Scott, Dohm, Rice, 1995]* and that 36 percent of all Martian channels are younger than Noachian (Plate 1, Figure 12C).

To review these stratigraphic ages further, we next considered the morphology of individual channels and classified them, according to the appearance of their walls and floors, as fresh, subdued, or degraded; for example, a fresh-appearing highland channel (Plate 1, Figure 13) that cuts Upper Noachian rock (maximum age of Noachian shown on map) and has similar morphology to a channel that cuts known Hesperian material (Plate 1, Figure 14) was reassigned an Early Hesperian age and added to the revised channel data (Plate 1, Figures 12B, D). Plate 1, Figure 15 shows a younger, v-shaped, sharp-rimmed channel (reassigned and Early Hesperian age) within an older degraded channel that cuts Noachian material. The ages of only a few channels, however, were revised from Noachian to Amazonian. One example (Plate 1, Figure 16) is a v-shaped, sharp-rimmed channel in Noachian highland material; the channel has cut through an old crater and debouched onto an Amazonian surface. Our study showed that the 35 percent of highland channels probably younger that Noachian (Plate 1, Figure 12B) is comparable with the 32 percent of highland surface that are probably younger that Noachian [*Tanaka*, 1986]. The comparison indicates that the densities of highland channels longer than 30 km per unit area for Noachian and for post-Noachian rocks are about the same. However, most investigators think that the Noachian Period was shorter that the combined duration of the Hesperian and Amazonian Periods. Therefore, although highland channel formation continued throughout the planet's history, the rate probably declined during later geologic periods.

In particular, the decline of valley systems that are most often found in the cratered highlands is commonly viewed as indicative of a change from a warm, wet climate to a colder, drier one [*Masursky*, 1973; *Sagan et al.*, 1973; *Pollack*, 1979; *Carr*, 1989]. *Craddock and Maxwell* [1993] determined that densities of fresh craters generally decrease at progressively lower elevations, which they interpret to indicate an extended period of atmospheric thinning and cooling. By comparing channel sources and their relative age of formation to their elevation, *Dohm and Scott* [1993] concurred with the ideas that volatiles gradually migrated to lower elevations, that Mars' early atmosphere was relatively thick, and that a gradual thinning may have resulted both in fewer channels forming at higher elevations and in a global decrease in the rate of channel formation. On the other hand, many of the younger channels and valley systems occur on diverse terrains at higher elevations; examples are found along the edges of structurally deformed regions such as the southern edges of both Solis Planum (lat 21° S., long 95°; Plate 1, Figure 17) and the provisionally named Thaumasia Planum (lat 22° S., long 65°) [*Tanaka and Schultz*, 1991].

Other locations of younger channels and valley systems include those (1) on the flanks of volcanoes, (2) along the highland-lowland boundary, and (3) around the rims and walls of impact craters. These varied occurrences suggest that channels may have formed in response to many different processes, including (1) local hydrothermal activity due to impacts [*Newsom,* 1980; *Brakenridge et al.,* 1985] and heating by intrusions [*Squyres et al.,* 1987; *Gulick et al.,* 1988; *Wilhelms and Baldwin,* 1989; *Mouginis-Mark,* 1990]; (2) local condensation and precipitation of water vapor from volcanoes [*Gulick and Baker,* 1990]; and (3) increased hydrologic activity due to tectonic deformation [*Mouginis-Mark,* 1990; *Tanaka,* 1991; *Tanaka and Schultz,* 1991; *Leyva and Clifford,* 1993].

Earlier studies [*Pieri,* 1980; *Carr and Clow,* 1981] of valley-network channels on Mars showed that more than 99 percent were in highland cratered terrain; on the basis of this association the channels were thought to have formed during the earliest period of Mars' history. This conclusion was not supported by our study, but a plausible explanation for the difference may lie in the data-formatting of the earlier study, the less detailed geologic base map used to assign ages to the channels, and the sizes and types of channels counted.

As the map shows, highland channels of different ages are common along the borders of the basins that we have described; they are far outnumbered, however, by channels that, on the surface at least, did not reach the lowland plains. Lowland channels of Amazonian age are most abundant in Utopia Planitia and may have been the chief water source of subbasin C. The low-relief, meandering channel forms in Arcadia Planitia resemble vestiges of waterways in mudflats and possibly may be related to the drying up of a former lake or lakes. The largest and most obvious suppliers of water to the lowlands were the huge outflow channels that emptied into the Chryse Basin and, to a lesser extent, the channels in Mangala and Ma'adim Valles that flowed into the Amazonis and Elysium Basins. Crater counts indicate that these channels are mostly Late Hesperian in age [*Scott and Tanaka,* 1986; *Greeley and Guest,* 1987; *Chapman et al.,* 1991; *De Hon,* 1992]. The wide range in age (Hesperian to Amazonian) of the small and large channels that supplied the basins with water suggests that the former lakes existed intermittently, possibly for long periods.

References:
Brakenridge, G.R., Newsom, H.E., and Baker, V.R., 1985, Ancient hot springs on Mars: Origins and paleoenvironmental significance of small Martian valleys: Geology, v. 13, no. 12, p. 859-862.

Carr, M.H.,1989, Recharge of the early atmosphere of Mars by impact induced release of CO_2: Icarus, v. 79, no. 2, p. 311-327.

Carr, M.H.,and Clow, G.D., 1981, Martian channels and valleys: Their characteristics, distributions, and age: Icarus, v. 48, no. 1, p. 91-117.

Chapman, M.G., Masursky, Harold, Dial, A.L., Jr., 1991, Geologic map of Science Study Area 1B, west Mangala Valles region of Mars: U.S. Geological Survey Miscellaneous Investigations Series Map I-2087, scale 1:500,000.

Craddock, R.A., and Maxwell, T.A., 1993, Geomorphic evolution of the Martian highlands through ancient fluvial processes: Journal of Geophysical Research, v. 98, no. 2, p. 3453-3468.

De Hon, R.A.,1992, Geologic map of the Pompeii quadrangle (MTM 20057), Maja Valles region of Mars: U.S. Geological Survey Miscellaneous Investigations Series Map I-2203, scale 1:500,000.

Dohm, J.M. and Scott, D.H., 1993, Relation between ages and elevations of Martian channels, in Abstracts of papers submitted to the Twenty-fourth Lunar and Planetary Science Conference, Houston, March 125-19, 1993: Lunar and Planetary Institute, p. 407-408.

Greeley, R., and Guest, J.E., 1987, Geologic map of the eastern equatorial region of Mars: U.S. Geological Survey Miscellaneous Investigations Series Map I-1802-B, scale 1:15,000,000.

Gulick V.C., and Baker, V.R., 1990, Origin and evolution of valleys on Martian volcanoes: Journal of Geophysical Research, v. 95, no. 9, p. 14,325-14,344.

Gulick, V.C., Marley, M.S., and Baker, V. R., 1988, Hydrothermally supplied ground water: A mechanism for the formation of small Martian valleys, in Abstracts of papers submitted to the Nineteenth Lunar and Planetary Science Conference, Houston, March 14-18, 1988: Houston, Lunar and Planetary Institute, p. 441-442.

Leyva, I.A., and Clifford, S.M., 1993, The seismic response of an aquifier to the propagation of an impact generated shockwave: A possible trigger of the Martian outflow channels?, *in* Abstracts of papers submitted to the Twenty-fourth Lunar and Planetary Science Conference, March 15-19, 1993: Houston, Lunar and Planetary Institute, p. 875-876.

Masursky, Harold, 1973, An overview of geologic results from Mariner 9: Journal of Geophysical Research, v. 78, no. 20, p. 4009-4030.

Mouginis-Mark, P.J., 1990, Recent water release in the Tharsis region of Mars: Icarus, v. 84, no. 2, p. 362-373.

Newsom, H.E., 1980, Hydrothermal alteration of impact melt sheets with implications for Mars: Icarus, v. 44, no. 1, p. 207-216.

Pieri, D. C., 1980. Martian valleys: Morphology, distributions, age, and origin. Science 210: 895-897.

Pieri, D. C., 1980, Geomorphology of Martian valleys, in Advances in Planetary Geology: National Aeronautics and Space Administration Technical Memorandum 81979, 160 p.

Pieri, D.C., 1976, Distribution of small channels on the Martian surface: Icarus, v. 27, no. 1, p. 25-50.

Pollack, J.B., 1979, Climate change on the terrestrial planets: Icarus, v. 37, no. 3, p. 479-533.

Sagan, Carl, Toon, O.B., and Gierasch, P.J., 1973, Climate change on mars: Science, v. 181, no. 4104, p. 1045-1049.

Scott, D.H. and Carr, M.H., 1978, Geologic map of Mars: U.S. Geological Survey Miscellaneous Investigations Series Map I-1083, scale 1:25,000,000.

Scott, D.H. and Tanaka, K.L., 1986, Geologic map of the western equatorial region of Mars: U.S. Geological Survey Miscellaneous Investigations Series Map I-802-A, scale 1:15,000,000.

Squyres, S.W., Wilhelms, D.E. , and Moosman, A.C., 1987, Large-scale volcano-ground ice interactions on Mars: Icarus, v. 70, no. 3, p. 385-408.

Tanaka, K.L., 1986, The stratigraphy of Mars, in Lunar and Planetary Science Conference, 17th, Houston, March 17-20, 1986, Proceedings: Journal of Geophysical Research, v.91, no. B13, p. E139-E158.

Tanaka, K.L., and Schultz, R.A., 1991, Late Noachian development of the Coprates rise, Mars, in Abstracts submitted to the Twenty-second Lundar and Planetary Science Conference, Houston, Lunar and Planetary Institute, p. 1379-1380.

Tanaka, K.L., and Scott, D.H., 1987, Geologic map of the north and south polar regions of Mars: U.S. Geological Survey Miscellaneous Investigations Series Map I-1802-C, scale 1:15,000,000.

U. S. Geological Survey, 1991, Topographic map of the western region of Mars, U. S. Geol. Surv. Misc. Inv. Ser. Map I-2160, Sheet 2, scale 1:15,000,000.

U.S. Geological Survey, 1989, Topographic maps of the western, eastern equatorial, and polar regions of Mars: U.S. Geological Survey Miscellaneous Investigations Series Map I-2030, scale 1:15,000,000.

Wilhelms, D.E., and Baldwin, R.J., 1989, The role of igneous sills in shaping the Martian uplands, in Lunar and Planetary Science Conference, 19th, Houston, 1988, Proceedings: Cambridge Universtiy Press and Lunar and Planetary Institute, p. 355-365.

MOC IMAGE
9.8 X 18.5 Km

CANYON
2.5 Km WIDE

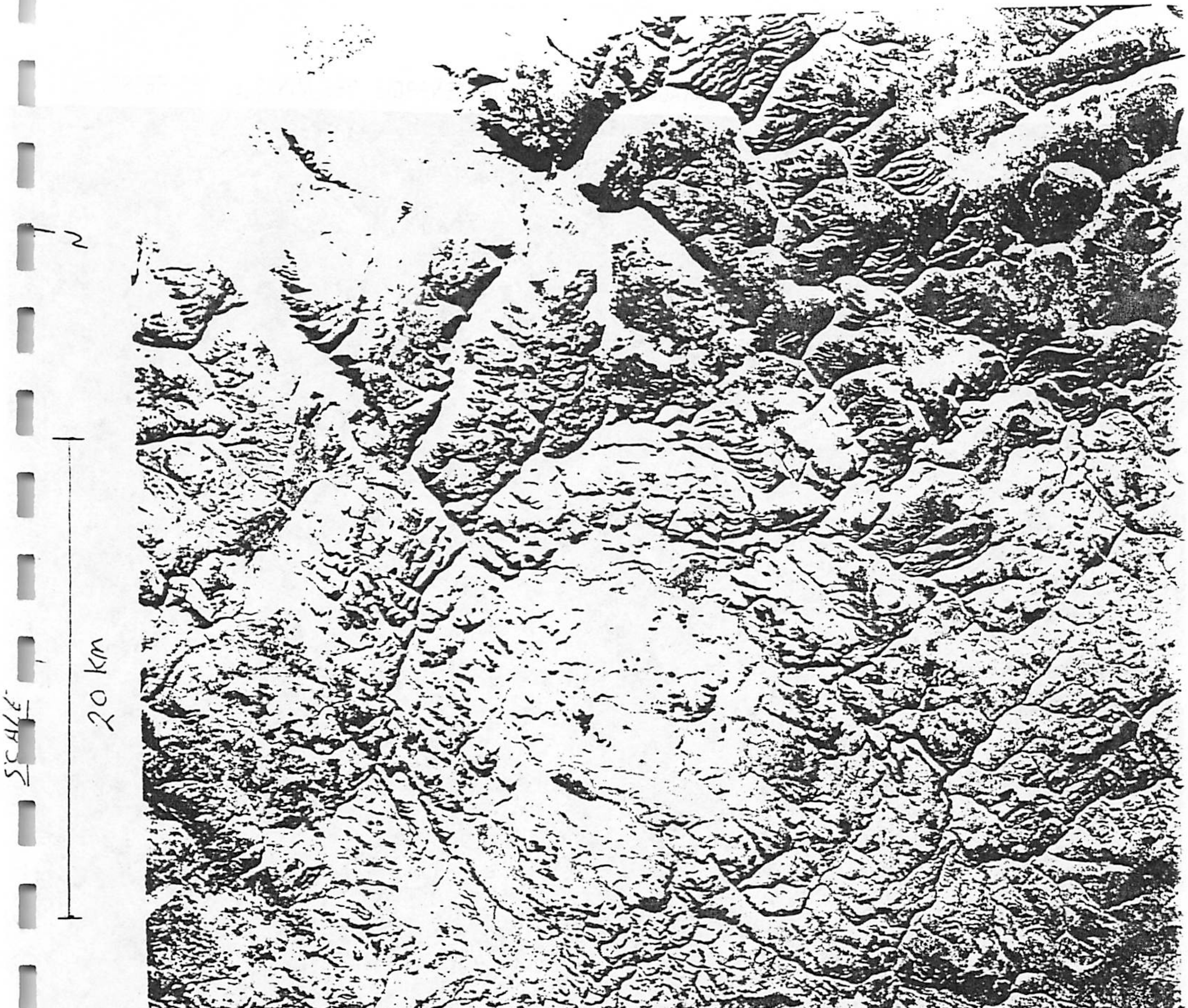
N
SCALE
20 km

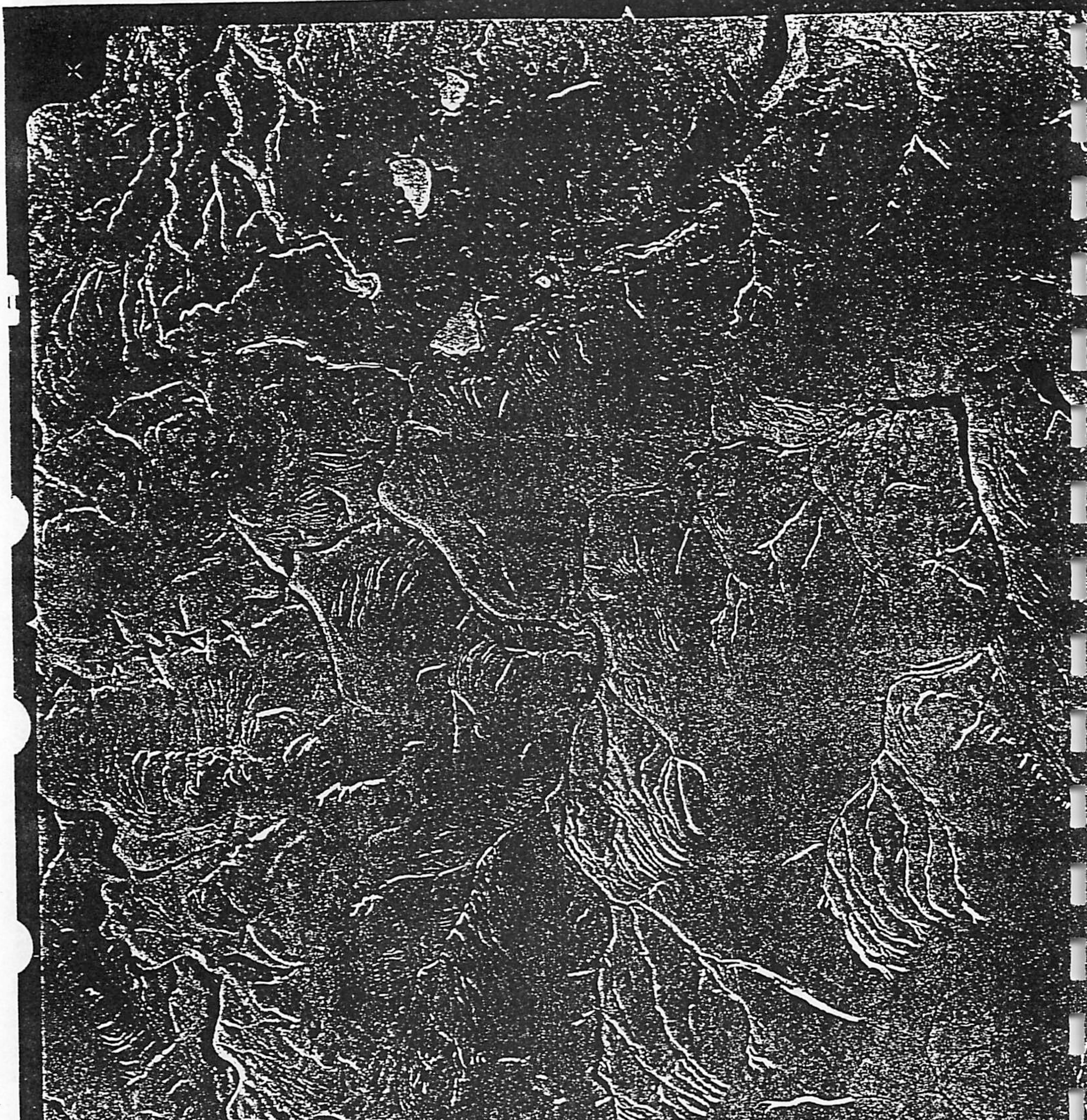

Washboards

Ralph D Lorenz

Washboard surfaces are a corrugated profile frequenctly encountered on surfaces trafficked by wheeled vehicles. They are most familiar in arid regions, forming ridges spaced by about 1 metre, but can be found on asphalt and concrete surfaces too.

One early (1938) theory, due to Renton of the University of Cairo, was one of 'relaxation oscillation' (i.e. increment/threshold) where it was believed that a wheel pushed material ahead of it slightly, until the material piled up enough that the resistance was such that the wheel rolled over it. The cycle would then begin again.

The canonical (only?) serious investigation of the underlying phenomenon is that by Keith Mather, then at the University of Melbourne (Australia has an extensive network of unpaved roads, so washboards are very common). Using a simple experimental setup, he found that it was basically the bounce of a wheel in the wake of a disturbance or bump that caused the phenomenon - when the wheel impacts the ground it pushes some material down (and/or ahead/behind). After several passages of a wheel, several bumps downstream of the original disturbance are created. Eventually a steady state is attained, with the bumps slowly marching downstream.

Although vehicles clearly differ widely in shape, mass etc., their suspension systems share generally similar characteristics, since their principal function is to limit oscillations that are uncomfortable to humans - see ch.2 of Bastow and Howard. (One early, but basically sound, argument was that since walking with a 30 inch stride at between 2.5 and 4 mph is comfortable for most people, the corresponding excitation frequency - between 1.5 and 2.3 Hz - must be acceptable) Above 5 Hz or so, the human visceral cavity resonates, with unpleasant effects.

Since, on a given stretch of road, vehicle speeds are likely to have typical values (especially if frequented by vehicles in convoy, or trucks/trailers with many axles) it follows then that the excitation lengths are likely to be clustered around some value. Traffic in both directions will cause the washboards to grow.

Washboards form most easily on easily-deformed surfaces (sand etc) - which can often be hardened after rainfall. They can form also on asphalt, concrete, etc. Similar features, often in two dimensions rathar than 1, are found as moghuls on ski pistes.

Certain streetcar power lines show corrugated surfaces, although the relation of the corrugations to bumps in the rails is a little different from those of roads - here the erosion of the surface is strongest just after the bump - in this case the erosion is due to arcing when the wheel loses contact with the surface, rather than maximized when the wheel re-impacts it.

References

D Bastow and G Howard, Car Suspension and Handling, SAE, Inc, 1993 (TL 257.B37)
K Mather, Why do Roads Corrugate, Scientific American, January 1963
J Henry and J Wambold (eds) Vehicle, Tire, Pavement Interface ASTMSPT-1164 , 1992 (TK 251.5 V44)
N C Yang, Design of Functional Pavements, McGraw Hill, 1972 (TE251.Y35)

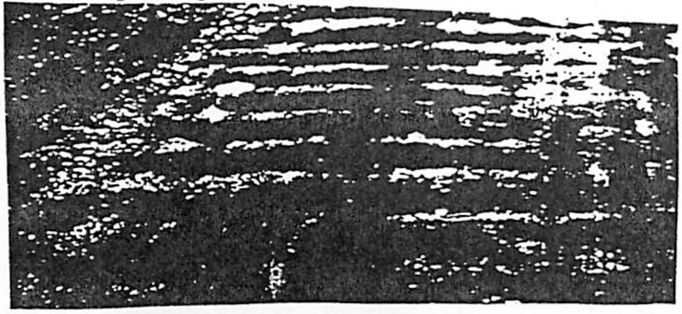

Washboards on a dirt road in Australia

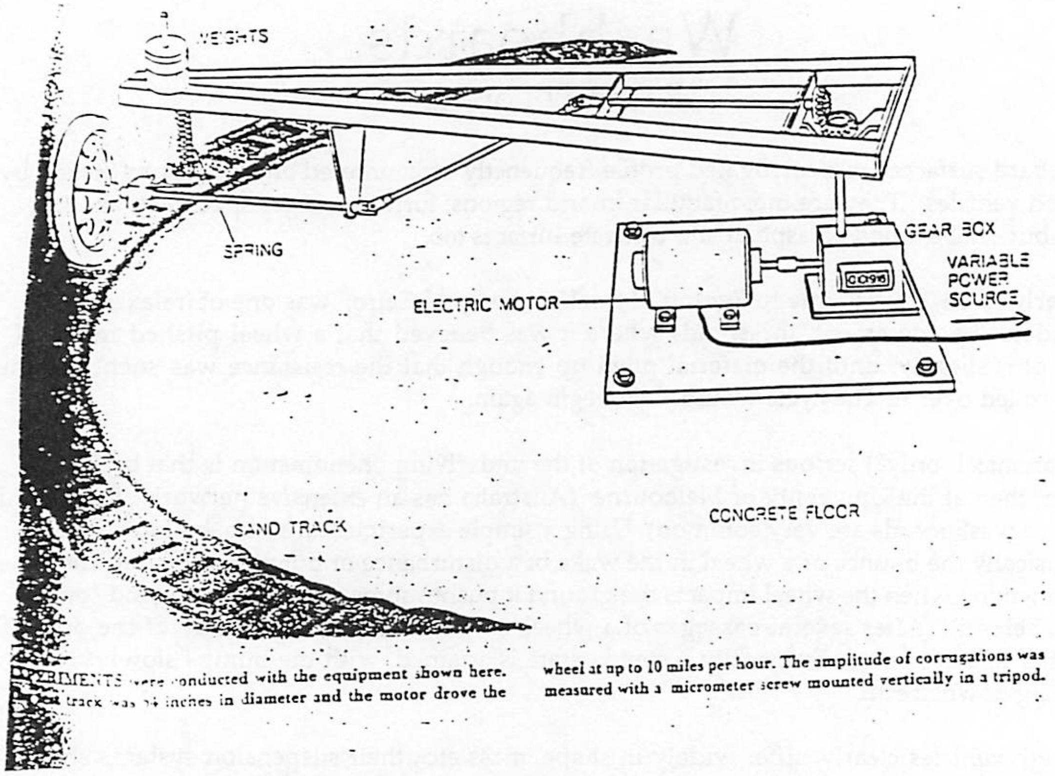

EXPERIMENTS were conducted with the equipment shown here. Test track was 34 inches in diameter and the motor drove the wheel at up to 10 miles per hour. The amplitude of corrugations was measured with a micrometer screw mounted vertically in a tripod.

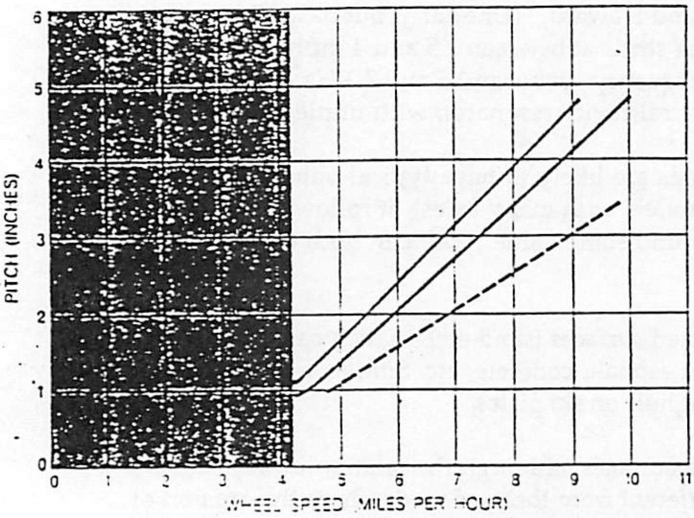

CORRUGATIONS are not generated until a critical speed is reached, about four miles an hour in the experiments. Thereafter the pitch, or distance between crests, increases with speed. The solid black curve is for the author's basic test situation with a hard rubber tire. Increasing the sprung weight and stiffening the spring shortened the pitch (*broken curve*); transferring the extra weight to the wheel lengthened the pitch (*gray curve*).

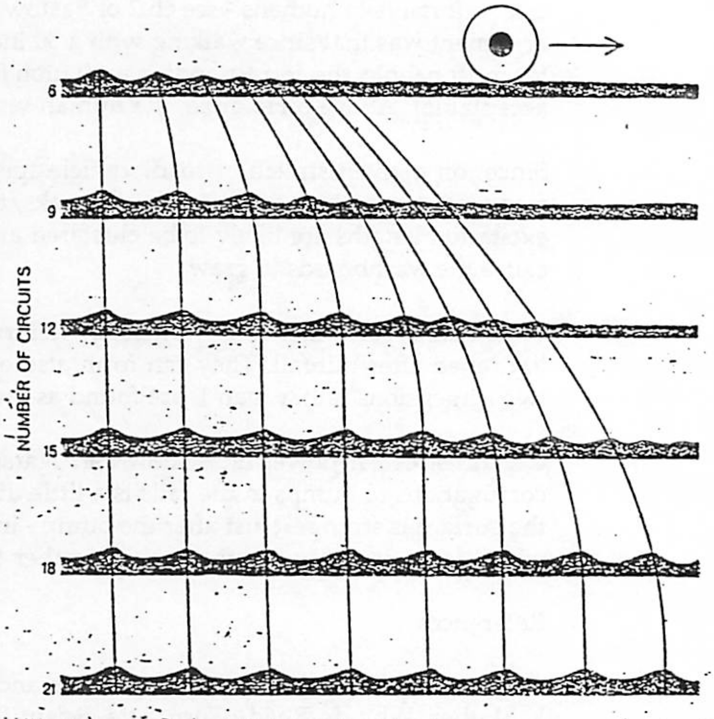

SET OF CORRUGATIONS develops from one major irregularity (*top left*). The crests increase rapidly in pitch and amplitude as the test wheel completes more circuits. After the pitch and amplitude become stable the crests migrate slowly in the direction of wheel travel.

MATHER'S
EXPERIMENTS

Ralph's Model

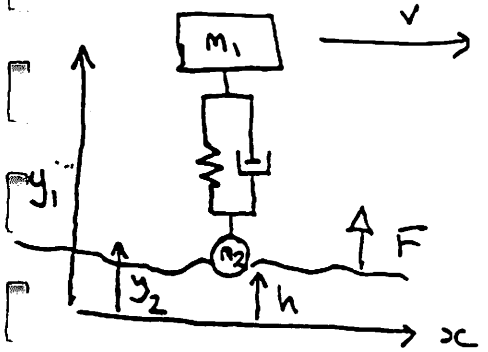

M_1 = vehicle, occupants (sprung mass) 200 kg
m_2 = rigid wheel, axle, etc 40 kg

Shock absorber = spring (~~ground~~ unloaded length L_0 30 cm, spring constant k_1) + dashpot k_2

4e4 N/m
1e3 N/m/s

$L = y_1 - y_2$

$$\ddot{y}_1 = (L_0 - L)\frac{k_1}{m_1} - \dot{L}\frac{k_2}{m_1} - g$$

$$\ddot{y}_2 = (L - L_0)\frac{k_1}{m_2} + \dot{L}\frac{k_2}{m_2} - g + \frac{F}{m_2}$$

k_3 = soil force constant 1e5 N/m

$F = 0$ $[y_2 > h]$
$F = k_3(h - y_2)$ $[y_2 < h]$

if $F > 0$ then
$h(x-\delta : x+\delta) = h(x-\delta : x+\delta) - \psi F$
$h(x+\delta : x+2\delta) = h(x+\delta : x+2\delta) + \psi F$

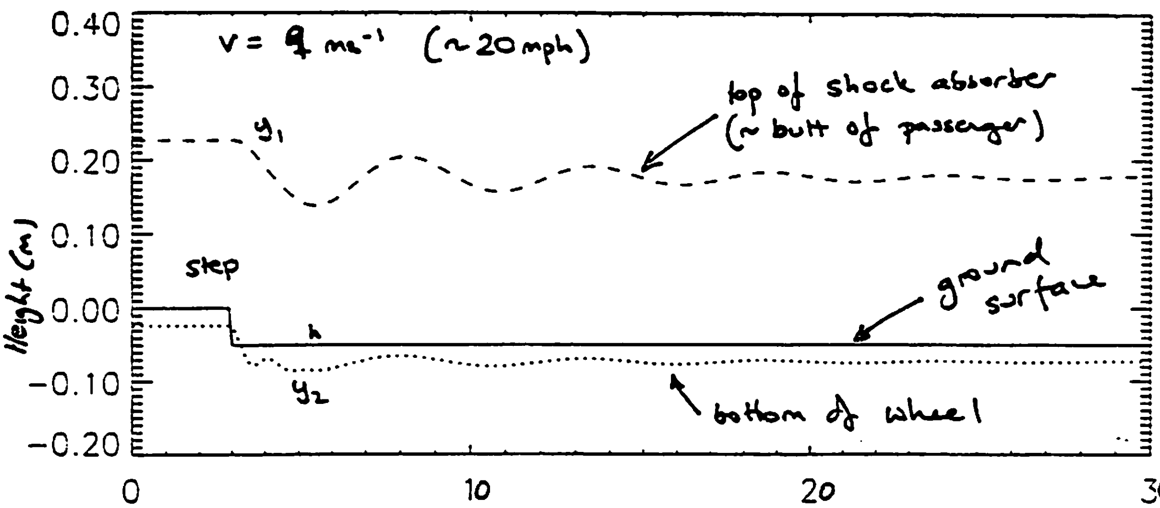

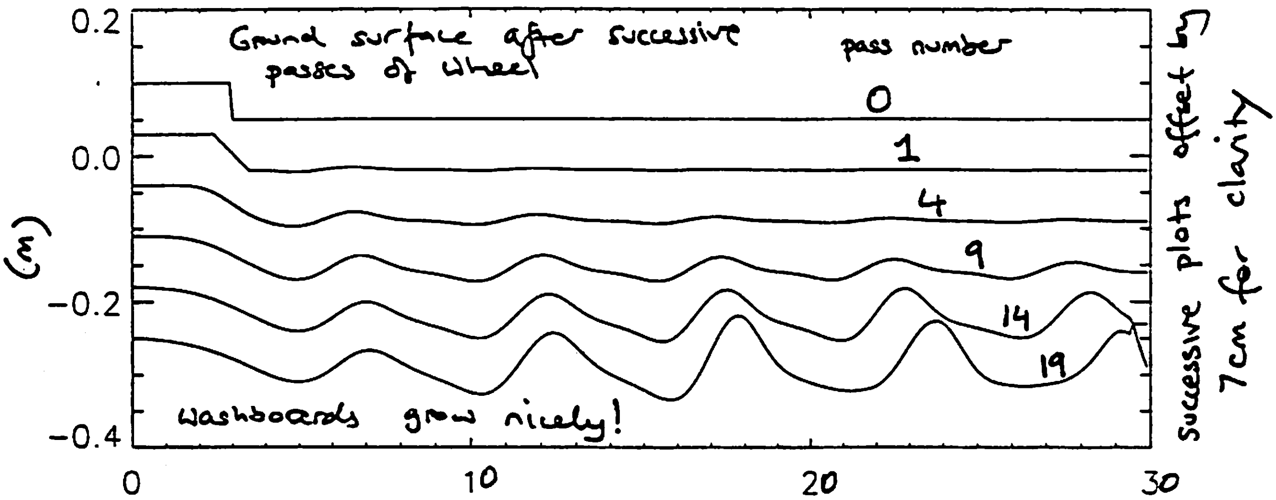

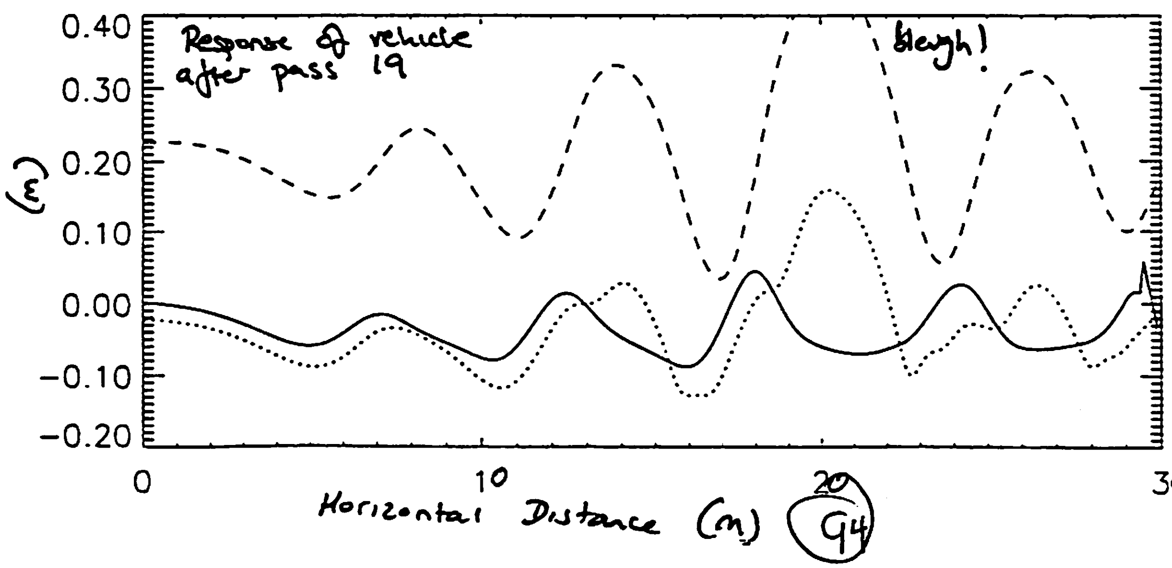

Dinosaur Tracks in Northern Arizona

Joseph Spitale

September 14, 1998

1 Introduction

Despite their relative fragility, dinosaur tracks are abundant in the fossil record. Although a given footprint is less likely to survive than a skeleton, an animal may leave millions of them during its lifetime. Footprints belong to class of fossils known as *trace fossils.* This category also includes droppings (coprolites) and stomach stones (gastroliths). Other fossils, such as bones, teeth, and claws, are generally classified as *body fossils.* The distinction is often unclear, as in the case of dinosaur eggs. In general, though, trace fossils are a record left by a living animal, while body fossils are generally left by a dead animal. Thus, trace fossils significantly enhance our picture of an animal's behavior while it was alive.

In the Western United States, dinosaur tracksites are found in Triassic, Jurassic, and Cretaceous sedimentary formations. The Moenave Road Tracksite near Tuba City occurs in the Lower Jurassic Moenave formation, overlying the Wingate formation and overlain by the Kayenta formation. These formations, along with the younger Navajo formation, are known as the *Glen Canyon Group* (figure 1). The Moenave Road tracksite is dominated by tracks of large and small therapods[5], as in figure 2.

2 Preservation of Tracks

The conditions which lead to the preservation of footprints are generally complementary to those which favor the preservation of bones. For this reason, it is rare to find footprint and bone fossils in close proximity to one another. Bones may be preserved when the carcass is quickly buried during an episode of rapid deposition, while footprints are more likely to be preserved if they are exposed for several days or weeks before burial.

In order to be preserved, footprints generally require water-lain clastic sediments, as found on shorelines, flood plains, deltas, etc. Such media are soft enough to allow the foot to sink in, but adhesive enough to retain the impression. The footprints which survive are usually those created during periods of slow deposition since those created during times rapid deposition are obliterated before they can lithify.

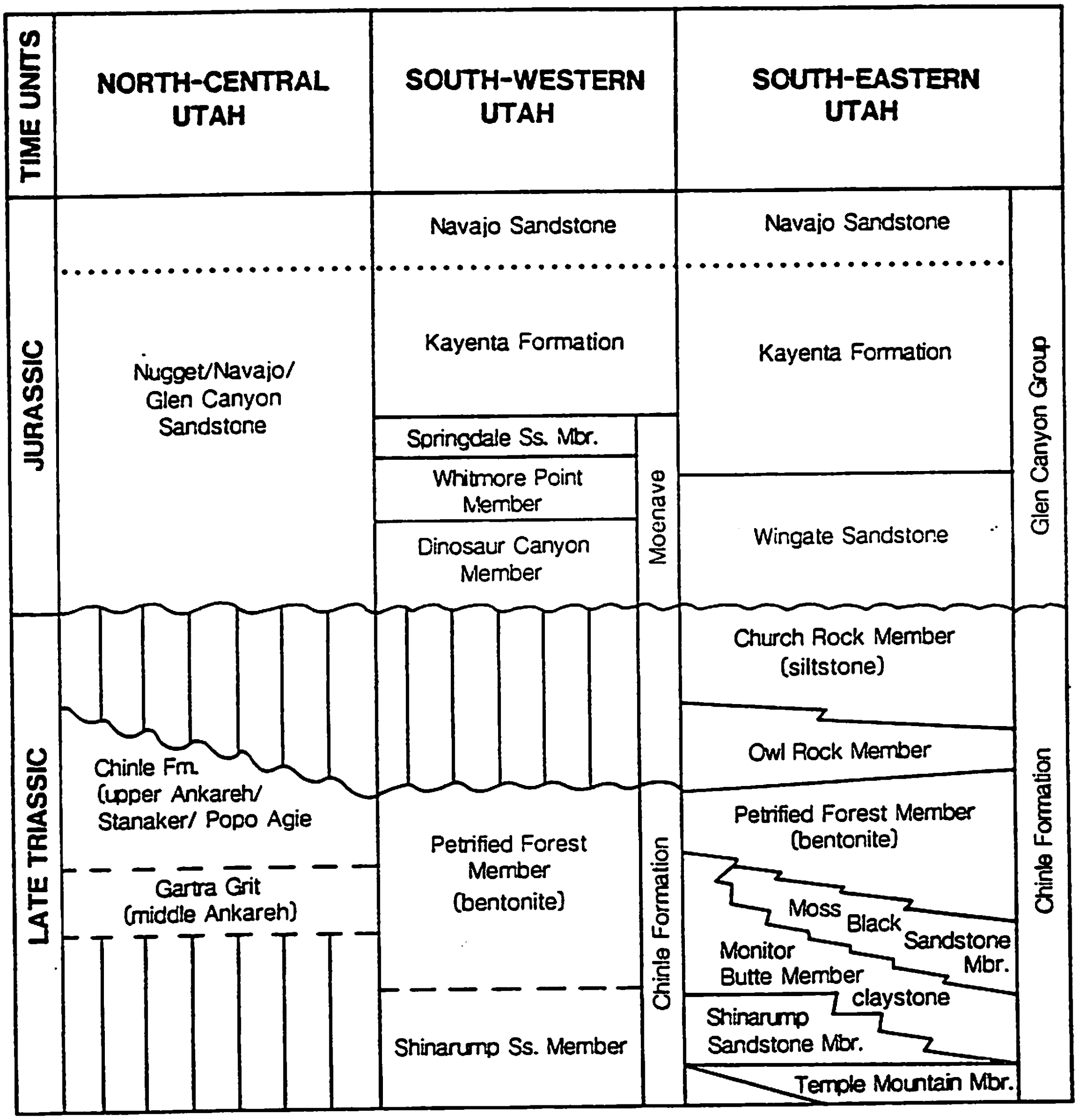

Figure 1: Stratigraphic columns in the vicinity of Tuba City. *From Gillette and Lockley (1989)*

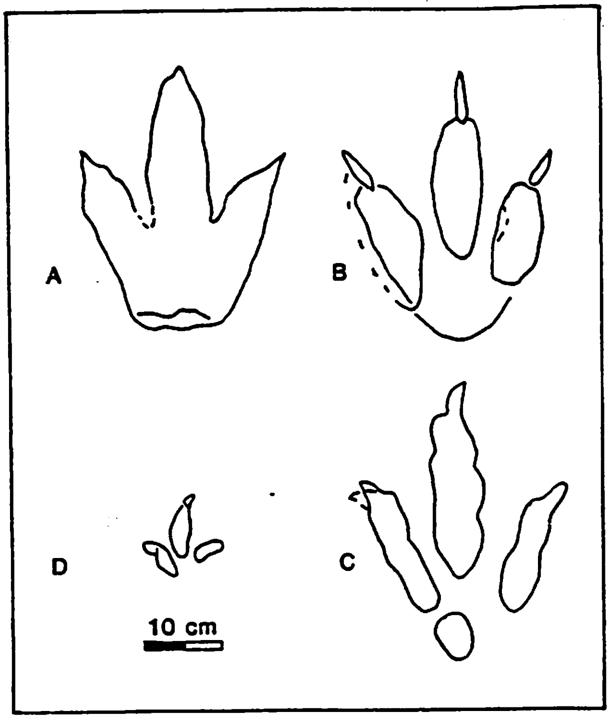

Figure 2: Therapod tracks typical of the Moenave Road tracksite. *From Lockley and Hunt (1995)*

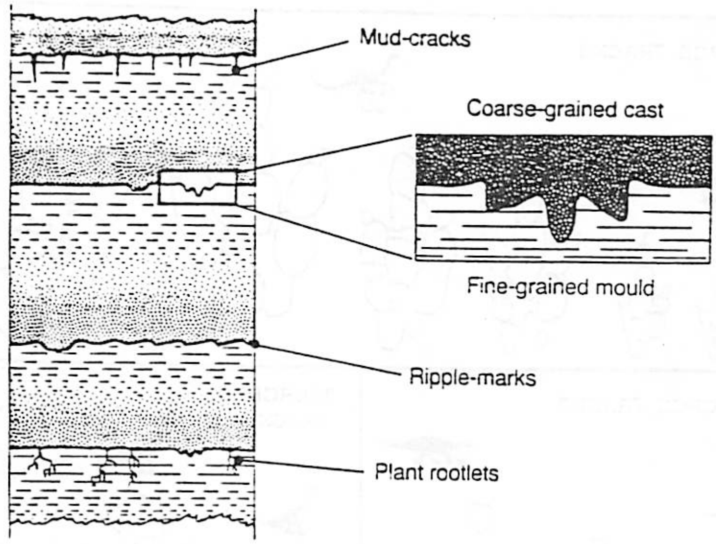

Figure 3: Sequence of sediments in which each horizon is fining-upwards. Footprints are preserved in the finer sediments near the top of each horizon. *From Thulborn (1990)*

A preserved footprint consists of two fossils – a *mold* and a *cast*. The mold is the actual footprint, depressed into the sediment. The cast is the image of the footprint in the overlying sediment. Molds tend to occur in fine-grained sediment, while casts usually consist of coarser material. This is a result of the sorting of sediment during deposition. Coarse-grained material is the first to drop out of suspension, followed by finer sand and silt. The resulting section contains a sequence of graded sediments, with the finest material at the top of each horizon, as in figure 3. The preserved footprints are created near the end of a depositional cycle, in the fine-grained sediments and are buried at the beginning of the next cycle by the coarse-grained sediments. This dicontinuity in grain-size facilitates the extraction of the fossil, as well as differential erosion. The fine-grained material is less resistant to erosion and often does not survive, leaving only the cast.

3 Identification of Trackmakers

Since it is unusual to find bones and tracks in the same vicinity, other evidence is required in identifying the trackmaker. Footprint locality, arrangement, and morphology all help to narrow down the selection, though a high level of confidence is often not possible.

Although body fossils are not usually found directly associated with fossil footprints, their geographic and stratigraphic distribution helps to establish whether or not it is likely that a particular species was present at the locality

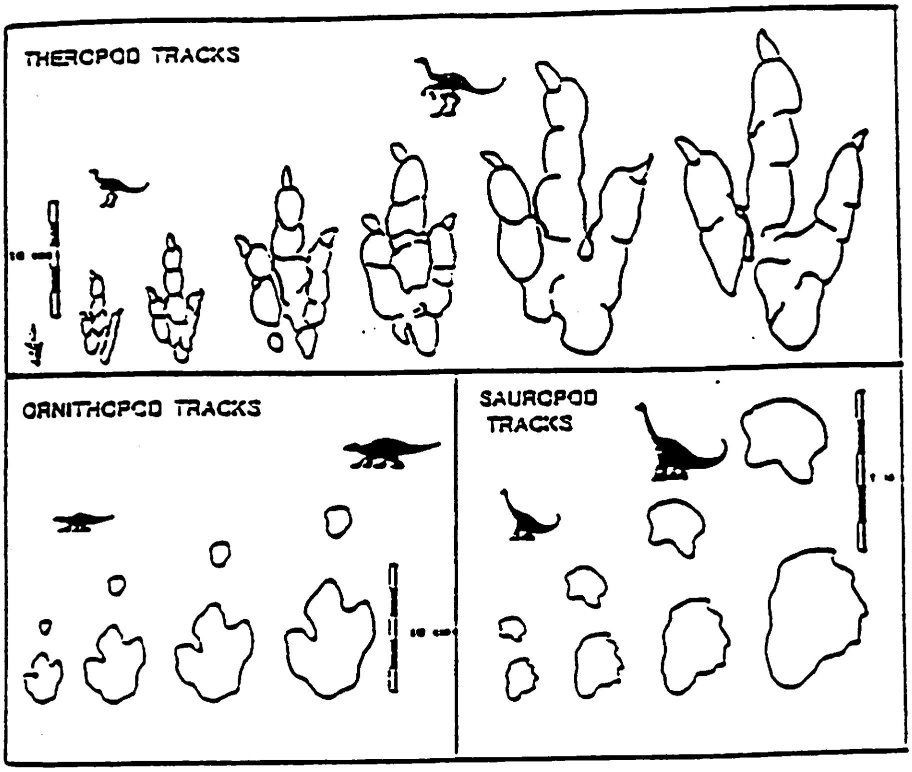

Figure 4: Shapes of various tracks created by various groups of dinosaurs. *From Lockley (1991)*

when the footprints were created. This is particularly useful for short-lived species or those with limited geographic ranges.

The arrangement of the tracks may indicate whether an animal was bipedal or quadrapedal. However, this is sometimes misleading for a number of reasons. First, many dinosaurs were not exclusively bipedal or quadrapedal. Some bipeds occasionally did walk quadrapedally[7]. Also, quadrapeds often planted their hindfeet in the prints of their forefeet or otherwise concealed their quadrapedal nature. Sometimes, there are just so many tracks that it is difficult to make the distinction.

Probably the most reliable method of identifying a species is to compare the morphology of a footprint directly to skeletal remains. It is at least necessary for the basic shape – number of toes, slender vs. wide, etc. – to match. Figure 4 shows typical footprints for various groups of dinosaurs. This criteria is still far from unique and much attention has been given to the study of the so-called *phalangeal formula*[7]. One counts the number of phalanges, proceeding from the innermost to the outermost digit. For example, the human hand has the phalangeal formula 2:3:3:3:3. Some of the footprints in figure 4 display distinct *nodes*, or bulges, along each digit. It was once expected that these

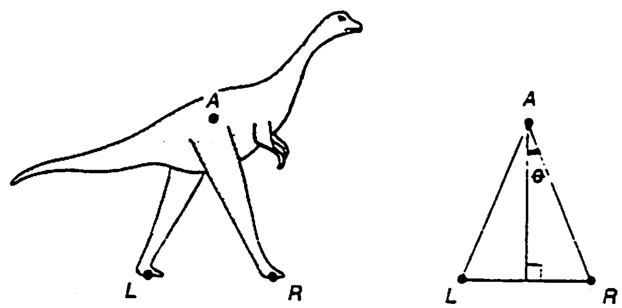

Figure 5: The angle of gait is defined in this drawing as 2ϕ. (From Thulborn (1990))

nodes corresponded directly to the phalanges and that the phalangeal formula could be determined by looking at a footprint. It has since been shown, by studying the feet of birds, that this is not necessarily a reliable assumption, though some degree of correspondence may be expected.

4 Interpretation of Footprints

Footprint morphology and the geometry of a trackway have been used to estimate properties of an animal, such as its size, gait, and speed. To esimate the size of a dinosaur from its footprint, one may attempt to estimate the height at the hip and extrapolate using skeletal specimens of the same species if the species has been identified. The height at the hip may be estimated if one assumes a value for the angle of gait (figure 5). It is well known, however, that the angle of gait may vary by as much as a factor of two or more depending on an animal's speed. To estimate the height at the hip without an assumption about the angle of gait, one can attempt to use the footprint to measure the length of the metatarsus and apply a scaling law to obtain the height at the hip. This may be a more reliable method since the assumptions can be corroborated using skeletal fossils. For small, lightweight dinosaurs, it has been observed that the length of the metatarsus may be roughly equal to the length of the footprint. Further, an empirical power-law relationship of the form

$$h = aMT^b \tag{1}$$

has been been demonstrated for each major group of dinosaurs, where h is height at the hip, MT is metatarsal length, and a and b are empirical constants. The data are plotted in figure 6 for ornithopods.

Various methods have been suggested for computing the speed of a dinosaur based on the geometry of the trackway. Alexander[1] proposed

$$v = 0.25g^{0.5}SL^{1.67}h^{-1.17}, \tag{2}$$

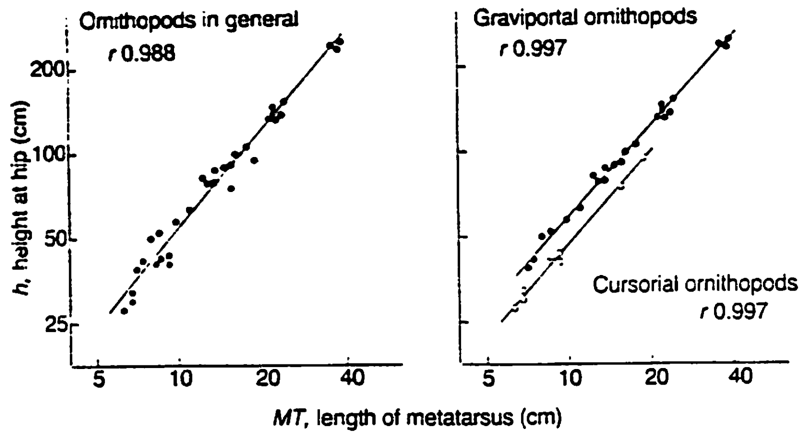

Figure 6: Empirical relationship between height at the hip (h) and metatarsus length (MT) *From Thulborn (1990)*

where v is the speed, g is the acceleration of gravity, and SL is the stride length (figure 7). Equation 2 was determined by observing various animals, including humans, horses, elephants and birds and may not be applicable to dinosaurs which were running. Values obtained from equation 2 range up to 40 km/h for a few theropods, though most rarely exceed 10 km/h. Thulborn and Wade[6] subsequently modified equation 2 for running dinosaurs;

$$v = [gh(SL/1.8h)^{2.56}]^{0.5}. \tag{3}$$

A seemingly more physical approach was given by Demathieu[2]. Based on a pendulum analogy, the result is

$$v = \frac{SL}{2\pi}\sqrt{\frac{g}{L}}, \tag{4}$$

where L is an effective length, whose value appears to be based on some rather arbitrary assumptions. The results are similar to those obtained using Alexander's method.

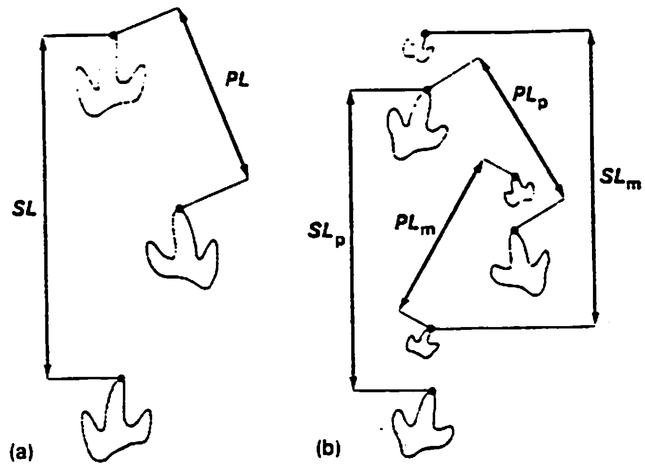

Figure 7: Measuring the dimensions of a dinosaur trackway. SL is the stride length and PL is the pace length. *From Thulborn (1990)*

References

[1] R.McN. Alexander. Estimates of the speed of dinosaurs. *Nature*, 261:129–130, 1976.

[2] G.R. Demathieu. Utilisation de lois de la mecanique pour l'estimation de la vitesse de locomotion des vertebres tetrapodes du passe. *Geobios*, 17:439–436, 1984.

[3] David D. Gillette and Martin Lockley, editors. *Dinosaur Tracks and Traces*. Cambridge University Press, 1st edition, 1989.

[4] Martin Lockley. *Tracking Dinosaurs: A New Look at an Ancient World*. Cambridge University Press, 1st edition, 1991.

[5] Martin Lockley and Adrian P. Hunt. *Dinosaur Tracks and Other Fossil Footprints of the Western United States*. Columbia University Press, 1st edition, 1995.

[6] R.A. Thulborn and M. Wade. Dinosaur trackways in the winton formation of queensland. *Memoirs of the Queensland Museum*, 21:413–517, 1984.

[7] Tony Thulborn. *Dinosaur Tracks*. Chapman and Hall, 1st edition, 1990.

Plateau Lands, and Their Formation

The Colorado Plateau Povince is dominated by plateaus and canyons, e.g., most important and impressive the well known Grand Canyon. The whole area extends about 460 miles from north to south, and 480 miles from east to west, with altitudes between 5000 and 11000 feet.

The apparent dryness of the region seems to be in contradiction with the erosion taking place in this region: The amount of sediments in alluvial deposits and the sediments transported to the Pacific Ocean via Colorado River indicate, that about **1 foot** of surface can be eroded during a time period of about 1260 years, indicating relatively rapid erosion.

The existing dry climate with its sparse vegetation and thin soil forms in collaboration with short but intense rain falls a unique scenery composed of **Mesas, Cliffs and Monuments** as indicated in **Fig. 1**, which is geologically described as **"Differential Erosion"**:

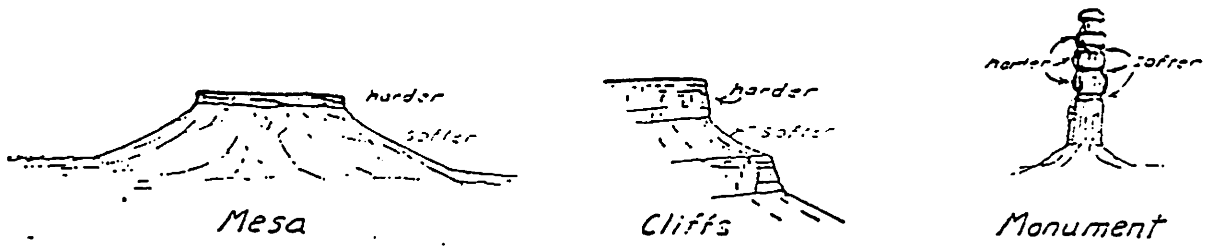

Differential Erosion
How it Works

The basic reason for this scenery and for the differential erosion are differences in the hardness of the layers in the rocks. A harder layer is sitting on top of a more soft layer. Harder rocks are less destroyed by erosion than softer rocks, and in consequence the harder layer persists longer against erosion, protecting the softer layer underneath against it as well. Therefore erosion of the harder layer can only take place from cracks or joints in which originate already from times when the rock was still a part of the crust, and target for the great strains and stresses inside the crust.

Is water penetrating the harder rock once along a crack as indicated in the "Carving of Monument Valley"(1) in **Fig. 2**, it starts to cut narrow washes and river beds into the hard rock. These carves get deeper and deeper with time, and finally reach the until then protected layer of softer material. From that moment on the softer material is more quickly eroded away than the harder material above. This erosion of the softer material underneath the e.g. hard sandstone gets the formed cliffs statically more and more instable, while water from above widens further existing joints and cracks. This leads to an accelerated erosion as well as from the flanks of the existing hard rock cliffs. In water carrying river beds material is even carved away underneath the harder layer creating vertical rock walls and overhangs. Cliffs and overhangs get statically increasingly instable with time, break away along joints from the main Mesa rock and drop or slide down towards the softer material layer. This process is geologically called **rock sliding**, but better described with a **rock collapse** or **rock drop**.

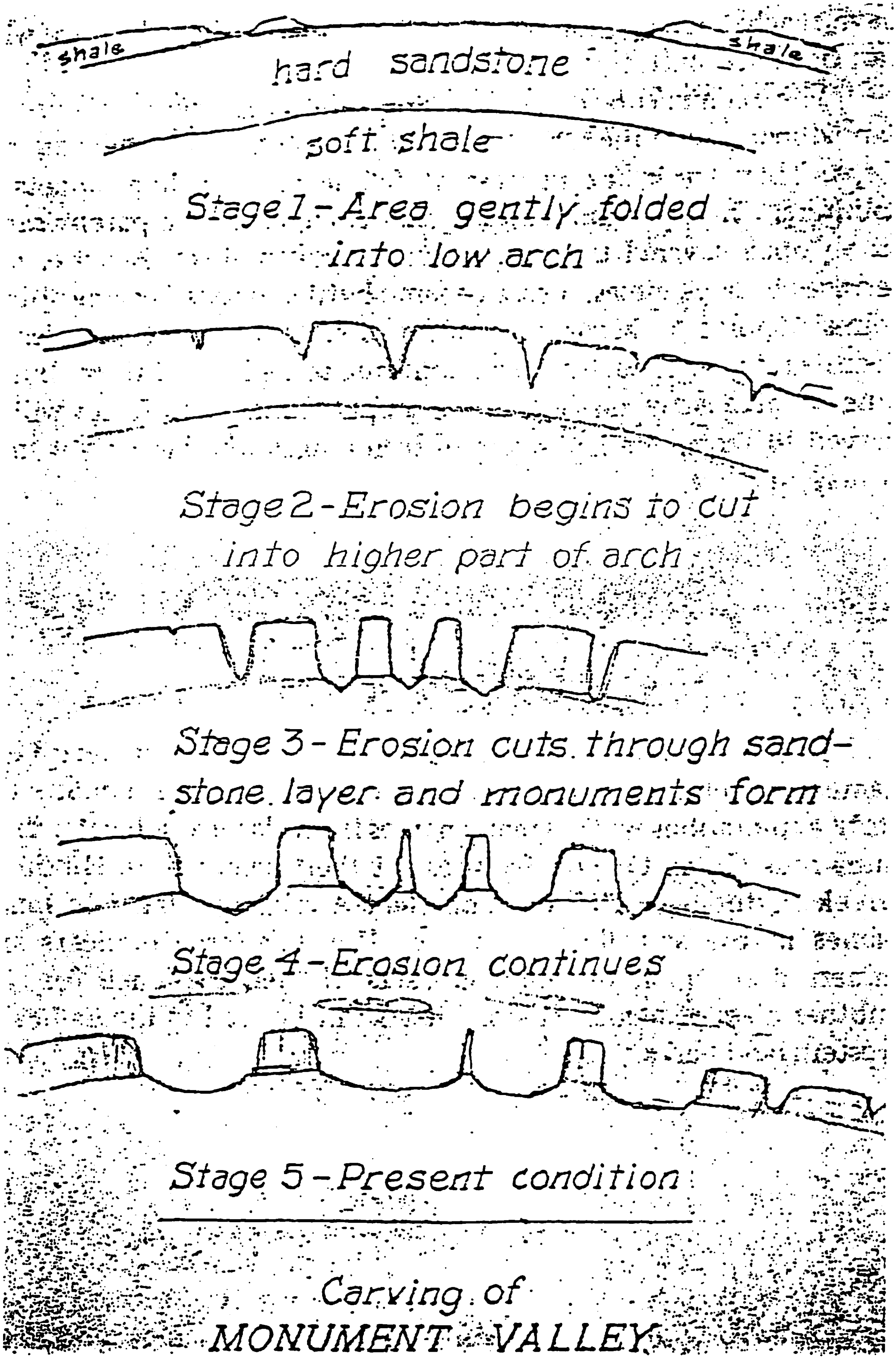
shale
shale
hard sandstone
soft shale
Stage 1 - Area gently folded into low arch
Stage 2 - Erosion begins to cut into higher part of arch
Stage 3 - Erosion cuts through sand-stone layer and monuments form
Stage 4 - Erosion continues
Stage 5 - Present condition
Carving of MONUMENT VALLEY

Plateau Land Scenery

1. Grand Staircase of a Plateau

Beside their impressive height and length, the cliffs have distinctive colours which gave them their popular names. Starting on the rim of the Grand Canyon a sequence of cliffs rises higher and higher northwards which geologists call the **Grand Staircase of Western Geology** as indicated in Fig. 3:

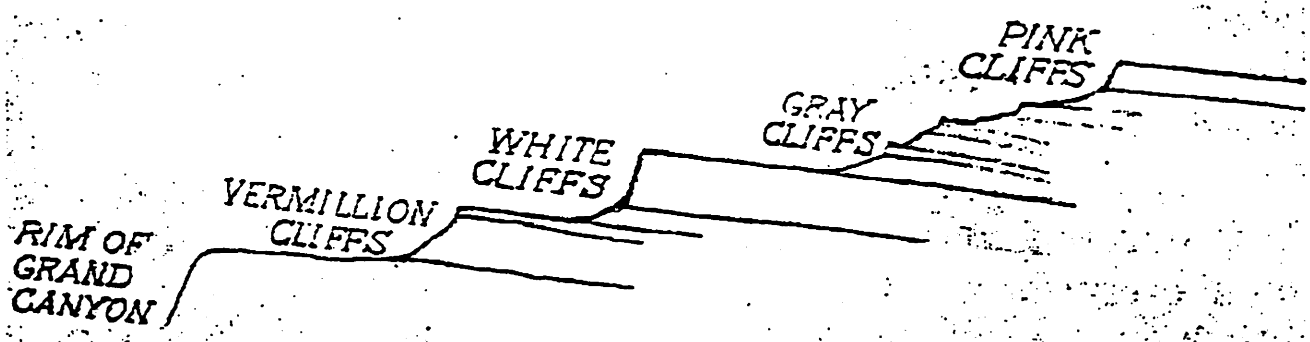

Grand staircase of Plateau geologic history

At the bottom is the Vermillion Cliff, followed by the White Cliffs, the Gray Cliffs, and the Pink Cliffs. The Vermillion Cliffs run almost parallel along the Arizona-Utah boundary, are brillantly red, and consist of a lower part made of shale, and an overlying part of conglomerate and sandstone. The are the grave yard for some Triassic dinosaurs, heqavy bodied amphibians, fish and marine shells. The conglomerate buries many fossil trees and even petrified forrest.

On top of the Vermillion Cliffs are the most famous White Cliffs because of their height and picturesque forms into which they are carved. The White Cliffs consists almost entirely of one great sandstone which is called the Navajo Formation (e.g., Glen Canyon, Rainbow Bridge). It represents a desert period in the Jurassic times, nearly empty of life, and in consequence only small amounts of dinosaur skeletons can be found.

Above this formation are the Gray Cliffs, which are originally Ocean-deposited, and made of soft shale. They bury all kinds of sea life (shark teeth) from the Cretaceous Period. Beside that coal beds can be found as well, indicating swamp and marsh vegetation present at that time.

On top of all are the Pink Cliffs, which are the youngest formation. They consist of limy siltstone, a product of an ancient freshwater lake that once covered most of southeastern Utah. From this layer Bryce Canyon and Cedar Breaks were carved.

2. Typical Formations

Pictures 3 to 6 on the right side show some typical formations from the Colorado Plateau:

Different resistant layers covering softer shales in Pict. 3 and 4:

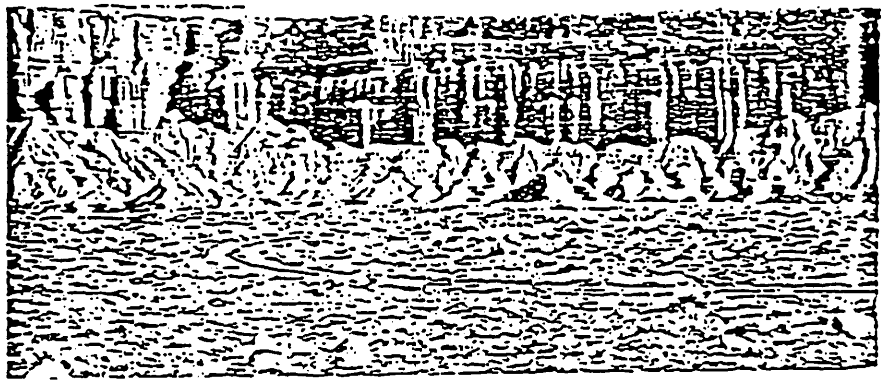

Photo 3. Compound scarp composed of resistant Shinarump Member of the Chinle Format overlying shales of Moenkopi Formation near Torrey, Utah; fluted middle portion of scarp composed of Moenkopi Formation.

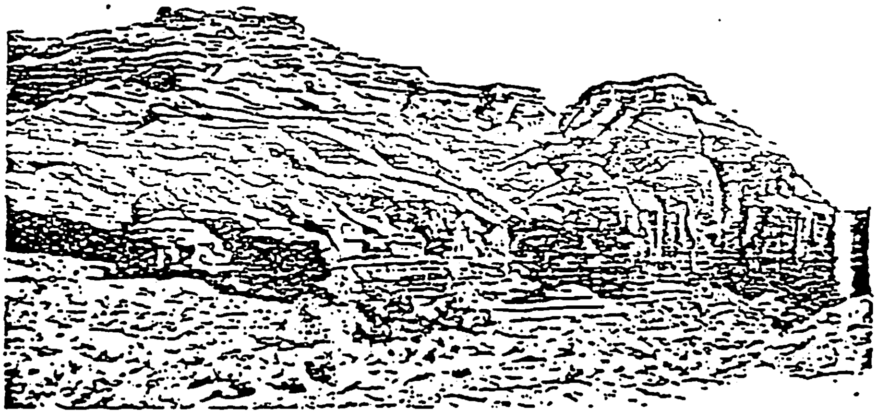

Photo 4. Complex scarp composed of four rock types near Gouldings Trading Post, Monum Valley, Utah. Rounding of De Chelly Sandstone Member of the Cutler Formation occurs thin cap of Shinarump Member of the Chinle Formation, and Hoskinnini Tongue and ov lying shales of the Moenkopi Formation of Triassic and Triassic(?) age are eroded. Shale und lying De Chelly is the Organ Rock Member of the Cutler Formation.

The "Skyline Arch" is a representative member for other sandstone arches. It was opened by a rock fall in November 1940.

Pict. 6 shows a typical rock fall area along the road to Turret Arch

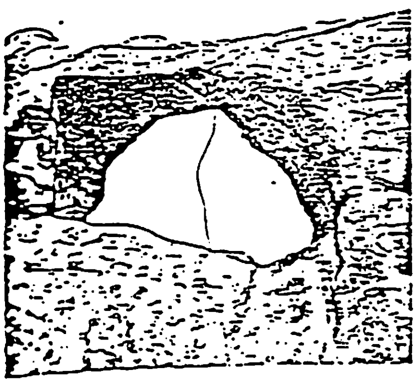

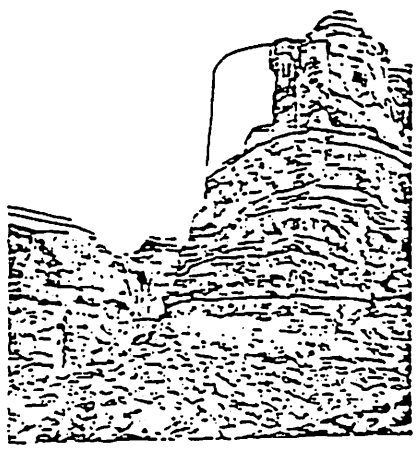

Photo 5

Photo 6

Skyline Arch, Arches National Monument, Utah. About one-half of the area under the arch, as outlined, was opened by a rock fall in November 1940 (S. G. Canton, written communication). Arch is composed of Entrada Sandstone.

Photo 6. Rock fall on road to Turret Arch, Arches National Monument, Utah. This rock fall occurred on October 7, 1942, when two large pinnacles, as outlined, of the Entrada Sandstone fell. Note relatively small caliber of debris.